Section 1
Executive Summary

Paraffinic hydrocarbon liquids, including both crude oils and condensates, will form a paraffin or wax solid phase when the temperature falls below the cloud point of the liquid. Once formed, the wax will either be transported with the liquid (and gas) or will deposit on the pipe wall.

In this JIP, the effects of multiphase flow variables on wax deposition rates and wax deposit composition were to be assessed and correlated to single-phase liquids. These multiphase flow variables include pipe inclination angle, flow pattern, gas and liquid superficial velocities and liquid holdup. The impact of wax deposition on pressure drop (pipe roughness and/or diameter reduction) and flow rate were also addressed. These data could then be used to develop or improve wax deposition prediction models.

A test facility for conducting single-phase deposition tests was identified at the Alberta Research Council (ARC) in Edmonton, Alberta, Canada. The facility was shipped to Tulsa in 1995, reassembled, and significantly upgraded with new instrumentation, pumps, chilling system and a data acquisition and control system. The test section consists of a near-horizontal, 50-m (164 ft) long, U-shaped steel pipe with an inside diameter of 43.6 mm (1.71 in.). This pipe is held in place with PVC centralizers in the center of a PVC pipe jacket with an inside diameter of 102 mm (4.0 in.).

A second test facility for conducting high pressure, two-phase, natural gas-oil deposition tests was designed, constructed and commissioned. The test section consists of a U-shaped, 52.5-mm (2.067 in.) I.D., stainless steel pipe and is 48.8-m (160 ft) long. It is mounted on a boom such that any inclination angle between horizontal and vertical can be selected using a hydraulic hoist attached to an 18.3-m (60 ft) high tower. One leg of this test section is partially jacketed with a 10.16-cm (4 in.) nominal diameter CPVC pipe, over a length of approximately 16.2-m (53 ft). The entire test facility was designed for a pressure level of 6.8948 MPa (1,000 psia) and temperatures up to 180 °F.

Separator and stock tank samples for use in this study were taken from two wells: South Pelto 10 Well 9-2 and Garden Banks 426 Well A-14. Most of the tests were conducted using oil from Mobil Oil Corporation's South Pelto Field, Well 10E, in the Gulf of Mexico. Deposition and physical properties of this crude had been previously determined as a part of the DeepStar Joint Industry Project. This oil contains approximately 5% wax by weight, and has a WAT of approximately 49°C (120°F). The density of this 35 °API (specific gravity of 0.85) crude oil was measured continuously with a Micro Motion mass flow meter.

Single-phase paraffin deposition was studied extensively with a 50-m (164 ft) long flow loop with a 43.6-mm (1.71 in.) internal diameter. Most of the tests were conducted with crude oil from Mobil Oil Co.'s South Pelto field and two tests were conducted with condensate from Shell Oil Co.'s Garden Banks field, both from the Gulf of Mexico. All the laminar flow tests and one low velocity condensate turbulent test produced soft deposits. Estimates of wax thickness were made using methods based on pressure drop and heat transfer in the test section, using an ultrasonic sensor designed and constructed by Norsk Hydro and Christian Michelson Research (CMR), and from visual observations and manual measurements. The remaining tests produced hard deposits. The trapped oil concentration in the deposits ranged from 20 to 90% and the deposit thermal conductivities ranged from the oil thermal conductivity to 6 times the oil thermal conductivity, depending on test conditions and duration. The effect of flow regime on wax deposition was demonstrated clearly by the tests at different flow rates with the same difference between the oil and glycol inlet temperatures. The deposit thickness was found to decrease rapidly with increasing flow rate in laminar flow; after the flow became turbulent, the thickness was much less sensitive to an increase of flow rate. The aging effect was studied by conducting tests of different time durations. The oil

concentration was found to decrease with time. The wax deposit changed from "shoe polish" like wax after 24 hours, to a "candle" wax after 120/140 hours. In laminar tests, there was no change observed in the oil concentration for different time durations. All deposits contained approximately 90% oil.

Multiphase deposition tests involved flowing the fluids at horizontal (0°), inclined upward (2°), and vertical (90°) positions for up to 24 hours, and utilized one inlet mixture temperature and one inlet glycol temperature. In addition to the techniques discussed above, wax measurements were made with the Liquid Displacement-Level Detection (LD-LD) device. Wax deposition was found to be flow pattern dependent and occurs only along the pipe wall in contact with the waxy crude oil. The deposition buildup trend at low mixture velocities is similar to that observed in laminar single-phase flow tests. The buildup trend at high mixture velocities is similar to that observed in turbulent single-phase flow tests. Thinner and harder deposits at the bottom than at the top of the pipe were observed in horizontal intermittent flow tests. Thicker and harder deposits were observed at low liquid superficial velocity than at high liquid superficial velocity annular flow tests. No wax deposition was observed along the upper portion of the pipe in stratified flow tests.

A computer program was developed by the JIP for the prediction of wax deposition during single-phase and two-phase gas-oil flow in horizontal and near-horizontal flowlines, and vertical wellbores. The program is modular in structure, and assumes a steady-state, one-dimensional flow, energy conservation principal. The program performs wax deposition prediction during multiphase flow in pipelines and wellbores by coupling mechanistic two-phase flow hydrodynamic models, solid-liquid-vapor thermodynamics, two-phase flow heat transfer and flow pattern dependent wax deposition kinetics into one modular program. This program has been integrated with a Graphical User Interface (GUI) developed by MSI, with graphical input, output and plotting supports.

Section 2
Acknowledgements

The successful completion of a project of this type and magnitude requires significant contributions of time and other resources from a large number of individuals and organizations. We specifically acknowledge the following:

- Jeff Creek for outstanding leadership as the Chair of the important Flow Loop and Deposition Studies Committee. His regular monthly trips to Tulsa to monitor progress and travels with the Tulsa University co-Principal Investigators to Canada, the United Kingdom, Norway, the Netherlands, France and Mexico on behalf of the JIP members were of tremendous benefit in helping the research team remain focused. He also performed important simulations with commercial software to improve flow loop operating procedures, supported development of an ultrasonic sensor by Norsk Hydro and the Christian Michelsen Institute (CMR), and helped organize, write and edit several of the JIP reports.

- Chevron Petroleum Technology Corporation for significant laboratory HTGC analyses of deposits for all tests conducted.

- Shell Oil Co. for providing the Garden Banks condensate. Alan Leitco and George Broze for suggestions to improve flow loop operations, including incorporation of temperature trimming in the flow loops. Ulfurt Klomp for valuable discussions of Ostwald ripening as a mechanism for deposit aging.

- Jean Luc Volle of Elf for suggesting the LD-LD method to measure deposit thickness, for making wax solubility and DSC WAT measurements on the South Pelto crude oil, for performing flow loop paraffin deposition simulations, for valuable discussions about deposition mechanisms and flow loop design, and for sponsoring Emmanuel Delle Case as a visiting scholar to the JIP for a period of 18 months.

- Ivor Forsdyke, formerly with BP and now with Flowassurance Solutions Limited, for initially approaching TUFFP to form the JIP, for sharing his ideas on multiphase flow deposition mechanisms, and for performing flow loop deposition simulations.

- Vicki Niesen, formerly with Conoco and now with Multiphase Solutions Inc. (MSI), for initially approaching TUFFP to form the JIP, for performing CPM WAT measurements on the South Pelto crude oil, for her role in making the Conoco single-phase deposition computer program available to JIP members, for many valuable discussions on deposition mechanisms and solid-liquid-vapor equilibrium concepts, and for developing the GUIs for both the single-phase and multiphase deposition computer programs.

- Robert Kaminsky of Exxon for performing important initial consistency and quality checks on data from both single-phase and multiphase deposition tests, for analysis of temperature data to determine deposit thickness calculations, and for proposing methods to estimate film heat transfer coefficients under multiphase flow conditions.

- Knut Erik Grung of Norsk Hydro for his role in developing and making available an ultrasonic sensor for measuring paraffin deposit presence and thickness in the single-phase flow loop.

- Bill Martin, formerly of Norsk Hydro, for valuable initial discussions on flow loop design and deposition mechanisms, and for hosting a visit to observe the Hydro flow loops at Porsgrunn.

- Jack Hsu of Texaco for valuable discussions on the importance of rheology, shear dispersion and shear stripping in deposition and for arranging for Texaco to conduct a Hazop analysis of the single-phase and multiphase flow loops.

- Petronas for supporting Ahmadbazlee Matzain as a Research Assistant to the JIP for both his MS and PhD programs.

- Brad Pate and Nagi Nagarajan of Mobil for hosting an important initial meeting in Dallas of potential JIP members, and for assisting in obtaining 40 bbl of the South Pelto crude oil.

- Oyvind Isaksen, formerly of CMR and now with ABB, and Gunnar Wedvich of CMR for making an ultrasonic sensor available during single-phase deposition tests and for interpreting results that confirmed periodic shear stripping in some tests.

- United States Department of Energy for recognizing the importance of this project to the domestic oil and gas energy and funding approximately 25% of the total cost.

In addition, the following University of Tulsa staff members deserve special recognition for their contributions throughout the JIP:

- Jerry Wilson for his contributions as Project Engineer, including the design and construction supervision for site preparation, towers and booms, headquarters trailer and supervision of technicians.

- Charles Ingle, mechanical technician and supervisor, for ordering, receiving and assembly of all parts and equipment for both flow loops.

- Tony Butler, Senior Electronics Technician, for ordering, receiving and installation of all measurement devices.

- Pam Clark, Project Assistant, for all tasks related to accounting and organization of meetings.

- Linda Jones, Administrative Secretary, for tasks related to preparation of materials for meetings, formatting final reports, purchasing and communications with JIP members.

Section 3
Table of Contents

List of Tables

List of Figures

Section 4
Introduction

The frontier for oil and gas exploration and production is deepwater; however, as oil and gas production moves to deeper and colder water, subsea multiphase production systems become critical for economic feasibility. It will also become increasingly imperative to adequately identify the conditions for paraffin precipitation and predict paraffin deposition rates to optimize the design and operation of these multiphase production systems. Accurate information about the potential for, and extent of, wax deposition is very critical, not only towards the operation and design of these systems, but also for assuring their economic feasibility. Although several oil companies have paraffin deposition predictive capabilities for single-phase oil flow, these predictive capabilities are not suitable for the multiphase flow conditions encountered in most flowlines and wellbores. DeepStar was formed to identify and develop the required technology. This $4.5 million JIP formed in May 1995 is a spin-off from DeepStar.

New petroleum production horizons at water depths greater than 500m have driven industry to develop new technologies for preventing and controlling the deposition of petroleum wax. Traditional methods of management, prevention, and remediation have been established for many years (Mendes and Braga (1996) and Jessen and Howell (1958)). The greater water depths mean lower temperatures, no fixed platforms (TLP's and FPSO's are expensive) and subsea wellheads. The longer and fewer production lines in deeper water make economic solutions to prevention, management, and remediation key to economic development of these new deep water resources.

The cost of remediation due to pipeline blockage from paraffin deposition is on the order of $200,000 when the water depth is 100m, but on the order of $1,000,000 when the remediation occurs in water depths near 400m. The cost is proportionately greater as development depth increases (Pate (1995)).

Since its inception, the petroleum industry has been plagued by paraffin. Its long time nature as a nuisance, easily and inexpensively treated onshore with chemicals and scrappers, has resulted in a lack of basic research regarding the actual deposition phenomena. However, paraffin deposition can be the determining factor for not producing deep-water fields, many of which are tied to nearby platforms with subsea flowlines. These remote facilities at low temperatures are vulnerable to deposition of paraffin in tubulars. It could lead to a potentially expensive, catastrophic event in the history of a project.

This inherent engineering and economic challenge has led to a renewed interest in studying the problem within the petroleum industry. Many oil and gas related companies have studied paraffin deposition and have predictive capabilities for paraffin deposition during single-phase oil flow. However, these predictive capabilities are still unproven and not suitable for multiphase flow conditions encountered in most flowlines and wellbores. It is important to model the deposition rate to optimize pigging schedules, to design appropriate chemical treatments, or to design insulated systems to minimize or alleviate paraffin deposition in wellbores or flowlines.

Section 5
Scope of Problem

Paraffinic hydrocarbon liquids, including both crude oils and condensates, will form a paraffin or wax solid phase when the temperature falls below the cloud point of the liquid. Once formed, the wax will either be transported with the liquid (and gas) or will deposit on the pipe wall.

In this JIP, the effects of multiphase flow variables on wax deposition rates and wax deposit composition were to be assessed and correlated to single-phase liquids. These multiphase flow variables include pipe inclination angle, flow pattern, gas and liquid velocities and liquid holdup. The impact of wax deposition on pressure drop (pipe roughness and/or diameter reduction) and flow rate were also addressed.

Prediction of paraffin deposition under multiphase flow conditions requires a synergistic approach that builds on current technologies in the areas of thermodynamics, multiphase flow and heat transfer. Figure 5.1 illustrates the synergism among the various tasks performed in this JIP or deferred to the follow-on Consortium.

The work plan for the wax deposition JIP involved two phases (Phases I and II) that had to be conducted according to a logical time schedule. A third phase (Phase III) was originally planned but could not be accomplished due to a lack of available funds. Phases I – III are shown in Figure 5.2 and are described below.

Phase I

The first phase of the study involved a collection of initial tasks that had to be completed in preparation for conducting deposition tests under single-phase and two-phase conditions. These tasks included building two paraffin deposition test facilities, conducting single-phase wax deposition studies, and screening and evaluating existing thermodynamic and heat transfer models. Each is discussed in greater detail below.

Test Facilities Development

A test facility for conducting single-phase deposition tests was identified at the Alberta Research Council (ARC) in Edmonton, Alberta, Canada. The facility was shipped to Tulsa in 1995, reassembled, and significantly upgraded with new instrumentation, pumps, chilling system and a data acquisition and control system. The test section consists of a near-horizontal, 50-m (164 ft) long, U-shaped pipe with an inside diameter of 43.6 mm (1.71 in.). This pipe is held in place with PVC centralizers in the center of a PVC pipe jacket with an inside diameter of 102 mm (4.0 in.). Please see Section 6 and the MS Theses of Matzain (1997) and Lund (1998) for more details.

A second test facility for conducting high pressure, two-phase, natural gas-oil deposition tests was designed, constructed and commissioned. The test section consists of a U-shaped, 52.5-mm (2.067 in.) I.D., stainless steel pipe and is 48.8-m (160 ft) long. It is mounted on a boom such that any inclination angle between horizontal and vertical can be selected using a hydraulic hoist attached to an 18.3-m (60 ft) high tower. One leg of this test section is partially jacketed with a 10.16-cm (4 in.) nominal diameter CPVC pipe, over a length of approximately 16.2-m (53 ft). The entire test facility was designed for a

Figure 5.1 - Paraffin Deposition Task Synergism

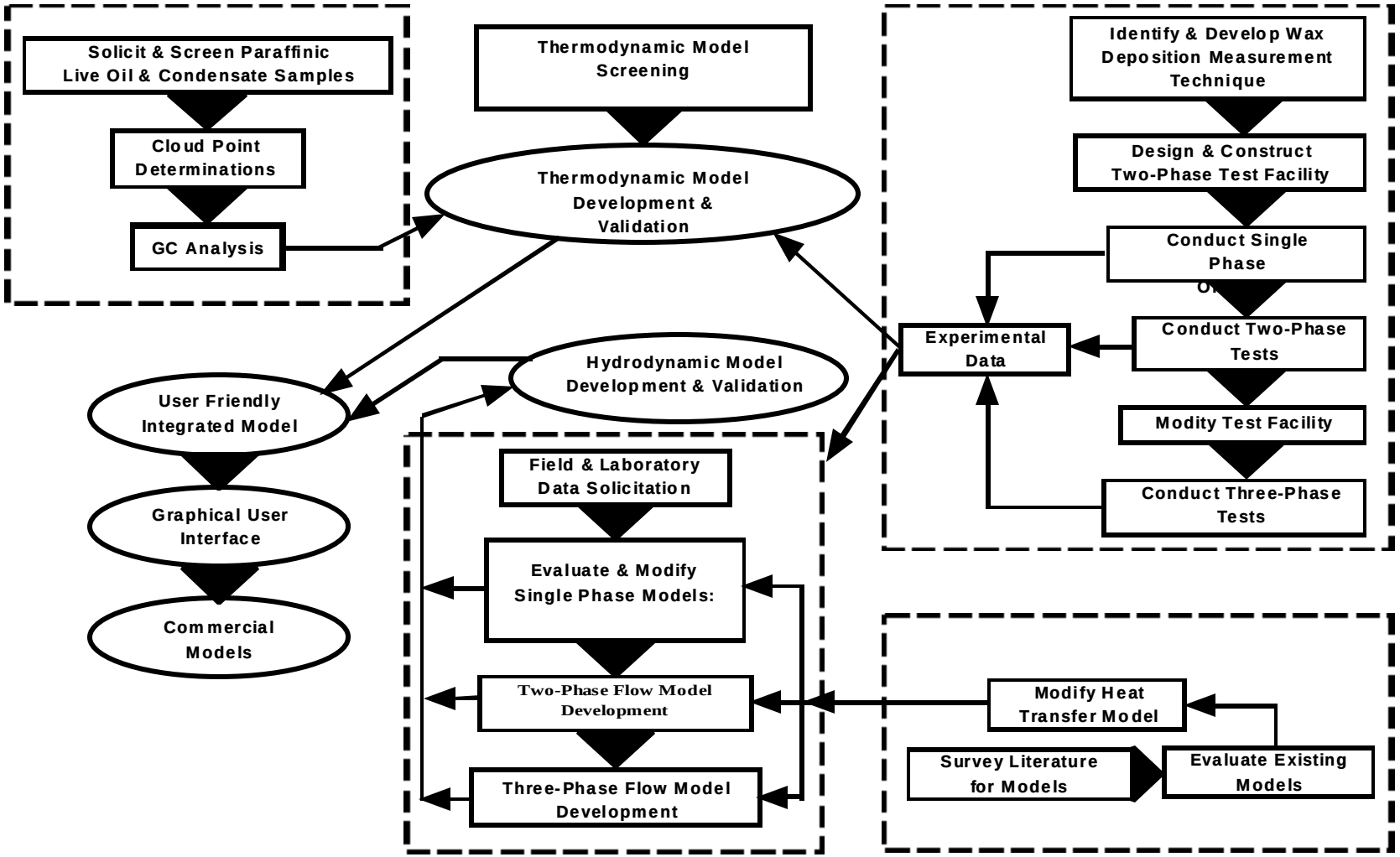

Figure 5.2a – Thermodynamic and Heat Transfer Studies

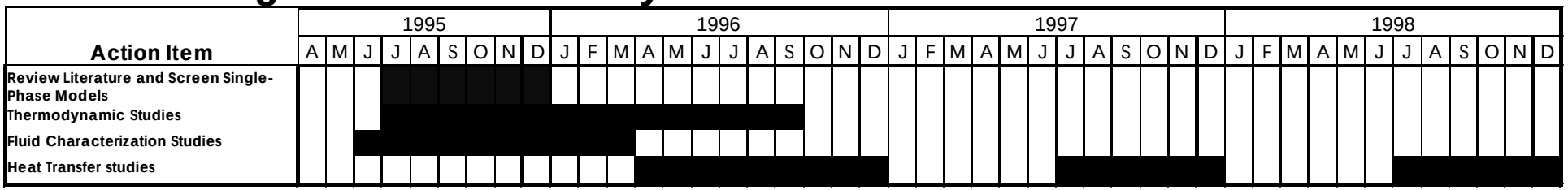

Figure 5.2b - Wax Testing Schedule

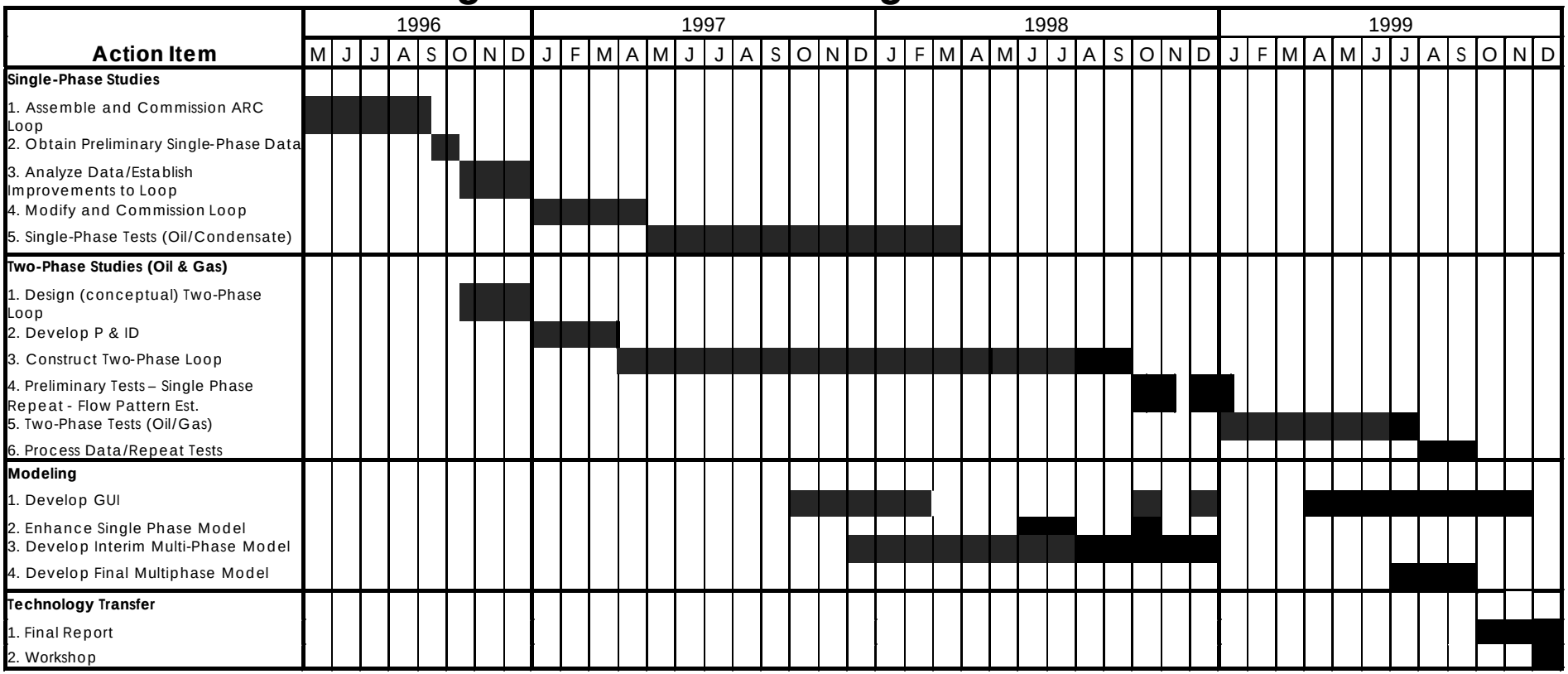

pressure level of 6.8948 MPa (1,000 psia) and temperatures up to 180 °F. Of special significance is the outstanding level of instrumentation and control installed in all parts of the flow loop. Please see Section 6 and the MS Thesis by Apte (1999) and the PhD Dissertation by Matzain (1999) for more details.

Single-Phase Deposition Tests

The single-phase deposition facility was used to obtain limited single-phase tests by Matzain (1996), following which extensive modifications were made to improve the facility. More detailed single-phase tests were then conducted by Lund (1998) using both South Pelto crude oil and Garden Banks condensate. Please see Lund's MS thesis for more details.

Thermodynamic Tasks

A solicitation and screening of possible paraffinic oil and condensate samples was completed, resulting in the selection of Mobil Oil Corporation's South Pelto oil and Shell Oil Company's Garden Banks condensate as the liquid phases to be tested. Approximately 40 bbl of each liquid were delivered to The University of Tulsa.

Marathon Oil Co. was contracted to perform the thermodynamic characterization analysis of the liquids in equilibrium with Tulsa city natural gas. Marathon also measured the cloud points and the wax content vs temperature of the samples. Please see Section 7 and the report by Creek and Volk (1999) for more details. Chevron performed HTGC analyses of all deposits generated during the tests.

After identifying possible single-phase deposition computer programs, the Conoco program was made available to all interested JIP members at a cost of $2,000. The program included the capability of performing solid-liquid equilibrium calculations.

Heat Transfer Tasks

The Mechanical Engineering Department at Oklahoma State University (OSU) performed an exhaustive literature search for identification of existing models and correlations for predicting convective heat transfer in gas-liquid pipe flows with different flow patterns. The OSU investigators also identified possible heat transfer data. For more information, please see the reports "Multiphase Heat Transfer in Flowlines and Wellbores Literature Survey – Part I" prepared by A. J. Ghajar and R. L. Dougherty, Oklahoma State University (1996) and "Multiphase Heat Transfer in Flowlines and Wellbores Literature Survey – Part II" prepared by A. J. Ghajar, R. L. Dougherty, D. Kim and Y. Sofyan, Oklahoma State University (1997).

Phase II

The second phase of the study involved conducting two-phase paraffin deposition tests and using the data to develop an improved deposition model. Also included were enhancements in both thermodynamic models and prediction of heat transfer coefficients. Finally, a user friendly computer program was to be developed that integrates improved paraffin deposition, two-phase flow hydrodynamic, thermodynamic and heat transfer models. Each is discussed in greater detail below.

Two-Phase Flow Tests

Twenty-three two-phase tests were conducted at different oil and gas superficial velocities and at inclination angles of 0° (horizontal), +2° (upward inclined) and 90° (vertical). All tests were conducted with the South Pelto crude oil and Tulsa city gas. Experimental data generated were used to improve our understanding of two-phase flow deposition, helped in the development of enhanced deposition models and identified necessary areas of future research. Please see Sections 8-10, the MS Thesis by Apte (1999) and the PhD Dissertation by Matzain (1999) for more details.

Thermodynamic Tasks

Multiphase Solutions Inc. (MSI) was contracted to modify the Conoco thermodynamic module to include a vapor phase and to utilize both the Peng-Robinson and SRK equations of state. Experimental data from the Marathon report in Phase I were used to verify predictions from the MSI computer program. Please see Sections 7 and 11 for more details.

Heat Transfer Tasks

After evaluating existing methods against the experimental data, OSU recommended correlations for predicting heat transfer for the multiphase flow of hydrocarbon gases and liquids. The resulting heat transfer methods were provided in the form of Fortran code. For more information, please see reports "Multiphase Heat Transfer in Flowlines and Wellbores Final Report – Phase I" prepared by A. J. Ghajar, R. L. Dougherty, D. Kim, Y. Sofyan, and V. K. Ryali, Oklahoma State University (1997) and "Multiphase Heat Transfer in Flowlines and Wellbores Final Report – Interim Phase" prepared by R. L. Dougherty, A. J. Ghajar, D. Kim and V. K. Ryali, Oklahoma State University (1999).

Computer Program Development

A Fortran computer program was written that numerically integrates the pressure gradient and enthalpy gradient equations for single-phase and two-phase flow through interconnected pipe segments that make up a pipeline or a wellbore. The program uses modern mechanistic models for calculation of pressure gradient, the JIP models for performing solid-liquid-vapor equilibrium calculations and generation of transport properties, heat transfer correlations recommended by OSU, and kinetic paraffin deposition models from the JIP. MSI was contracted to provide a graphical-user-interface (GUI) to enhance use of the computer program by JIP members. Please see Section 11, Appendix D and the MS Thesis by Apte (1999) for more details.

Phase III

Phase III proposed to conduct a feasibility study on the effects of water on paraffin deposition under multiphase flow conditions. Included were modification of the two-phase test facility to accommodate water as an additional liquid phase. A sufficient number of gas-oil-water tests would then have been conducted to permit developing a preliminary three-phase deposition model from the two-phase deposition model, and evaluate the potential need to conduct more extensive tests in a follow-on study not included in this JIP. Unforeseen experimental problems and a loss of some membership income resulted in total depletion of JIP funds at the conclusion of Phase II.

Section 6
Test Facilities

The wax test facilities are shown in Figure 6.1. They consist of a single-phase test facility, a multiphase test facility, a large trailer that houses staff as well as the single-phase control room and a small trailer that houses the multiphase control room. A description of each facility follows.

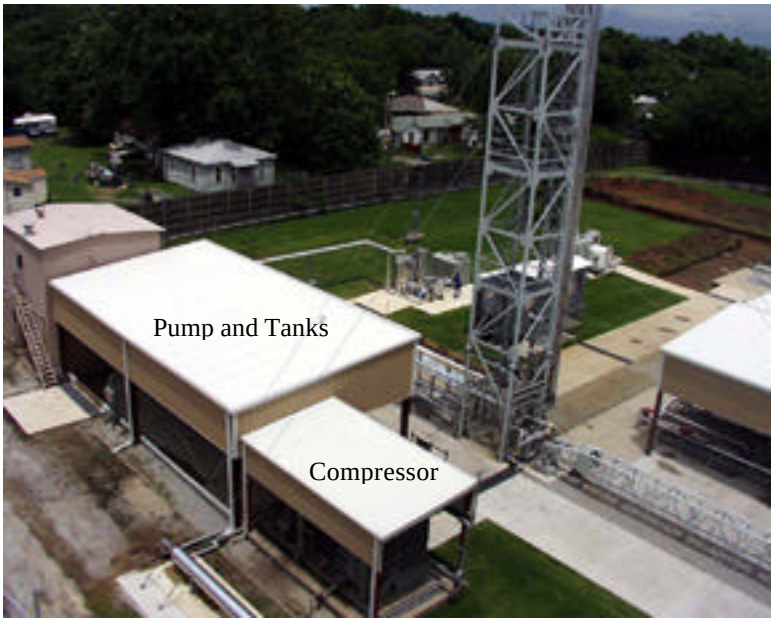

Oil System:
Moyno Pump:
85 GPM (19.3 m^3/s)
Capacity:
Oil Tank 25 bbl (4m^3)

Gas System:
Knight Compressor
Up to ≈45 ft/s (14 m/s) @
100°F and 350 psi through the test section
Two Receivers:
21 $ft.^3$ (0.6m^3)

Figure 6.1 – Overall View of Two-Phase Facility

Single-Phase Test Facility

Flow Loop

The single-phase paraffin deposition flow loop consists of a test section, a test fluid circulation system, a cooling system, a hot glycol-water mixture system, a heat tracing system and a data acquisition system. During tests, the data acquisition system gathers data from 87 input channels. Five different pumps are used to circulate the test fluid and the four separate glycol-water mixture systems used for temperature control. The inlet temperatures of the test fluid and one of the glycol-water mixture systems are kept stable to within ±0.05°C (±0.1°F) by adjusting the settings on the two boilers, the chiller, the two impedance heating systems, the two computer-controlled valves, and many manual valves. Figure 6.2 is a simplified schematic of the flow loop. It shows the oil circulation system, the cooling system, the hot glycol-water mixture system, and the test section, which is briefly described below. For detailed descriptions of the flow loop and the consisting systems, please refer to Matzain's (1997) and Lund's (1998) M.S. theses.

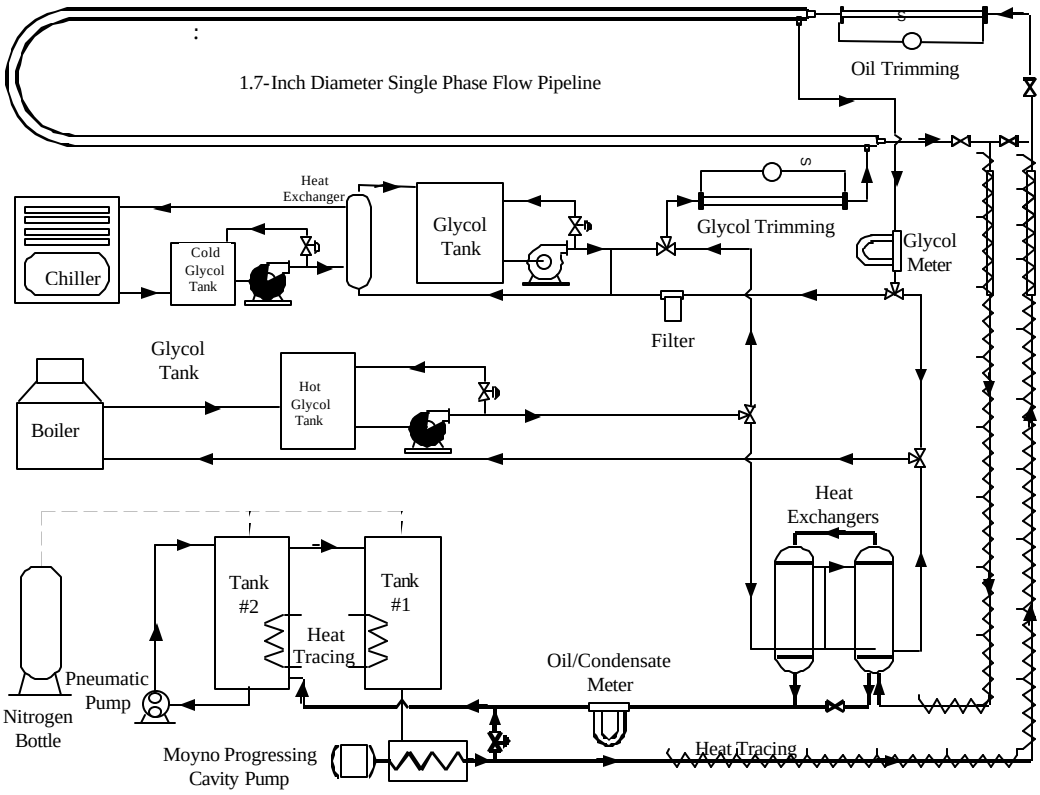

Figure 6.2 - Simplified Schematic of the Single-Phase Flow Loop

Test Section

The test section consists of a 50-m (164 ft) long U-shaped pipe with an inside diameter of 43.6 mm (1.71 in.). This pipe is held in place with PVC centralizers in the center of a PVC pipe jacket with an inside diameter of 102 mm (4.0 in.). The PVC pipe is insulated on the outside to reduce heat transfer to the surroundings. During a test, the test fluid flows in the inner pipe with a water-glycol mixture (50% ethylene glycol) flowing counter-current in the jacket. Temperatures and pressures were measured at 10 different locations along the test section. These locations are all approximately 5 m (16.4 ft) apart from each other. There are two removable spool pieces in the test section to allow visual inspection of the wax deposit. The two spool pieces are each approximately 1-m (3.28 ft) long, and are interchangeable. One of the spool pieces contains an ultrasonic sensor designed and constructed by Norsk Hydro and Christian Michelsen Research (CMR) to measure the deposit thickness on the pipe wall. Figure 6.3 is a photograph of the test section.

Pressures:
2 Gauge Pressures (GP) (beginning and end of test section)
9 Differential Pressures
Temperatures:
10 Temperatures for glycol
10 Temperatures for oil
4 Temperatures for reference sections
27 Temperatures inside pipe for top, bottom and side, at nine different locations.
Trimmer:
Current < 1500 amps
Transformer: 10-kw

Two Spool Pieces

Figure 6.3 – Single-Phase Test Section

Multiphase Test Facility

Flow Loop

The multiphase test facility was constructed to conduct paraffin deposition tests for a two-phase mixture of natural gas and crude oil flowing in horizontal, near-horizontal, and vertical pipes. Matzain *et al*. (1998) and Apte *et al*. (1999) gave detailed descriptions of the facility. The test facility, in general, consists of an oil system, a gas system, a multiphase system with an oil/gas temperature trimming section, a test section, an oil/gas separator, a chilling system, and a heating system. The facility is capable of flowing natural gas, and a waxy-crude simultaneously at pressures up to 6.8948 MPa (1000 psig). A schematic diagram of the flow loop is given in Fig. 6.4.

Crude oil is drained from the oil storage tank and pressure boosted by a Moyno Progressing Cavity (PC) pump. The oil is metered with either of two Micro Motion mass flow meters, and the flow rate is regulated by either of two automated control valves. After the oil is metered, it flows through a heat exchanger where it is warmed to the desired test temperature using a hot glycol-water mixture from the heating system.

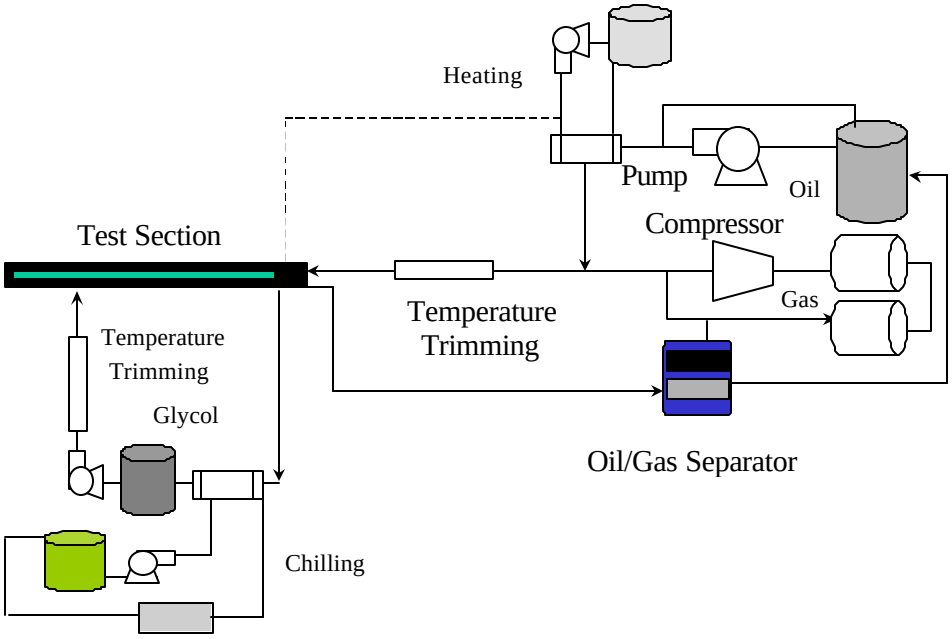

Figure 6.4 – Schematic of the Multiphase Flow Loop

Natural gas is stored in two receivers. A two-stage reciprocating compressor driven by a 149-kW (200 HP) engine recycles gas through the test facility. Discharged gas from the compressor is cooled in a gas cooler using a cold glycol-water mixture from the chilling system. The gas is metered with either of two Micro Motion mass flow meters, and the flow rate is regulated by either of two automated control valves. After being metered, the gas flows to the mixing tee where it mixes with the oil phase. The mixture then flows to a heat trimming section where the inlet temperature of the multiphase mixture is maintained at the desired test inlet temperature. After passing the test section, the multiphase mixture then flows into a 121.9-cm (48 in.) O.D., 4.3-m (14 ft) high gas-liquid separator. The separated gas is then directed to a gas receiver and the oil phase is transferred to the top of the oil tank.

Test Section

The test section consists of a U-shaped, 52.5-mm (2.067 in.) I.D., stainless steel pipe and is 48.8-m (160 ft) long. It is mounted on a boom such that any inclination angle between horizontal and vertical can be selected using a hydraulic hoist attached to an 18.3-m (60 ft) high tower. One leg of this test section is partially jacketed with a 10.16-cm (4 in.) nominal diameter CPVC pipe, over a length of approximately 16.2-m (53 ft). A chilled (50%) mixture of glycol and water is circulated in the jacket, countercurrent to the multiphase mixture flowing in the inner pipe.

The partially jacketed leg of the test section consists of five segments: hydraulic developing segment; thermal developing segment; longitudinal wax measuring segment; a removable spool piece segment; and a gamma densitometer segment. The 3.35-m (11 ft) long hydraulic developing segment allows the multiphase flow mixture to reach fully developed flow prior to making any measurements. The 7-m (23 ft) long thermal developing segment allows the multiphase mixture to be thermally developed prior to making any measurements.

The third segment is a 7-m (23 ft) long longitudinal (axial) wax measurement segment. At each end, automated valves are installed for isolating the fluids while making wax thickness measurements using the Liquid Displacement - Level Detection (LD-LD) method (see Section 8 and Appendices for more details). For this purpose, a liquid volume measurement drum having the same diameter and length as the stainless steel inner pipe in the segment is mounted beside the longitudinal wax measurement segment, and is connected at each end of the segment using 0.64-cm (1/4 in.) diameter stainless steel tubing. Differential pressure transducers were used to detect the liquid levels in the wax deposition pipe and the volumetric drum, respectively, so that the measurements can be performed at high pressures. The longitudinal wax measurement segment has five multiphase mixture temperature transmitters and five glycol-water mixture temperature transmitters located equidistant along the segment.

The fourth segment is a 1.52-m (5 ft) long take-out section for visual inspection and sampling of the wax deposit. The fifth segment is a 1.52-m (5 ft) long unjacketed pipe on which a gamma densitometer is installed for measuring liquid holdup and inferring flow pattern. Figure 6.5 is a photograph of the test section.

Test Section:
48.8-m (160 ft) long U-shaped, stainless steel pipe; 7-m (23 ft.) long thermal developing segment; 7-m (23 ft.) long measurement segment.

Figure 6.5 – Two-Phase Test Section – Slightly Inclined

Section 7
Test Fluids

Separator and stock tank samples were taken from two wells: South Pelto 10 Well 9-2 and Garden Banks 426 Well A-14. The following field samples were taken from each well:

South Pelto 10 Well 9-2
(8) one liter cylinders of separator gas
(4) one liter cylinders of separator liquid
(2) five gallon DOT cans of stock tank oil

Garden Banks 426 Well A-14
(16) 500 cc cylinders of separator gas
(6) 500 cc cylinders of separator liquid
(2) one gallon DOT cans of stock tank oil

A 43.8-liter cylinder containing a synthetic five-component gas blend representing The University of Tulsa's natural gas stream was prepared by Marathon Oil Company. These gas and liquid samples were recombined to create the reservoir and flow loop fluids studied in this work. Most of the tests were conducted using oil from Mobil Oil Corporation's South Pelto Field, Well 10E, in the Gulf of Mexico. Deposition and physical properties of this crude had been previously determined as a part of the DeepStar Joint Industry Project. This oil contains approximately 5% wax by weight, and has a WAT of approximately 49°C (120°F). The density of this 35 °API (specific gravity of 0.85) crude oil was measured continuously with a Micro Motion mass flow meter. Appendix 3.1 of the Final Report on Fluid Characterization and Property Evaluation (Creek, et al. 1999) reports data measured on oil from Mobil Oil Corporation's South Pelto Field.

Differential Scanning Calorimetry (DSC) tests were performed by Elf Aquitaine (Volle, 1996) on the South Pelto crude oil and results were reported in the October 1996 Paraffin Deposition JIP Advisory Board Meeting Report. Table 7.1 gives the results of the DSC analyses in terms of percent solids by weight at different temperatures.

Temperature, °C (°F)	Solid Weight %
45 (113)	0.020
40 (104)	0.110
35 (95)	0.193
30 (86)	0.310
25 (77)	0.469
20 (68)	0.703
15 (59)	1.072
10 (50)	1.555
5 (41)	2.166

Table 7.1 – DSC Analyses of South Pelto Crude Oil: Paraffin Solid Concentrations by Weight

Solid weight fractions at various temperatures and pressures were also estimated with the Conoco thermodynamic solid-liquid equilibrium model (Brown et al., 1993). Table 7.2 shows the solid weight percent versus temperature predictions as reported by Matzain (1996). Figure 7.1 compares solid concentrations predicted by the thermodynamic code with the measured solid concentrations.

Temperature °C (°F)	Pressure kPa (psia)	Solid Weight %
48.9 (120.0)	103 (14.9)	0.063
48.9 (120.0)	234 (33.9)	0.060
40.6 (105.1)	103 (14.9)	0.158
40.6 (105.1)	234 (33.9)	0.154
32.3 (90.1)	103 (14.9)	0.303
32.3 (90.1)	234 (33.9)	0.297
24.0 (75.2)	103 (14.9)	0.547
24.0 (75.2)	234 (33.9)	0.535
15.5 (59.9)	103 (14.9)	0.991
15.5 (59.9)	234 (33.9)	0.969

Table 7.2 – Paraffin Solid Concentrations from Conoco Thermodynamic Code

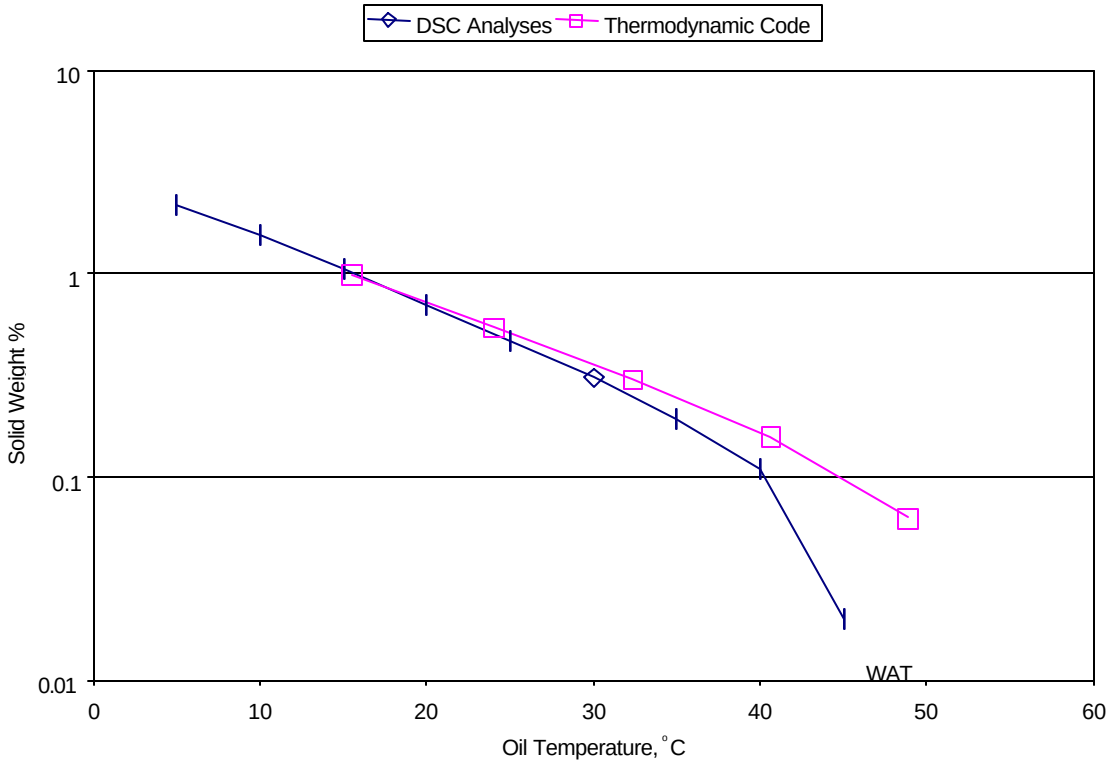

Figure 7.1 – South Pelto Solid Concentration Versus Oil Temperature

Viscosity and Rheological Behavior

The viscosity of the South Pelto crude oil was measured by several companies (Marathon (Tackett et al. (1997)), Shell (Broze (1997)), Conoco (Niesen (1995)). The reference pipes in the single-phase flow loop were used to verify that the crude oil in the loop had the same viscosity and rheological behavior as the South Pelto crude oil tested by the companies. Creek (1996 – 1998) combined the data sets from the companies and developed the following correlation for the viscosity of the oil.

$$\ln m_o = 14.023469 - 11.906456\frac{1000}{T_o} + 2.533129\left(\frac{1000}{T_o}\right)^2 \quad \text{.....(7.1)}$$

where T_o is in K, and μ_o is in cp.

The viscosity was also calculated based on the measured pressure drop in the reference sections, which were heat traced to ensure deposit-free pipe-walls. Resulting viscosity values calculated from the reference sections data are plotted in Figure 7.2, along with the viscosities calculated using Equation 7.1. Although there is some scatter in the data from the reference sections, there seems to be good agreement between the correlation and the viscosity values calculated based on the frictional pressure drop in the reference sections.

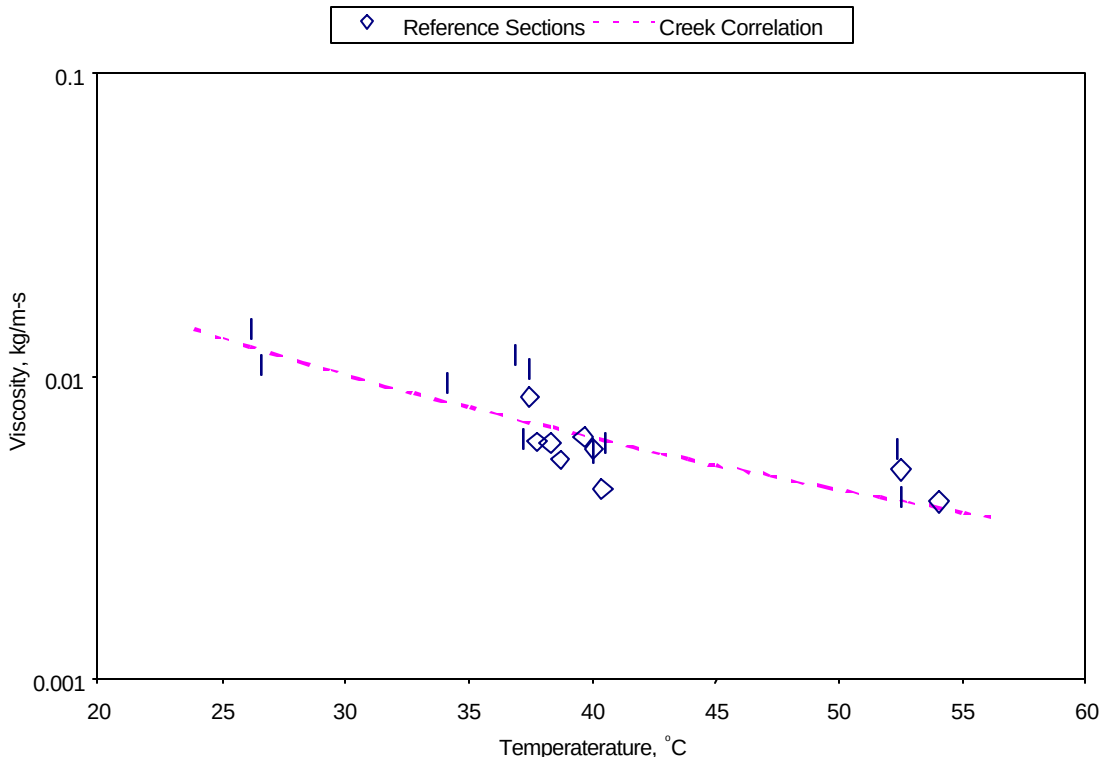

Figure 7.2 – Calculated Viscosity of the South Pelto Crude Oil at Various Temperatures for Several Tests

Two tests were conducted using a condensate from Shell Oil Company's Block 426, Well A-14, Garden Banks condensate in the Gulf of Mexico. This is a 42 °API (specific gravity of 0.82) condensate with approximately 0.5 percent wax by weight. The WAT of the condensate is approximately 43.3°C (110°F) as measured using Cross-Polar Microscopy (CPM). Appendix 3.2 of the Final Report on Fluid Characterization and Property Evaluation (Creek et al., 1999) reports data measured on the condensate from Shell's Garden Banks 426 Field.

Section 8
Facility Proving

This section briefly describes the steps taken to ensure the accuracy of reported measurements. Separate sections describe the proving of the single-phase and multiphase flow loops. Details of the test facility proving are given in Matzain (1996), Lund (1998), Apte (1999) and Matzain (1999).

Confirmation of Operability and Procedures

Single-Phase Flow Loop

Proving of the single-phase flow loop was accomplished as follows.

The instruments used (flow meters, pressure and temperature sensors) were factory calibrated before being installed in the flow loop. Control charts were generated showing the stability of operating conditions, possible measurement fluctuations and any start-up issues. Control charts for flow rates of the test fluid and the glycol-water mixture, inlet temperatures and temperature profiles were constructed.

Fluctuations in the oil flow rate were less than ± 1%, with or without control by the DAQ system. Although, the glycol-water mixture flow rate was less stable than the oil flow rate, its stability was adequate, and the average fluctuations of the glycol flow rate after the flow stabilized after a few hours were about ± 1%. After the first three tests, the oil and glycol inlet temperatures were maintained stable within ±0.1 F.

The final measured wax thickness was compared with the estimated wax thickness from two independent methods, the pressure drop method and the energy balance method.

Multiphase Flow Loop

Proving of the high-pressure multiphase flow loop was accomplished as follows.

The instruments used in this flow loop were factory calibrated before being installed in the flow loop. Control charts showing the stability of operating conditions, possible measurement fluctuations and any start-up issues were generated during every test. Control charts for flow rates of the test fluids (oil and gas) and the glycol-water mixture, inlet temperatures and temperature profiles were constructed. The variations observed in parameters such as oil and gas superficial velocities, glycol flow rate and the inlet temperatures were listed in Apte (1999).

Several 24-hour long single-phase wax deposition tests were conducted in the high-pressure multiphase facility to compare with results from similar tests conducted using the single-phase flow loop.

The multiphase flow wax deposition tests were preceded by a series of non-depositional tests to identify the flow patterns for selected oil and gas flow rate combinations. These flow patterns were detected using the densitometer signal. For horizontal and two-phase tests, the flow patterns detected were verified against the Taitel-Dukler (1976) flow-pattern prediction model, using FLOPAT subroutines developed at TUFFP. Similarly, for vertical flow, flow patterns detected were verified against the Taitel-Barnea-Dukler (1980) flow pattern prediction model in TUFFP. The oil and gas flow rates for multiphase

flow wax deposition tests were then selected based on this information, so that the test points were not close to a flow pattern transition boundary.

Effect of Wax Depletion on Observations

The single-phase wax deposition tests were carried out in a system with a small volume of test fluids. Therefore, depletion of wax in the system during a test was a concern. The depletion was studied by several methods.

The WAT depends on the composition and as the heavy components are depleted, WAT decreases. WAT was measured using Cross Polar Microscopy (CPM) by MSI for oil samples taken before and after selected tests (Test #14 and Test #21). For Test #14, a turbulent flow test, and for test #21, a laminar flow test, the change in WAT was about 3 F. This is of the same order as the accuracy of the CPM. Therefore, the depletion caused only a minimal change in the WAT.

HTGC compositional analysis results for the oil samples taken before and after Test #2, a 140-hour long test, are shown in Lund (1998) Figure 4.41. This also includes the compositional analysis results of the deposit sample from this test. The HTGC tests did not show any signs of depletion.

The MSI/Conoco paraffin deposition program was modified by MSI for Chevron to model closed loop systems. Lund presented the results of this model for both turbulent and laminar flow tests, with different fluid volumes in the closed loop. The model predicted a small, but noticeable depletion when 10 bbl, the volume used in single-phase tests, of fluid volume is used for a 24-hour test. The depletion is negligible when the fluid volume was 40 bbl. However, Lund stated that when the accuracy of the deposit thickness calculation methods is considered, the depletion would not affect the experimentally measured deposit thickness.

Pressure and Temperature Measurements

Pressure, differential pressure and temperature measurements in the single and multiphase flow loops were obtained using Rosemount pressure and differential pressure transducers and thermocouples for oil temperatures and RTDs for glycol temperatures. Pressure probes were protruded into the oil, thereby keeping them from becoming blocked with wax. The transducers were factory calibrated, and the ranges and accuracy of each instrument were listed. Measurements were smoothed after data acquisition. Smoothing provides a first order digital filter to reduce noise from the incoming signal. The smoothing process calculates the output by adding part of the previous output and part of the new input.

Flow Rate Stability and Pressure-Temperature Stability

Single-Phase Flow Loop

Operating control charts showing the variation of test fluid and glycol-water mixture flow rates, inlet temperatures and temperature profiles were developed for tests conducted. Selected charts for the single-phase loop tests were shown in Lund (1988). For most of the tests, the oil flow rate was manually controlled, and the DAQ system controlled this for Tests 5 and 6. The oil flow rate could be adequately controlled with or without the DAQ computer.

For the laminar tests conducted in the single-phase flow loop, the temperature readings were somewhat inconsistent, especially around the bend of the loop. The temperature in the bend would read higher than the readings upstream from the bend. After the testing was completed, Kaminsky (1998) suggested a possible explanation for the curious temperature readings in laminar flow. As the test fluid is heated in the heat trimmer, a concave radial temperature profile is developed in which the test fluid is warmest at the wall and coolest in the center of the pipe. Only the test fluid at the wall is rapidly cooled down after the oil enters the jacketed section. The temperature probes are located in the center of the pipe, missing the actual maximum temperature in the pipe. This temperature profile is skewed toward the outer wall at the bend. Since the thermal conductivity of the test fluid is low, this profile could possibly exist even at the outlet of the test section for laminar flow tests. Additional explanation of this hypothesis is given in Lund (1998).

The glycol-water mixture flow rate in the annulus was more difficult to control. This flow rate was controlled by the manual adjustment of a bypass valve. The pump vibrations caused the bypass valve to drift and sometimes jump, resulting in changes in the mixture flow rate. The flow rate tended to stabilize itself after several hours of drifting. This problem was not solved. An alarm would sound whenever the flow rate drifted out of the acceptable range, and it was then manually adjusted. Although the glycol-water mixture flow rate was less stable than the oil flow rate, the flow rate stability was adequate. The average fluctuation of the glycol flow rate is now about ±1%.

The oil and glycol-water mixture inlet temperatures were controlled only by the use of heat exchangers for the first three tests. The inlet temperature control improved dramatically after the third test. The reason for this dramatic improvement was the computer control of the heat trimmers. This allowed the inlet temperatures to be maintained stable to within ±0.056ºC (±0.1ºF).

Multiphase Flow Loop

For multiphase flow loop operations, operating control charts and histories were constructed to assess the stability of operating conditions, to identify possible measurement fluctuations and start-up issues. These charts are for the oil superficial or oil velocity, gas superficial velocity, glycol-water mixture flow rate, oil or oil-gas mixture and glycol-water mixture inlet temperatures, oil or oil-gas mixture and glycol-water mixture temperatures at various locations in the test section, differential pressure across the test section, and pressure and liquid height fraction in the test section. These charts are provided by Matzain (1999) in Appendix A for all of the 24-hr tests. Events and operational problems, if any, are noted in these charts.

Overall flow rate control performances were excellent, especially at high oil and gas superficial velocities. At low gas superficial velocity, especially below 0.305 m/s (1.0 ft/s), flow control variations within ±0.091 m/s (±0.3 ft/s) could be achieved. However, in some cases e.g. Test 4MR, flow control at 0.305 m/s (1.0 ft/s) gas superficial velocity was good, i.e., within ±0.030 m/s (±0.1ft/s). Oil flow rate control was excellent, even at low oil superficial velocity. Inlet temperature controls were excellent in most test cases except for low superficial velocity tests. Control performances of up to ±0.11 C (±0.2 F) can be achieved in most cases, except for low superficial velocity tests. Variations of ±3.18 m3/day (±20 BPD) in the glycol flow rate were observed in most tests.

In all multiphase tests, a "saw tooth" pressure response appearance resulted from a gas leak in the Knight compressor and addition of natural gas to the system at regular intervals during each test to maintain the system pressure. The liquid level in the separator continued to increase during the high oil and gas flow rate tests. A long duration test, especially at high oil and gas flow rates, can not be run until

a solution to the problem is obtained. The temperature probe T52, which is located in the removable spool piece, may have been damaged during spool piece removal and/or installation operations.

The rises and dips in flow rates, temperatures, differential pressures and liquid height fraction at different times throughout each test were due to stopping and/or interrupting the flow to the test section for a 15-20-min duration during LD-LD and/or single-phase temperature and differential pressure measurements. No abrupt change in the oil/gas mixture temperature profile was observed when single-phase oil flow was introduced at 6-hr intervals or after conducting the LD-LD measurements in all tests, except for Test 19M (a laminar single-phase flow test). It was postulated that the accumulated wax was removed when the LD-LD measurements were performed in Test 19M. An increase in the oil/gas mixture temperatures with time was observed in all tests, which corresponds to the insulation effect of the wax deposited in the test pipe.

Verification Test Procedure

Single-Phase Flow Loop

The operating procedure can affect the results of the tests. Therefore, it is important to understand how the tests were conducted to understand the possible impact of the start-up procedure on the data collected. The difficult part of operating these tests was to start the tests properly. Following the start-up procedure, the remaining operating procedure was the same for most of the tests.

Most of the tests were started after melting the deposit off the pipe wall from the previous test. The deposit was melted by flowing the test fluid in the inner pipe and the glycol-water mixture in the jacket, with both fluids approximately 17ºC (30ºF) above the WAT. The entire system was flowed at this temperature for at least 12 hours to ensure that the pipe wall was clean and that all the wax was re-dissolved into the oil. The temperature of the glycol-water mixture and the test fluid was then lowered to just above the WAT of the test fluid.

Cooling down the test fluid to the desired temperature required it to be pumped through the test section, and wax deposition during this start up period needed to be minimized. During this stage the test fluid was flowed at a high flow rate, for which the deposition rate was low. The higher flow rate also increased the heat transfer, which decreased the time it took to cool the test fluid to the desired temperature. The test fluid flow rate was then adjusted to the desired flow rate as the oil inlet temperature approached the desired temperature.

After the fluids had cooled down, the system was stabilized using both manual and computer-controlled valves, as well as the heat trimmers. After stabilization, the computer kept the system stable with the help of occasional manual adjustments. At the end of each test, the system was turned off in preparation for removing the two spool pieces. Pressurized nitrogen was used to push the test fluid out of the test section and back into the test fluid tanks. The test section was then closed off from the rest of the system and depressurized. The two spool pieces were removed from the test section after the system was depressurized. The deposit thickness in the spool pieces was then measured using the LD-LD device, which uses liquid displacement to measure deposit thickness. Deposit samples were scraped off the pipe wall adjacent to the spool pieces before the spool pieces were reinstalled in the test section.

This start-up procedure will create some deposits before the test conditions are reached, but this deposit thickness can be calculated and modeled. There are two additional problems with the single-phase flow loop start-up procedure that were identified and discussed in Lund (1998).

Multiphase Flow Loop

For the multiphase flow loop, the general operating stages followed during a typical paraffin deposition test are discussed in Matzain (1999). A typical test begins by first melting wax in the flow loop from the previous test for at least 6-8 hrs to ensure that the pipe wall was clean and that all the wax has re-dissolved into the oil.

The gas and oil systems were started, and were circulated, bypassing the test section, especially if the oil requires some cooling to reach the test temperature. This avoids any deposition in the test section before a test starts. The primary cold glycol mixture was simultaneously cooled down and circulated, bypassing the test section, at the desired flow rate. When the desired oil, gas and glycol temperatures were reached, the oil and gas mixture and the glycol were directed into the test section. The necessary inlet flow rates for the oil and gas phases and glycol were then achieved using the control valves. Deposition begins as soon as the wall temperature falls below the cloud point.

The heat tracing circuits were turned on and were automatically set to control the pipe wall temperature above the bulk oil temperature. The heat trimmers for both the glycol and the gas-oil mixture were turned on and were put on automatic mode to regulate the inlet temperatures. The desired oil inlet temperature was maintained using the heater and the hot glycol system. The desired gas inlet temperature was maintained by controlling the temperature at the discharge of the Knight KO2 compressor. The inlet temperatures of the two-phase mixture and glycol were tuned with the impedance heating temperature-trimming systems. For tests involving low flow of oil, only the impedance heater was used as a heat source and the hot glycol system was not used. There were no special issues associated with the shutdown which cause any additional wax deposition. The gas used to displace oil in the test section was slowly injected so as not to strip the wax deposit in the test section. The gas in the test section was then flared. The spool piece was then removed and wax deposit observations were made and samples were taken.

Sample Analyses

Single-Phase Tests

During single-phase testing, many test fluid samples were taken for analysis. Samples were taken from the test section before each test started, during the tests, and at the end of each test. Multiphase Solutions Inc. (MSI) measured the WAT using Cross-Polar Microscopy (CPM). Chevron Petroleum Technology Company (CPTC) performed compositional analyses on samples taken before and after tests using High Temperature Gas Chromatography (HTGC).

After each test was completed, the two spool pieces were taken out of the test section. Samples of the deposit were then scraped off the pipe wall adjacent to the spool pieces. The deposit thickness in each of the spool pieces was measured twice using the LD-LD device. The deposit was washed with Methyl Ethyl Ketone (MEK) between the two measurements to wash off any excess oil remaining on the deposit (Leitko (1997)). After the second measurement, another deposit sample was taken from each of the spool pieces. All the deposit samples were sent to CPTC for HTGC analyses to determine the trapped oil content of the deposit.

Multiphase Tests

For the multiphase flow tests, crude oil compositions were determined from a fluid characterization and property evaluation study by Marathon Oil Company (JIP Technical Report, 1999a). The purpose of the fluid characterization and property evaluation study was to provide fluid property data on hydrocarbon fluids used in the single-phase and multiphase flow deposition tests. The crude oil with a wax appearance temperature of 51.0 C (124 F) measured by Fourier Transform Infrared Spectroscopy at 34.5 MPa (5000 psig) contains approximately 6.6% by weight of C17 to C80 fractions n-paraffin components in the original stock tank oil (JIP Technical Report, 1999a).

The quantitative weight percent of n-paraffin carbon number distribution in the original stock tank oil as well as in separator oil flashed at standard conditions, 1 atm (14.7 psia), and 293 K (68.0 F) were obtained. Flash calculations were performed by MSI. Natural gas compositions for Oklahoma Natural Gas were determined by Southwest Laboratory of Oklahoma (1999). The natural gas contains approximately 94.0% by weight of methane.

After each test, the spool piece was removed and wax deposit observations were made and samples were taken. Collected wax samples during the test duration were sent to Chevron Petroleum Technology Company for compositional analyses using High Temperature Gas Chromatography (HTGC). The analyses also provide information on the percentage of oil trapped in the wax deposit. The percent oil in the deposits was estimated as the ratio of C19-C70+ area to total area in the deposit divided by the ratio of C19-C70+ area to total area from the original oil.

Techniques of Wax Thickness Measurement

A main objective of this experimental study was to measure kinetic or time-dependent wax deposit thickness values for the proposed test conditions. These data could then be used to develop or improve wax deposition prediction models.

A Liquid Displacement-Level Detection (LD-LD) technique was implemented in the multiphase flow loop. It can give accurate measurement of wax thickness without changing the system pressure and temperature. In single-phase tests, the LD-LD measurements were obtained with a spool piece, which was removed from the test section after each test. In the absence of any reliable device that could make continuous wax thickness measurements during a test without interference, estimates of wax thickness were made using methods based on pressure drop and heat transfer in the test section. The wax deposit thickness was also estimated during several single-phase tests using an ultrasonic sensor designed and constructed by Norsk Hydro and Christian Michelson Research (CMR). Visual observations and manual measurements were obtained at the end of both single-phase and multiphase tests by use of spool pieces. For detailed descriptions of these deposit measurement techniques, please refer to Appendix A.

Error Analysis of Wax Thickness Measurement

In Lund's (1998) M.S. thesis, an error analysis was performed for the single-phase tests to determine how sensitive the different deposit thickness measurement methods are to errors in the data. For the LD-LD method, an error of ±7.62 mm H_2O (±0.3 in.) in the differential pressure measurements to determine fluid height would give an error of ±0.1 mm (±0.0039 in.) in the deposit thickness for the spool piece studied. For the pressure drop method, no problem was encountered with the turbulent case when the entire loop (50-m long) was used to measure pressure drop. As shown in Table 1 of Appendix B, for a typical turbulent flow, an error of ±254 mm H_2O (±10 in.) in pressure drop only produces a ±0.13 mm

(±0.0051 in.) error in the computed thickness. However, for the laminar flow case, an error of only ±5.08 mm H_2O (±0.2 in.) in pressure drop causes a 0.17 mm (0.0067 in.) error in the deposit thickness calculated from the pressure drop data. The problem in laminar cases is even more acute if the 5-m (16.4 ft) long test sections are used to determine thickness. For the heat transfer method, the laminar flow case is relatively insensitive to temperature measurement errors. An error of ± 0.1 °C (0.18 °F) gave an error of about ±0.3 mm (±0.012 in.) in the deposit thickness. The turbulent case indicated that an error of ±0.01 °C (±0.018 °F) gave an error in calculated deposit thickness of about ±0.1 mm (±0.0039 in.). This implies that the measurement accuracy would need to be on the order of ±0.011 °C (±0.02 °F) to obtain the desired precision, a value not attainable with the instruments used.

Error analyses were also conducted for the LD-LD, pressure drop and heat transfer methods used to measure the thickness of the wax deposit in the multiphase flow tests. The results show that the LD-LD method gave the most reliable measurement. When the largest differential pressure (corresponding to full pipe liquid displacement) is used, the error in the wax thickness is only ±0.015 mm. The pressure drop method can give accurate measurement at high flow rates, but is not applicable for low flow rate situations. On the other hand, the heat transfer method is only applicable when the flow rate is low and the difference between the inlet and outlet oil temperatures is sufficiently large. The uncertainty of the thermal conductivity of the wax deposit may cause significant error when using the heat transfer method. For details of the error analysis of wax thickness measurement methods, please refer to Appendix B.

Flow Pattern Verification

Flow pattern maps of the two-phase mixture flowing in the 52.5-mm (2.067 in.) ID test section pipe were initially generated using the FLOPAT computer library. These flow pattern maps were used as guidelines when formulating the test matrix for the wax deposition tests. A series of dedicated flow pattern tests were conducted in the present study to verify and assess the applicability of the flow pattern maps generated by the FLOPAT computer library. The flow pattern tests identified the regions around the transition boundaries, thus ensuring that the selected wax deposition tests are not close to transition regions.

Multiphase Heat Transfer

The wax deposition scenario has been described as a non-isothermal flowing system that appears to be driven by heat flux. Consequently, the success in predicting wax deposition rates in single-phase and multiphase flow environments depends on how well heat transfer characteristics are evaluated. These include the forced convective film heat transfer coefficient, bulk and wall temperatures and local heat flux across the pipe wall. Heat transfer measurements during two-phase flow were obtained from a series of dedicated heat transfer tests. The purpose of the heat transfer tests was to assess the applicability of several two-phase flow convective film heat transfer coefficient correlations.

Section 9
Test Results

Test Matrices

Single-Phase Tests

Using existing theoretical expressions for wax deposition, a test matrix was developed to study the effects of the most important variables affecting paraffin deposition. The first two variables can be identified from the molecular diffusion equation given in Equation 9.1.

$$\frac{dm_w}{dt} = -\rho_o D_{ow} A_i \frac{dC_w}{dr} = -\rho_o D_{ow} A_i \left(\frac{dC_w}{dT}\right)\left(\frac{dT}{dr}\right) \quad \text{.....(9.1)}$$

Equation 9.1 shows that the deposition rate should be proportional to the radial temperature gradient, dT/dr. Controlling the difference between the test fluid inlet temperature and the glycol-water mixture inlet temperature into the annulus determines the radial temperature gradient. Thus, the difference between the test fluid and glycol-water mixture inlet temperatures was chosen as a variable to study. Since both the diffusion coefficient, D_m, and the dissolved wax concentration, dC_w/dT, are functions of the test fluid temperature, the effect of test fluid inlet temperature was also chosen as a variable to be studied.

The test fluid flow rate in the pipe is expected to affect the deposit in several ways. Increasing the flow rate will increase the shear rate at the wall, where the wax deposits. This will change the nature of the deposit according to rotating disk experiments presented by Eaton and Weeter (1976). Increasing the shear rate could also cause sloughing or removal of deposited wax from the wall. This has been reported from small tube deposition experiments by both Weingarten and Euchner (1988) and by Creek and Hobson (1996). By changing the flow rate, one can also change the flow regime between laminar and turbulent flow. Increasing the shear rate has been reported to decrease the deposition rate (Brown *et al.*, 1993). Changing the flow regime will change the heat transfer from the oil to the wall, the radial temperature gradient, and the shear rate, as well as other phenomena. Since flow rate has many effects on the deposition, it was chosen as a variable to study the effects of flow regime and velocity on paraffin deposition.

Eaton and Weeter (1976) reported that the deposit characteristics change with time. One of the anticipated changes was an increase in the concentration of wax crystals and a decrease in the concentration of trapped oil in the deposit, leading to a hardening of the deposit with time. The duration of the tests was varied by running identical test conditions for different time durations. Deposit samples taken at the conclusion of each test can then be analyzed to give the change of wax concentration with time.

Although many investigators (*e.g.* Brown *et al.*, 1993, and Mendes and Braga, 1996) consider deposition by shear dispersion to be insignificant relative to the molecular diffusion deposition rate, it was decided to verify these observations in this study. Verification tests were designed for zero and even negative heat flux. The deposition rate due to molecular diffusion equals zero when the oil and glycol-water mixture temperatures are the same. Thus, these conditions leave shear dispersion as the only possible deposition mechanism.

The resulting test matrix consists of five "phases," each of which is designed to investigate the effect of one variable or phenomenon. The resulting testing matrix for single-phase flow is given in Tables 9.1 through 9.6:

Test #	Q_o m^3/s (BPD)	T_{oin} °C (°F)	$DT = T_{oin} - T_{gin}$ °C (°F)	Duration hours
2, 2R	0.00028 (150)	51.7 (125)	8.3 (15)	24
1	0.00028 (150)	51.7 (125)	16.7 (30)	24
7, 7R	0.00028 (150)	51.7 (125)	25 (45)	24

Table 9.1 - Phase 1: Effect of DT in Laminar Flow

Test #	Qo m3/s (BPD)	Toin °C (°F)	DT = Toin – Tgin °C (°F)	Duration hours
8	0.0028 (1500)	40.6 (105)	8.3 (15)	24
12	0.0028 (1500)	40.6 (105)	16.7 (30)	24
14, 14R	0.0028 (1500)	40.6 (105)	25.0 (45)	24

Table 9.2 - Phase 1: Effect of DT in Turbulent Flow

Test #	Qo m3/s (BPD)	Toin °C (°F)	DT = Toin – Tgin °C (°F)	Duration hours
2, 2R	0.00028 (150)	51.7 (125)	8.3 (15)	24
4	0.00028 (150)	40.6 (105)	8.3 (15)	24
10, 10R	0.00028 (150)	29.4 (85)	8.3 (15)	24

Table 9.3 - Phase 2: Effect of Initial Oil Temperature

Test #	Qo m3/s (BPD)	Toin °C (°F)	DT = Toin – Tgin °C (°F)	Duration hours
9	9.20E-05 (50)	40.6 (105)	8.3 (15)	24
4	0.00028 (150)	40.6 (105)	8.3 (15)	24
18	0.000920 (500)	40.6 (105)	8.3 (15)	24
17, 17R, 17RR	0.00184 (1000)	40.6 (105)	8.3 (15)	24
8	0.0028 (1500)	40.6 (105)	8.3 (15)	24
6	0.00368 (2000)	40.6 (105)	8.3 (15)	24

Table 9.4 - Phase 3: Effect of Flow Regime and Flow Rate (Velocity) on Deposition

Test #	Qo m3/s (BPD)	Toin ºC (ºF)	DT = Toin – Tgin ºC (ºF)	Duration hours
4	0.00028 (150)	40.6 (105)	8.3 (15)	24
5	0.00028 (150)	40.6 (105)	8.3 (15)	60
11	0.00028 (150)	40.6 (105)	8.3 (15)	120
8	0.0028 (1500)	40.6 (105)	8.3 (15)	24
3R	0.0028 (1500)	40.6 (105)	8.3 (15)	120
3	0.0028 (1500)	40.6 (105)	8.3 (15)	140

Table 9.5 - Phase 4: Effect of Aging

Test #	Qo m3/s (BPD)	Toin ºC (ºF)	DT = Toin – Tgin ºC (ºF)	Duration hours
15, 15R	**0.00028 (150)**	**26.7 (80)**	**0**	**24**
20	**0.00028 (150)**	**26.7 (80)**	**-2.8 (-5)**	**24**
19	**0.00028 (150)**	**40.6 (105)**	**0**	**24**
16	**0.0028 (1500)**	**26.7 (80)**	**0**	**24**

Table 9.6 - Phase 5: Viability of Shear Dispersion Deposition as a Mechanism

We should be able to determine a relationship for the diffusion coefficient from the first three phases to allow paraffin deposition thickness predictions. Phases one, three and four should provide some qualitative information about the hardness and wax concentration to expect in a paraffin deposit. These phases should also make it possible to determine estimates of the wax concentration in paraffin deposits. Phase 5 will determine if paraffin deposition can occur when the pipe wall is not colder than the oil. If deposition occurs in Phase 5, it should be a result of shear dispersion.

Multiphase Tests

The test matrices for the wax deposition tests with the multiphase flow loop are given in Tables 9.7 to 9.9. The test conditions involved flowing natural gas and South Pelto crude oil in the test section at horizontal (0°), inclined upward (2°), and vertical (90°) positions for up to 24 hrs. The test conditions utilized one inlet mixture temperature; 40.56 °C (105 °F), and one inlet glycol temperature; 15.56 °C (60 °F). A total of 23 tests were conducted. The tests covered a wide range of operating conditions with oil superficial velocities ranging from 0.061 m/s (0.2 ft/s) to 1.829 m/s (6 ft/s), and gas superficial velocity ranging from 0.152 m/s (0.5 ft/s) to 9.144 m/s (30 ft/s). The glycol-water mixture flow rate was maintained at 317.78 m^3/day (2000 BPD) in all tests. The tests covered a wide range of the flow patterns often encountered in multiphase pipelines and wellbores.

Table 9.7 - Test Matrix for Horizontal Flow

Tag	v_{sl}, m/s (ft/s)	v_{sg}, m/s (ft/s)	Flow Pattern	Wax Thickness Calculation Methods
TEST1M	1.31 (4.3)	0	SGL(Dead)	SP/HT/PD/LD
TEST2M	1.22 (4.0)	0	SGL	SP/HT/PD
TEST5M	0.061 (0.2)	0	SGL	HT/SP
TEST6M	0.061 (0.2)	0.305 (1)	SS	SP
TEST10M	0.061 (0.2)	2.134 (7)	SW	SP
TEST7M	0.061 (0.2)	9.144 (30)	ANN	SP/LD
TEST7MRS	0.061 (0.2)	9.144 (30)	ANN	LD
TEST3M	1.219 (4)	0	SGL	SP/PD/HT/LD
TEST4M	1.219 (4)	0.305 (1)	ITMI	SP
TEST4MR	1.219 (4)	0.305 (1)	ITMI	SP/LD/1P
TEST4MRS	1.219 (4)	0.305 (1)	ITMI	LD
TEST9M	1.219 (4)	1.524 (5)	ITMI	SP/LD/1P
TEST9MRS	1.219 (4)	1.524 (5)	ITMI	LD
TEST12MR	1.219 (4)	4.572 (15)	ITMI	SP/LD/1P
TEST12M	1.219 (4)	4.572 (15)	ITMI	SP/LD/1P
TEST12MRS	1.219 (4)	4.572 (15)	ITMI	LD

Note:

1. Test duration is 24 hrs for most tests, except for tests where tag name ends with RS. Tests where tag name ends with RS are 8-hr or 12-hr tests.

2. All tests, except TEST2M, are conducted at an inlet mixture temperature of 40.56 °C (105 °F), and at an inlet glycol temperature of 15.56 °C (60 °F).

3. TEST 2M was conducted at an inlet mixture temperature of 40.56 °C (105 °F), and at an inlet glycol temperature of 32.22 °C (90 °F).

Nomenclature:

SGL	Single-Phase Oil
ITMI	Intermittent
SW	Stratified Wavy
ANN	Annular
SS	Stratified Smooth
PD	Single-Phase Pressure Drop Method – 7-m Test Section
HT	Single-Phase Heat Transfer Method – 7-m Test Section
SP	Volumetric Method - Spool Piece
LD	LD-LD – 7-m Test Section
1P	Single - Phase PD/HT Methods

Table 9.8 - Test Matrix for Vertical Flow

Tag	v_{sl}, m/s (ft/s)	v_{sg}, m/s (ft/s)	Flow Pattern	Wax Thickness Calculation Methods
TEST19M	0.152 (0.5)	0	SGL	SP/LD
TEST16M	0.152 (0.5)	0.305 (1)	ITMI	SP/LD
TEST15M	0.152 (0.5)	1.219 (4)	ITMI	SP/LD
TEST8M	0.152 (0.5)	6.096 (20)	ANN	SP/LD
TEST22M	0.305 (1)	0	SGL	SP//LD
TEST23M	0.609 (2)	0.914 (3)	ITMI	SP/LD
TEST20M	1.219 (4)	0	SGL	SP//LD
TEST18M	1.219 (4)	0.152 (0.5)	BBLY	SP/LD
TEST17M	1.219 (4)	9.144 (30)	ANN	SP/LD
TEST21M	1.829 (6)	0	SGL	SP/LD

Note:

1. Test duration is 24 hrs for all tests.
2. All tests are conducted at an inlet mixture temperature of 40.56 °C (105 °F), and an inlet glycol temperature of 15.56 °C (60 °F).

Nomenclature:

SGL	Single-Phase Oil
ITMI	Intermittent
ANN	Annular
BBLY	Bubbly
DP	Single-Phase Differential Pressure Method – 7-m Test Section
TT	Single-Phase Temperature Method – 7-m Test Section
SP	Volumetric Method - Spool Piece
LD	LD-LD – 7-m Test Section

Table 9.9 - Test Matrix for Upward Flow

Tag	v_{sl}, m/s (ft/s)	v_{sg}, m/s (ft/s)	Flow Pattern	Wax Thickness Calculation Methods
TEST11M	0.305(1)	0	SGL	SP/PD/HT/LD
TEST13M	0.305(1)	1.219 (4)	ITMI	SP/LD/1P
TEST13MRS	0.305(1)	1.219 (4)	ITMI	LD
TEST14M	0.305(1)	9.144 (30)	ANN	SP/LD/1P
TEST14MRS	0.305(1)	9.144 (30)	ANN	LD

Note:

1. Test duration is 24 hrs for most tests, except for tests where tag name ends with RS. Tests where tag name ends with RS are 8-hr or 12-hr tests.

2. All tests are conducted at an inlet mixture temperature of 40.56 °C (105 °F), and an inlet glycol temperature of 15.56 °C (60 °F).

Nomenclature:

SGL	Single-Phase Oil
ITMI	Intermittent
ANN	Annular
PD	Single-Phase Pressure Drop Method – 7-m Test Section
HT	Single-Phase Heat Transfer Method – 7-m Test Section
SP	Volumetric Method - Spool Piece
LD	LD-LD – 7-m Test Section
1P	Single - Phase PD/HT Methods

Test Data

The single-phase and multiphase test data are all included in the attached CDs. Detailed descriptions of the test results can also be found in Lund's (1998) and Apte's (1999) theses and Matzain's (1999) dissertation.

Confirmation of Known Effects

Several investigators, e.g., Bern *et al.* (1980), Brown *et al.* (1993), and Burger *et al.* (1981) have suggested that molecular diffusion is the primary paraffin deposition mechanism in single-phase flow. The classical Fick's mass diffusion law in Eq. 9.1 describes the rate of transport of dissolved paraffin through the molecular diffusion mechanism, where the radial concentration gradient is expressed in terms of a temperature concentration gradient and a radial temperature gradient. The diffusion coefficient D_m is often expressed either as an experimental constant divided by the viscosity or by empirical correlations developed for normal paraffins by Wilke and Chang (1955) or Hayduk and Minhas (1982).

According to Eq. 9.1, wax deposition rate increases with an increase of the radial temperature gradient, dT/dr. This was confirmed in the tests with different temperature differences between the oil inlet temperature and the glycol inlet temperature. Figures 9.1 and 9.2 show the overall deposit thickness after approximately 24 hours versus temperature difference. The heat transfer and the pressure drop methods were used to measure the deposit thickness. In both laminar and turbulent flow regimes, the deposit thickness increases with an increase of the temperature difference.

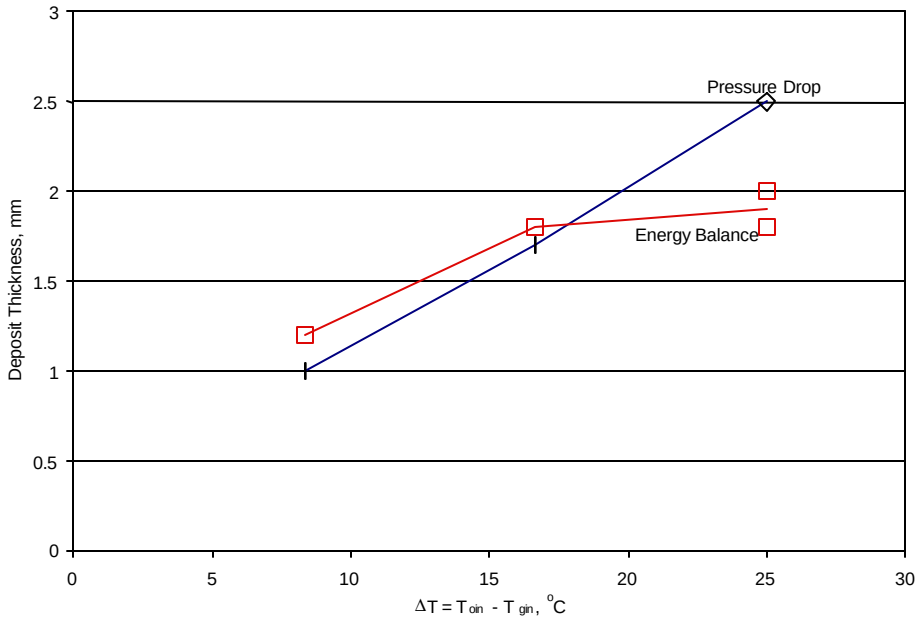

Figure 9.1 – Final Deposit Thickness Versus DT for Laminar Flow

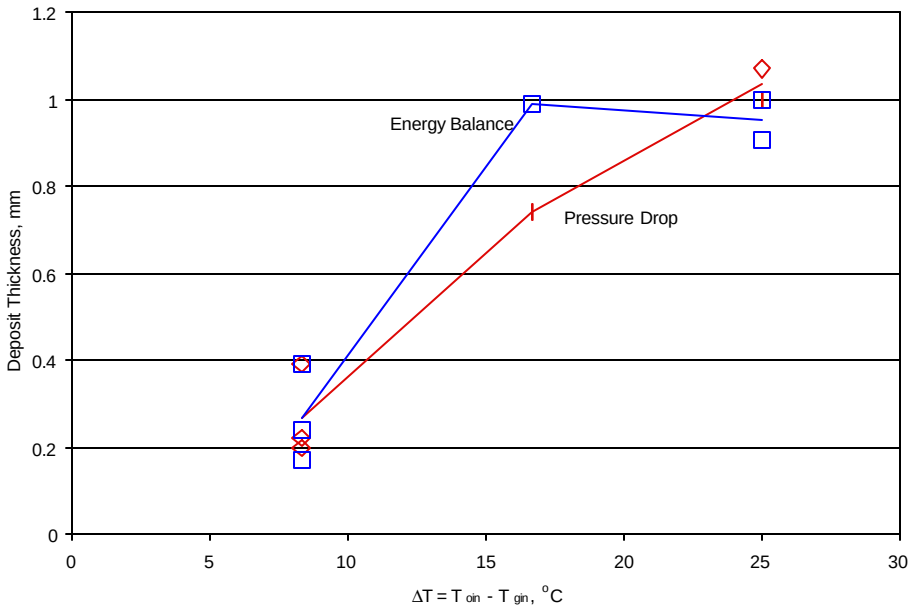

Figure 9.2 – Final Deposit Thickness Versus DT for Turbulent Flow

The oil temperature affects the deposition rate in two ways, according to the molecular diffusion equation (Eq. 9.1). The dC_w/dT term increases with decreasing oil temperature, and this causes an increase in the deposition rate. The molecular diffusion coefficient is believed to be a function of the inverse of the oil viscosity. An increase in the oil viscosity will therefore decrease the deposition rate. Theoretically, the two effects of the temperature should cause a maximum deposition rate at a certain oil temperature. This inference was also proved by the test results with different oil temperatures.

Wax deposition rate due to molecular diffusion should be zero if the radial temperature gradient is zero. Therefore, by setting the oil and glycol at the same temperature, the shear dispersion deposition mechanism was assessed in the single-phase study. There was no deposit observed during the turbulent test indicating that shear dispersion is not an important deposition mechanism.

Forsdyke (1995) suggested that the principal effects of multiphase flow on wax deposition would be those of composition and flow patterns. The presence of additional gas (light-ends) will make the crude more 'lively', and will reduce the WAT of the oil. This in turn will reduce the wax deposition rate. Flow patterns will govern the extent, duration and shear stress severity of the contact of the liquid phase with the pipe wall. This contact will affect the rate of heat transfer, which in turn will affect the temperature gradient and the rate of wax deposition. A higher flow rate will also increase the wall shear stress that might lead to the stripping of deposits away from the wall. These postulations were found to be in agreement with the multiphase test results.

Section 10
Discussion of Results

Single-phase paraffin deposition has been studied extensively with a 50-m (164 ft) long flow loop with a 43.6-mm (1.71 in.) internal diameter. Most of the tests were conducted with crude oil from Mobil Oil Co.'s South Pelto field and two tests were conducted with condensate from Shell Oil Co.'s Garden Banks field, both from the Gulf of Mexico. All the laminar flow tests and one low velocity condensate turbulent test produced soft deposits. The remaining tests produced hard deposits. The oil concentration in the deposits ranged from 20 to 90% and the deposit thermal conductivities ranged from the oil thermal conductivity to 6 times the oil thermal conductivity, depending on test conditions and duration.

Twenty-three multiphase tests at different oil and gas superficial velocities were conducted. The test conditions involved flowing the fluids at horizontal (0°), inclined upward (2°), and vertical (90°) positions for up to 24 hours, and utilized one inlet mixture temperature and one inlet glycol temperature. Wax deposition was found to be flow pattern dependent and occurs only along the pipe wall in contact with the waxy crude oil. An increase in mixture velocity results in harder deposits, but with a lower deposit thickness. The deposition buildup trend at low mixture velocities is similar to that observed in laminar single-phase flow tests. The buildup trend at high mixture velocities is similar to that observed in turbulent single-phase flow tests.

Single-Phase Results

The effect of flow regime on wax deposition is demonstrated clearly by the tests at different flow rates with the same difference between the oil and glycol inlet temperatures. Figure 10.1 shows that the deposit thickness decreases rapidly with increasing flow rate in laminar flow. After the flow becomes turbulent, the thickness is much less sensitive to an increase of flow rate. This is similar to the observation made by Bern at al. (1980). The effect of flow rate on the oil concentration in deposit is shown in Fig. 10.2. It appears that the oil concentration decreases with increasing flow rate. There seems to be a problem with the samples from Test #9 (the lowest flow rate), whose deposit exhibits an oil concentration similar to those of hard deposits.

The aging effect was studied by conducting tests of different time durations. Figure 10.3 shows the oil concentrations in deposits from turbulent tests (1500 BPD). Clearly, the oil concentration decreases with time. The wax deposit changed from "shoe polish" like wax after 24 hours, to a "candle" wax after 120/140 hours. In laminar tests, there was no change observed in the oil concentration for different time durations. All the deposits contained approximately 90% oil.

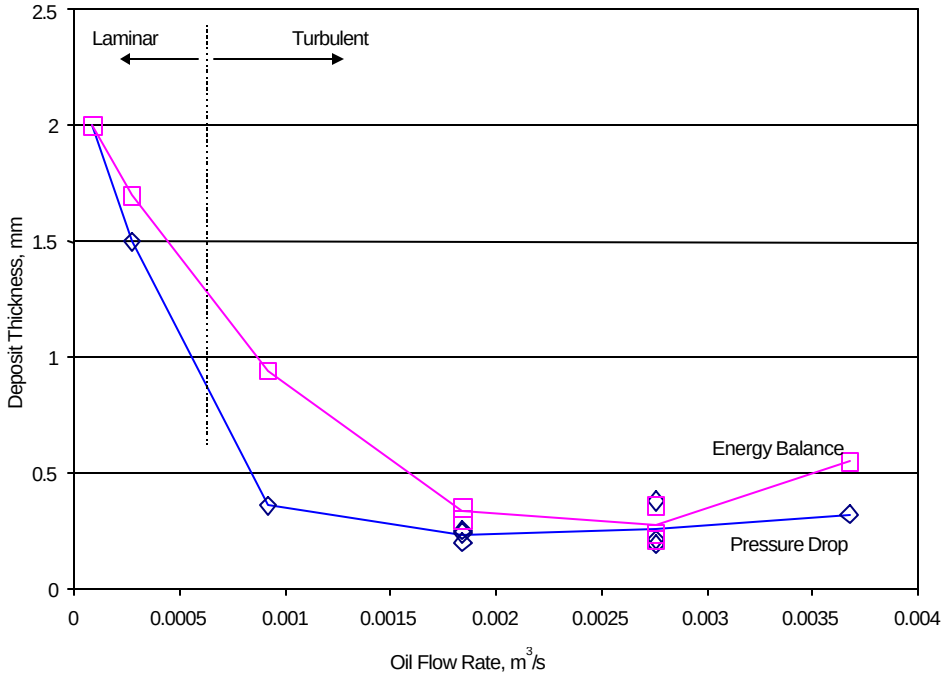

Figure 10.1 - Deposit Thickness Versus Flow Rate

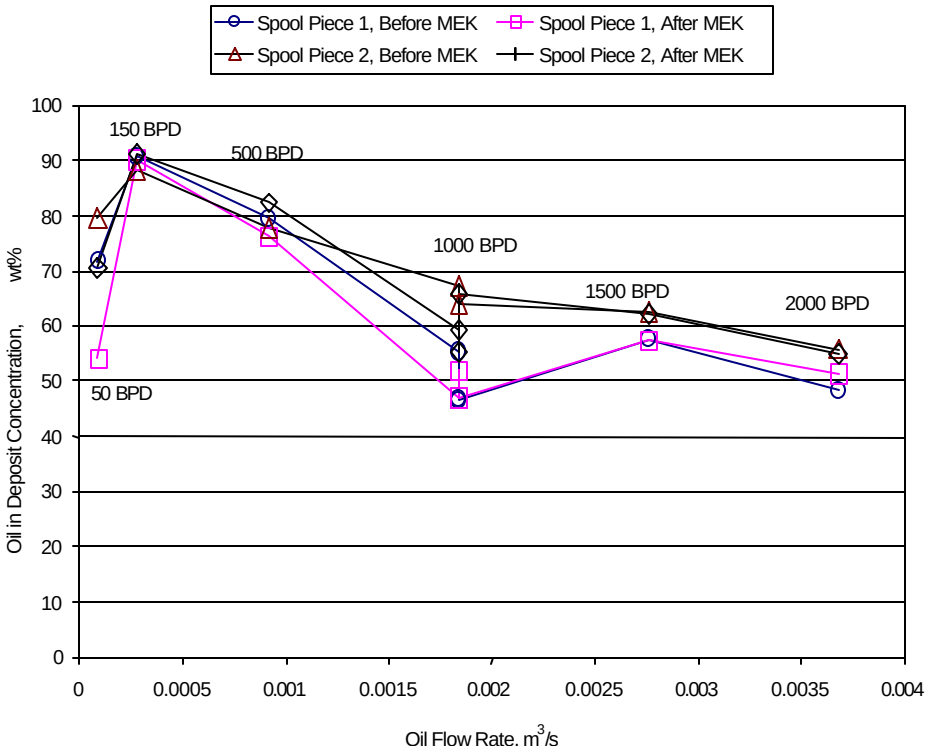

Figure 10.2 - Oil in Deposit Concentration Versus Flowrate

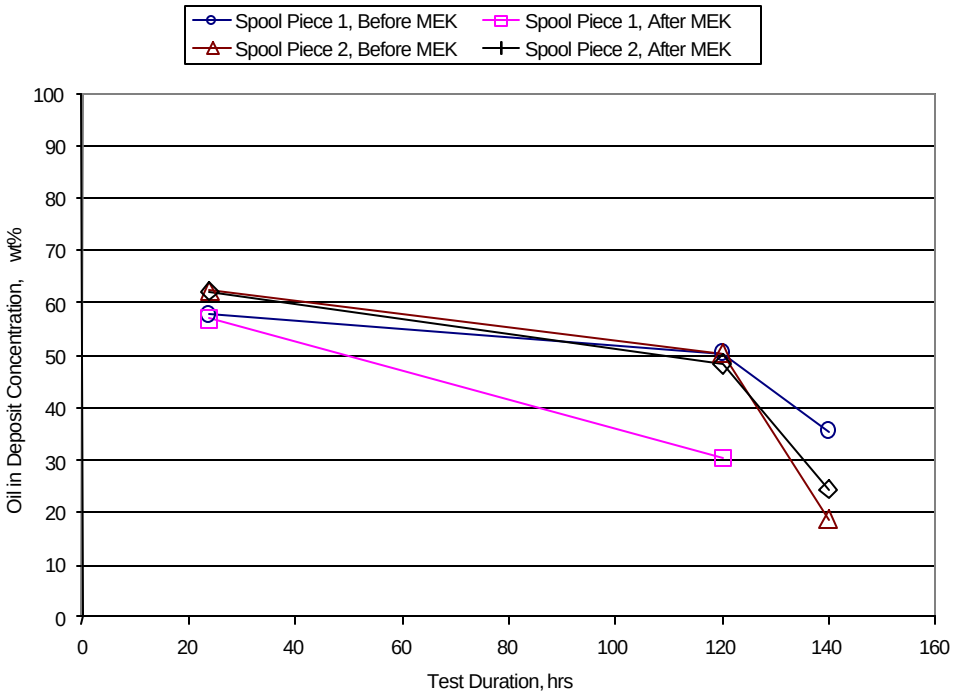

Figure 10.3 - Oil in Deposit Concentration Versus Test Duration

In order to extrapolate the data gathered using the South Pelto oil to other fluids, two tests were also conducted on a different fluid, Garden Bank condensate, at similar test conditions for both laminar and turbulent flow. While the South Pelto crude contains approximately 5% wax, the Garden Bank condensate contains only 0.5% wax (by weight). The WAT of the condensate is also lower than that of the South Pelto crude oil. The 24-hour tests showed about half the deposit thickness of the corresponding tests with the South Pelto crude. Soft deposits were observed even at high flow rate (turbulent).

Visual observation of the deposit was carried out at the end of each test using the spool pieces. The appearance of the wax deposit varied significantly, depending on the test conditions. Basically, it changes from gelled oil to candle wax as the flow changes from laminar to turbulent. The hard deposits were all fairly evenly distributed around the pipe circumference. The soft deposits, however, tend to be thicker at the top of the pipe.

Multiphase Results

Wax deposition rate and the deposit hardness (inversely proportional to oil content) depend on flow rates, flow pattern and pipe inclination. Tables 10.1 to 10.3 list the deposit thickness and the visual observations of the deposit hardness for each multiphase flow test (including some single-phase tests) after 24 hours. The wax thickness was measured by use of the LD-LD method. Besides the thickness difference at the end of the test, the deposit growing trend was also different at different test conditions (please see Matzain's dissertation, 1999).

Table 10.1 - Test Results for Horizontal Flow

Tag	v_{sl}, m/s (ft/s)	v_{sg}, m/s (ft/s)	Flow Pattern	Nature of Deposit	Wax Thickness LD-LD/ Volume (mm)	Oil in Deposit (%)
TEST3M	1.22 (4.0)	0	SGL	Hard	0.57/0.47	55.5
TEST5M	0.061 (0.2)	0	SGL	Soft	NM/NM	
TEST6M	0.061 (0.2)	0.305 (1)	SS	Soft	NM/NM	82.1
TEST10M	0.061 (0.2)	2.134 (7)	SW	Soft	NM/NM	80.8
TEST7M	0.061 (0.2)	9.144 (30)	ANN	Hard	1.42/1.83	62.0
TEST4M	1.219 (4)	0.305 (1)	ITMI	Hard	0.64/0.66	53.0
TEST9M	1.219 (4)	1.524 (5)	ITMI	Hard	0.49/0.77	56.5
TEST12M	1.219 (4)	4.572 (15)	ITMI	Hard	0.49/0.72	50.4

Table 10.2 - Test Results for Inclined Upward Flow

Tag	v_{sl}, m/s (ft/s)	v_{sg}, m/s (ft/s)	Flow Pattern	Nature of Deposit	Wax Thickness LD-LD/ Volume(mm)	Oil in Deposit (%)
TEST11M	0.305(1)	0	SGL	Soft	0.82/0.87	75.0
TEST13M	0.305(1)	1.219 (4)	ITMI	Hard	0.98/1.10	64.3
TEST14M	0.305(1)	9.144 (30)	ANN	Hard	0.66/0.93	55.3

Table 10.3 - Test Results for Vertical Flow

Tag	v_{sl}, m/s (ft/s)	v_{sg}, m/s (ft/s)	Flow Pattern	Nature of Deposit	Wax Thickness LD-LD/ Volume (mm)	Oil in Deposit (%)
TEST19M	0.152 (0.5)	0	SGL	Soft	0.31/0.38	
TEST16M	0.152 (0.5)	0.305 (1)	ITMI	Medium Hard	0.90/0.99	61.9
TEST15M	0.152 (0.5)	1.219 (4)	ITMI	Hard	0.93/1.02	51.1
TEST8M	0.152 (0.5)	6.096 (20)	ANN	Hard	0.72/0.88	44.2
TEST22M	0.305 (1)	0	SGL	Soft	0.82/0.92	79.0
TEST23M	0.609 (2)	0.914 (3)	ITMI	Hard	1.12/1.24	57.9
TEST20M	1.219 (4)	0	SGL	Hard	0.56/0.52	53.5
TEST18M	1.219 (4)	0.152 (0.5)	BBLY	Hard	0.55/0.62	54.5
TEST17M	1.219 (4)	9.144 (30)	ANN	Medium Hard	0.57/0.66	55.5
TEST21M	1.829 (6)	0	SGL	Very Hard	0.44/0.46	47.0

The trapped oil concentration in wax deposit was obtained from HTGC analysis. The deposit thermal conductivity was estimated using the heat transfer data. The results clearly show that higher oil concentration gives lower thermal conductivity. The relationship between the oil concentration and the wall shear stress was also checked for the multiphase flow tests. Figure 10.4 shows a plot of oil concentration in the wax deposit versus shear stress on the wall. The shear stress was calculated using the differential pressure across the test section. As can be seen, a higher shear stress gives lower oil concentration in a wax deposit. Based on these results, a correlation was developed for the oil concentration and was used in the wax deposition modeling.

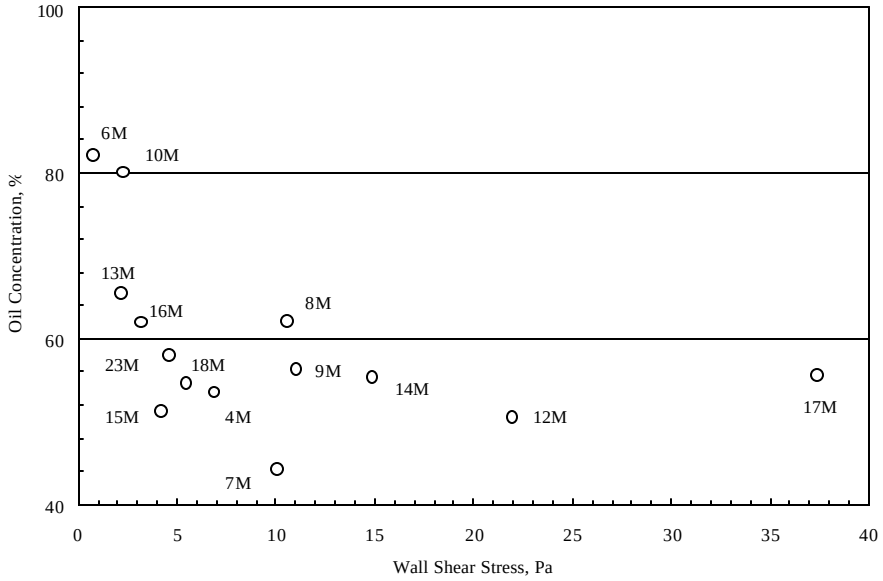

Figure 10.4 - Trapped Oil Concentration vs. Shear Stress for Multiphase Flow Tests

Figures 10.5 – 10.8 summarize the observations made from the multiphase wax deposition tests on flow pattern maps. Conclusions reached from analysis of the data are given below.

For horizontal and near-horizontal flow, wax deposition appeared to be flow pattern specific. For single-phase flow, an increase in oil velocity results in harder deposits, but with a lower deposit thickness. For stratified flow, a soft deposit is observed, similar to that in single-phase laminar flow, but only at the bottom of the pipe. For stratified wavy flow, a soft deposit, similar to that in single-phase laminar flow is observed only at the bottom of the pipe, with a harder and thicker deposit along the edge of the wave boundary, i.e., gas-liquid interface. The deposit in annular flow is uniform across the pipe circumference and very hard, especially at low oil superficial velocity. Intermittent flow results in a hard deposit with hardness increasing from top to bottom of the pipe. High gas superficial velocity intermittent flow results in harder deposits, but with a lower deposit thickness. A transition from stratified to annular flow yields a wax deposit thickness of the same order of magnitude, but there is a significant increase in its hardness. A transition from stratified to intermittent flow results in a lower deposit thickness but yields a deposit that is significantly harder. A transition from intermittent to annular flow results in a thicker deposit but without a significant change in the deposit hardness.

For vertical flow, wax deposition also appeared to be flow pattern specific. For single-phase flow, an increase in oil velocity results in harder deposits, but with a lower deposit thickness. The nature and the extent of wax deposit thickness in vertical flow are similar to horizontal flow. The deposit in annular flow is uniform across the pipe circumference and very hard for low oil superficial velocity. For high oil

superficial velocity, the deposit is not as hard and not as thick. Intermittent flow results in a medium hard to a hard deposit with uniform hardness around the pipe circumference. An increase in velocities results in harder deposits, but yields a deposit thickness of the same order of magnitude. A transition from intermittent to annular flow yields a wax deposit thickness of the same order of magnitude and without a significant change in the deposit hardness. High oil superficial velocity or high mixture velocity bubbly flow results in a hard deposit. A transition from bubbly flow at high oil superficial velocity to intermittent flow at low superficial oil velocity results in a thicker deposit and a significant decrease in hardness. A transition from bubbly flow at high oil velocity to intermittent flow yields a wax deposit thickness of the same order of magnitude, but without a change in the deposit hardness.

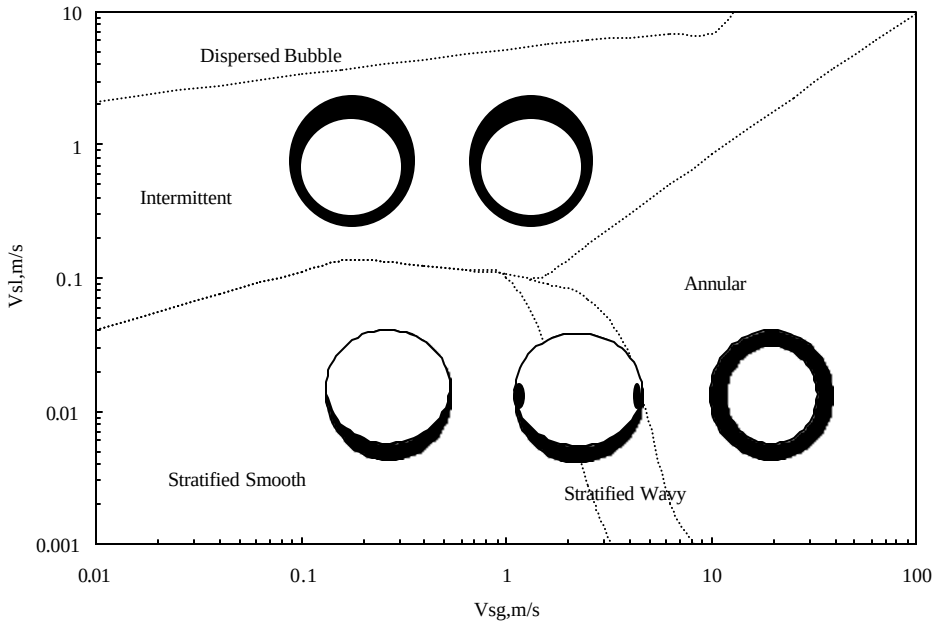

Figure 10.5 - Wax Thickness Distribution for Various Horizontal Flow Patterns

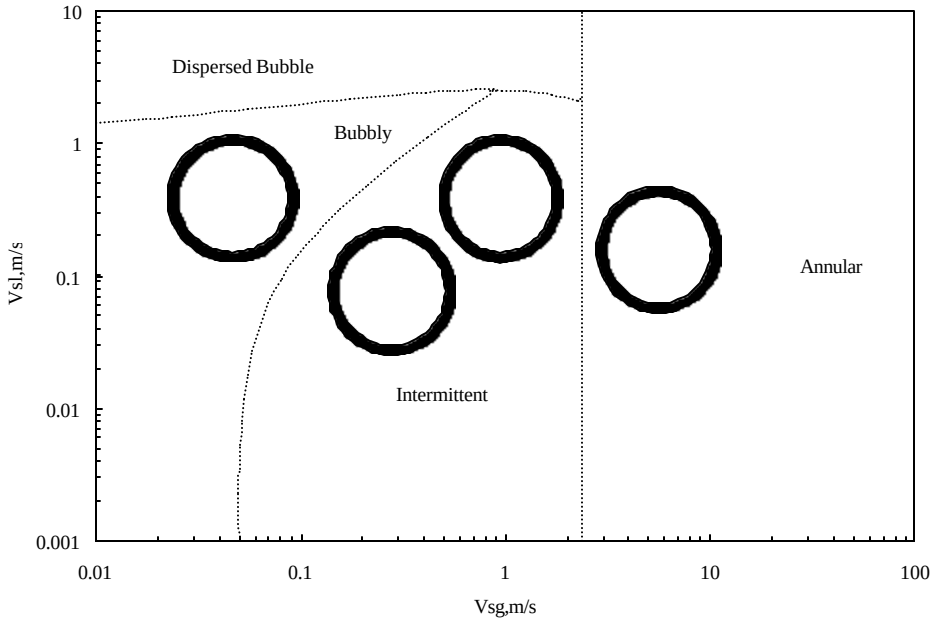

Figure 10.6 - Wax Thickness Distribution for Various Vertical Flow Patterns

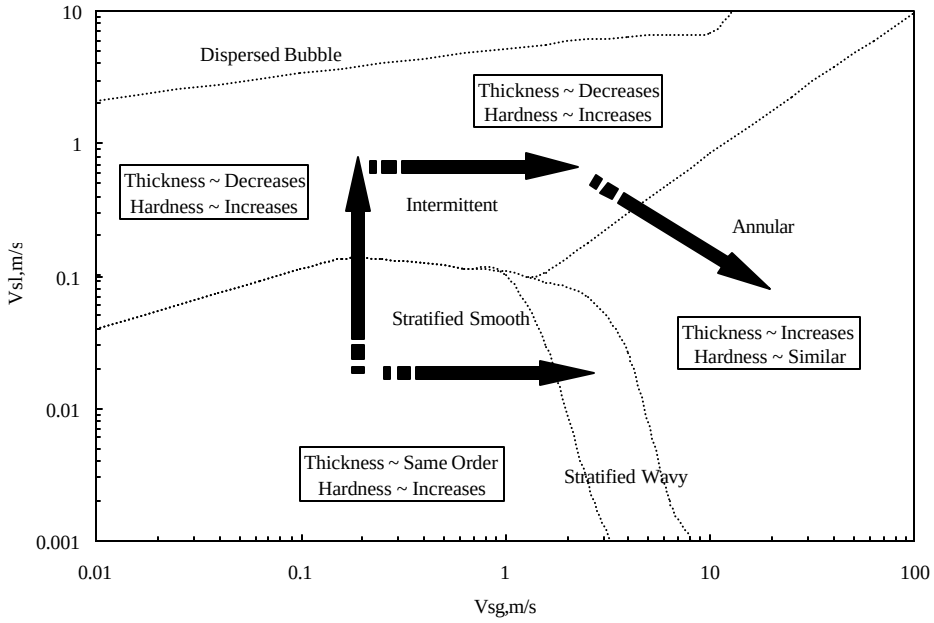

Figure 10.7 - General Observations in Horizontal Flow Tests

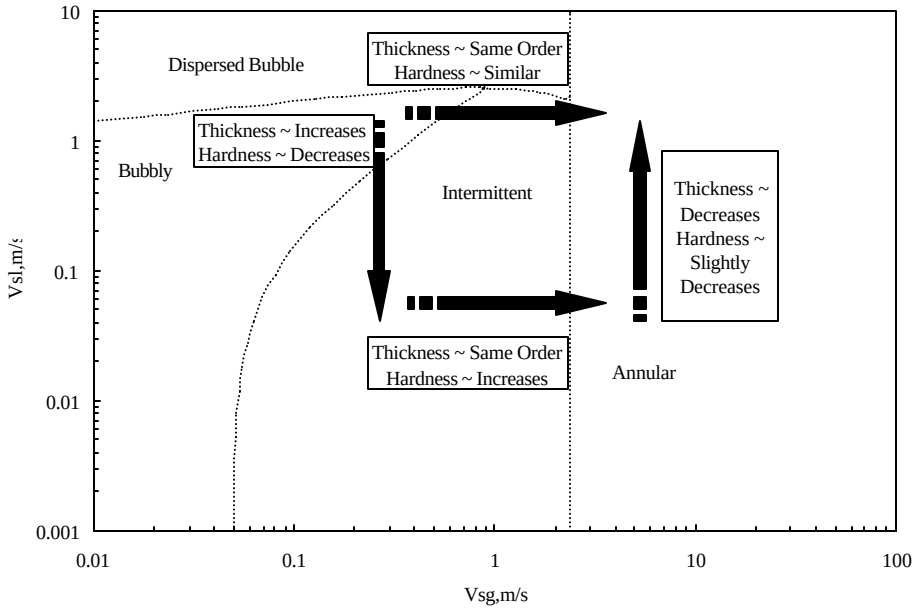

Figure 10.8 - General Observations in Vertical Flow Tests

Section 11
Modeling

Computer Program

A computer program was developed by the JIP for the prediction of wax deposition during single-phase and two-phase gas-oil flow in horizontal and near-horizontal flowlines, and vertical wellbores. The program is modular in structure, and assumes a steady-state, one-dimensional flow, energy conservation principal. The program performs wax deposition predictions during multiphase flow in pipelines and wellbores by coupling mechanistic two-phase flow hydrodynamic models, solid-liquid-vapor thermodynamics, two-phase flow heat transfer and flow pattern dependent wax deposition kinetics into one modular program. This program has been integrated with the Graphical User Interface (GUI) developed by MSI, with graphical input, output and plotting supports.

In the hydrodynamics module, the Xiao *et al.* (1990) and Kaya *et al.* (1998) mechanistic models are used to predict flow pattern, liquid holdup and pressure gradients in near-horizontal and near-vertical pipe flows, respectively. MSI's code for thermodynamics calculations is used to generate a transport property table and a thermodynamic table for the multiphase fluid system, with respect to temperature and pressure. For heat transfer calculations, the pipe inside convective heat transfer coefficient is evaluated by use of the correlations recommended by the OSU group (1997) for different flow patterns. The wax deposition is related to the mass transfer, which is controlled by molecular diffusion (Fick's Law) near the interface of the crude oil and deposit.

In the single-phase and two-phase tests of the Wax JIP, some factors were identified that affect the wax deposition process. These include: the oil content trapped in the deposit, the shear stripping of the deposit by the flowing fluids, the changes in the thermal conductivity of the deposit and the surface roughness, and the aging effect of the deposit. Accordingly, entry options were incorporated in the simulation program to allow users to input adjustment parameters according to laboratory or field measurement. The default values and recommended ranges of these adjustment parameters are given in Appendix D according to the single-phase and two-phase test results of the Wax JIP.

Two-Phase Flow Hydrodynamics

Two mechanistic models developed at the Tulsa University Fluid Flow Projects are used for the hydrodynamics calculation. They are Xiao *et al.* (1990) for horizontal and near-horizontal pipelines, and Kaya (1999) for inclined and vertical wellbores.

The flow patterns encountered during multiphase flow of liquid and gas in horizontal and near-horizontal pipes are categorized as stratified (smooth and wavy), intermittent (elongated bubble and slug), annular and dispersed bubble. The mechanistic model of Xiao *et al.* (1990) is used to predict flow patterns, pressure gradients and liquid holdups for pipe inclination angles from –15° to + 15°.

The flow patterns encountered during multiphase flow in inclined and vertical wells are categorized as bubbly, dispersed bubble, intermittent (slug and churn) and annular. The mechanistic model of Kaya (1999) is used to predict flow patterns, pressure gradients and liquid holdups for pipe inclination angles from +15° to +90° from horizontal.

MSI Thermodynamic Model

A thermodynamic model for predicting vapor-liquid-solid equilibria of hydrocarbon systems developed by Brown *et al.* (1997) was used to generate tables of dissolved paraffin (mole fraction) and concentration gradient (dC_w/dT) at various temperatures and pressures. The mole fraction and concentration gradient were obtained for the lumped paraffin components, where paraffin was considered as one pseudo component.

The thermodynamic model, *i.e.*, from the thermodynamic module of the JIP paraffin prediction program, is essentially the same as described by Erickson *et al.* (1993) and Brown *et al.* (1994). The multiphase flash algorithms are based on the Gibbs energy minimization methods as proposed by Michelsen (1982a,b). The algorithms initially assume the system to be single-phase and the stability of this phase is evaluated with respect to vapor-liquid phase split. If the single-phase is unstable, a vapor-liquid flash is performed.

The stability of the one or two-phase system is then evaluated with respect to formation of a solid paraffin phase. If the system is unstable, a two or three-phase flash is performed. For the stability analysis, the method of Michelsen (1982a,b) is used. Given an estimate of the composition of a new phase, the stability analysis converges on a composition for the new phase which, when split off in an infinitesimal amount, minimizes the Gibbs energy of the combined phases. If the Gibbs energy of the combined phases is less than of the original system, the original system is unstable.

Two-Phase Flow Heat Transfer

Wax deposition occurs in a non-isothermal flowing system and appears to be driven by the heat flux. Therefore, the success in predicting wax deposition rates in single-phase and multiphase flow environments depends on how well heat transfer characteristics are evaluated. They include the forced convective film heat transfer coefficient, bulk and wall temperatures and local heat flux across the pipe wall.

As a subcontractor to the Paraffin Deposition JIP, the OSU group (Dougherty *et al.*) performed a comprehensive literature review of heat transfer during gas-liquid two-phase pipe flow (JIP Report, 1997a,b). They assessed the validity of 20 non-boiling heat transfer correlations and compared them with 524 experimental data points available from the literature. Based on the results of the comparisons, appropriate correlations for different flow patterns and pipe orientations were recommended (JIP Report, 1997, JIP Report, 1999).

Recently, Kaminsky (1999) proposed a new heat transfer estimation method for non-boiling gas-liquid flow in pipes of high Prandtl number liquids, such as crude oil. The method was evaluated for engineering applications and was found to be applicable to all flow patterns except those with low liquid holdup. The method works in conjunction with existing prediction methods for two-phase flow pressure drop and liquid holdup.

In this JIP, a total of 39 heat transfer tests were conducted, with 16 for horizontal flow and 23 for upward vertical flow. The flow patterns included stratified, slug, annular and bubbly flows. The measured two-phase convective heat transfer coefficients were compared with the predictions of the OSU recommended correlations and Kaminsky's method for different flow patterns. For some cases, the predictions agreed reasonably well with the experimental data. For others, the comparisons were quite scattered. The reasons for this may be partially due to the uncertainties in experimental measurements and/or the insufficient temperature difference to resolve the heat transfer. In horizontal flow tests, the

temperature difference between oil and glycol was about 45°F. In vertical flow tests, the temperature difference was only 10°F.

The other and perhaps the most important reason for the scattered comparison may be due to the prediction ability of the correlations. All the correlations recommended by the OSU group were obtained from experimental studies with different fluids and at different flow conditions. The applicability of these correlations to the crude oil-natural gas system at high pressure (and temperature) needs to be tested before they are used in engineering calculations.

Considering the progress that has been made during the last 25 years in mechanistic modeling of the hydrodynamics of gas-liquid two-phase flow, mechanistic modeling of heat transfer should now be possible and may bring significant improvement to the prediction of heat transfer coefficients in different flow patterns. For details of the heat transfer study, please refer to the JIP Quarterly Report (1999).

Wax Deposition Kinetics

A semi-empirical wax deposition kinetic model was developed by Matzain (1999) for the prediction of wax deposition during the single-phase oil and two-phase gas-oil wax deposition tests conducted in his Ph.D. study. One-dimensional flow and pseudo-homogenous radial heat transfer and thermal balance relationships were developed for two-phase flow to provide closure for the kinetic model. The model utilizes key parameters that were measured or correlated from the experimental data, and employs vapor-liquid-solid equilibria from the thermodynamic model. In order to investigate the kinetics of wax deposition, a computer algorithm that predicts wax deposition buildup during single-phase and two-phase flow wax deposition tests was formulated. The algorithm applied measured key parameters to couple two-phase flow heat transfer and two-phase flow hydrodynamics to the wax deposition kinetics. Temperature, pressure and pressure gradient, inferred flow pattern and liquid holdup are the key measured parameters used in the kinetic deposition prediction. The use of these measured parameters allows a more focused investigation on the kinetics of wax deposition. Consequently, the rate reduction due to shear stripping and rate enhancement due to entrapment of oil were also correlated by use of dimensionless variables and empirical constants. These correlations are incorporated in the wax deposition program to minimize the tuning parameters. For details of the wax deposition kinetics modeling, please refer to Matzain's (1999) dissertation.

Section 12
Recommendations

Single-Phase Wax Deposition Study

A static mixer right after the heat trimmer is needed to generate a better temperature distribution in the oil flow.

The resistors used for the current to voltage conversion should be replaced with higher quality resistors with low temperature sensitivity. This will reduce the sensitivity of the data readings to the data acquisition room temperature.

A major concern has been whether or not the oil is being depleted of wax during a test. This problem will be even more severe when oils with low wax content are tested in the facility. The current oil storage tanks could be replaced by one larger tank to increase the oil volume used.

The glycol-water mixture flow rate was unstable due to the vibration of the bypass valve. The bypass valve can be moved to the tank side of the hose, thereby, isolating it from the pump vibrations.

More effort should be expended to better understand deposit properties, aging, the effect of shear rate and shear stress, deposition mechanisms, and the molecular diffusion coefficient.

Multiphase Wax Deposition Study

Experimental Program

At low gas superficial velocity, especially below 0.305 m/s (1.0 ft/s), flow control variations of ±0.091 m/s (±0.3 ft/s) could only be achieved. It is recommended that the control valve used for controlling gas flow rate at low superficial velocities be resized.

During the experimental tests conducted in this study, a slight leak was observed in the gas system. In order to maintain system pressure, gas was periodically added during the course of each test. Piping modifications are recommended that would allow automatic injection of the gas throughout the duration of a test in order to maintain a constant system pressure. Efforts should also be made to minimize the leak.

The level of oil in the gas-liquid separator rose throughout all tests, especially during tests at high oil and gas superficial velocities. Simultaneously, the level of oil in the oil tank decreased continuously which was caused by the accumulation of gas on top of the oil tank. Piping changes are recommended that would allow this accumulated gas in the oil tank to be flared during the course of the test, thereby allowing the oil in the separator to be at a relatively constant level.

For tests involving high oil flow rates, a significant amount of oil carry-over from the separator was observed. This oil accumulated in the gas receivers and in the gas scrubbers of the compressor. Oil carry-over could be detrimental to the operation of the compressor. It is therefore recommended to install a mist eliminator inside the separator.

The Intellution based data acquisition system used in the study was not fast enough to acquire data from the Gamma Densitometer. A faster data acquisition system would be helpful in detecting the transition boundaries between flow patterns. A LabView™ based data acquisition system that will allow faster data acquisition rates for the Gamma Densitometer is recommended to supplement the existing data acquisition system. It may also be necessary to use a different scintillation counter or a larger nuclear source to achieve a faster response time. A pair of high speed Gamma Densitometer devices is also recommended to allow for more detailed two-phase flow hydrodynamic studies.

During high winds, it is not possible to raise the boom due to safety concerns. When this occurs, LD-LD measurements can not be made. A solution should be pursued to ensure that the boom is equipped with safety features that can allow it to be raised during high winds. A safety stop feature should also be added to ensure that the boom does not damage the tower support when raising it to a vertical position.

A variation in the circumferential profile of the wax deposit was observed. The pressure transmitters used in the circumferential LD-LD setup could not detect small changes in oil level. It is recommended to install more sensitive transmitters for measuring the differential pressures in the circumferential LD-LD setup.

The wax deposition tests conducted in the present study lasted for only 24 hrs. It is recommended that future wax deposition tests last longer than 24 hrs. Wax thickness measurements using the LD-LD method should be performed more frequently.

The hardness of wax deposits was interpreted from visual observations and personal judgement, which is not supported by any scientific background. A more direct laboratory measurement of wax deposit hardness is thus recommended.

The deposit thermal conductivity was found to vary depending upon the amount of oil trapped in the wax deposit. However, these findings were derived from limited thermal conductivity information inferred from heat transfer data. A more direct laboratory measurement of wax deposit thermal conductivity is thus recommended.

Collected wax samples were taken with care so as to ensure that the wax samples do not mix with oil. However, oil may not be completely drained out during depressurization and this may cause wax at the bottom of the pipe to mix with oil during sampling. It is recommended that a more detailed sampling procedure be formulated to ensure that the deposit samples do not mix with oil during sampling. A method to perform sampling at various time intervals and at system pressure should also be investigated.

Collected wax samples were sent to Chevron Petroleum Technology Company for compositional analyses using HTGC. The analyses provide information on the percentage of oil trapped in the wax deposit. The capability to determine the amount of oil trapped in the wax deposit is not available in-house and should be developed to ensure that more detailed and frequent analyses can be performed.

Transport properties of the oil and gas were estimated from several correlations. Laboratory measurements of the transport properties are thus recommended in order to tune these correlations.

Many of the flow pattern prediction methods were established at low system pressure. The failure to verify some of the flow patterns for some flow pattern tests could be attributed to the fact that the tests were conducted at a much higher system pressure. A dedicated series of tests should be conducted to establish flow pattern transition maps for various pipe inclinations.

Additional heat transfer tests in a non-depositional environment are recommended to develop film heat transfer correlations for the gas-liquid two-phase flow. The number and quality of heat transfer instruments must be improved. This may include reliable instruments for measuring the outside wall temperature, eliminating the need to estimate of the outside convective film heat transfer coefficient. Considering the progress that has been made during the past 20 years in mechanistic modeling of the hydrodynamics of gas-liquid two-phase flow, mechanistic modeling of heat transfer is also recommended and may yield significant improvements to the prediction of convective film heat transfer coefficient in different flow patterns.

Modeling

Based on a thorough review of paraffin deposition data during single-phase flow, it can be concluded that the molecular diffusion theory alone cannot adequately describe the deposition phenomena. The influence of shear on wax deposition in multiphase flow and the effect of aging of the deposit should be studied in depth. A careful study of the deposition phenomena, often termed as 'deposition physics', is therefore recommended.

The solutions of mass transfer problems in many chemical engineering applications can be obtained by analogy with corresponding problems in momentum and heat transfer. The applicability of the analogy to the paraffin deposition problem needs to be investigated.

The kinetics of paraffin deposition has been recently associated with the theory of crystal growth. The applicability of this theory to the paraffin deposition problem needs to be investigated.

The semi-empirical kinetic deposition model in this study attempted to incorporate important factors such as deposition rate reduction due to shear stripping, rate enhancement due to entrapment of oil, and other mechanisms not accounted for by the classical Fick's mass diffusion theory. The incorporation was made empirically and was tailored for the wax deposition tests conducted for the present study. Furthermore, the empirical constants and the correlation for the trapped oil concentration were derived from limited wax deposition data. Their use needs to be verified for other test conditions, especially for different flow patterns and test duration.

Empirical correlations were developed for the deposit thermal conductivity based on the wall shear stress, and the trapped oil concentration. However, these correlations were derived from limited experimental data. It is recommended that more detailed investigation and laboratory measurements be conducted to acquire additional data for a more reliable correlation development.

Section 13
Conclusions

Single-Phase Wax Deposition Study

The flow loop is capable of producing high quality data that a small diameter loop is unable to produce.

The effects of bulk oil temperature and temperature difference between oil and glycol (ΔT) are consistent with the molecular diffusion model.

Shell Oil Company's Block 426, Well A-14, Garden Banks condensate is capable of producing significant deposits.

The roughness of the deposit from Test #14R was estimated to be 0.05 mm (0.002 in.), which is only slightly higher than the pipe roughness of 0.04 mm (0.0015 in.).

A linear relationship between the oil in deposit concentration after 24 hours and the bulk oil temperature was observed for the South Pelto tests that produce hard deposits.

The deposit thermal conductivity can vary from the oil thermal conductivity to at least six times the oil thermal conductivity, depending on operating conditions and aging of the deposit. The variations are much higher than that found in multiphase flow tests. This may be due to inaccuracies in data analysis.

The regressed molecular diffusion coefficients are not constant nor do they agree with the commonly used Wilke-Chang and Hayduk and Minhas correlations.

It was shown that, although some wax depletion did occur, it did not significantly impact the tests.

Neither a molecular diffusion nor a shear dispersion model can adequately predict all the paraffin deposition phenomena that were observed.

Multiphase Wax Deposition Study

Experimental Program

A new high-pressure state-of-the-art test facility was designed, constructed and operated to generate wax deposition data during single-phase waxy oil and two-phase gas-waxy oil flow in horizontal, near-horizontal, and vertical pipes. The test facility, proven to be capable of depositing wax on the inner pipe wall of the test pipe, was operated successfully with few operational problems. Wax thickness measurements using the LD-LD device gave the most reliable values for two-phase flow when compared to the widely accepted single-phase pressure drop and heat transfer methods. The test facility used in the study generated quality paraffin deposition data for a two-phase mixture of natural gas and South Pelto crude oil. Analysis of the data resulted in the following conclusions.

Horizontal and near-horizontal flow:

- Wax deposition appeared to be flow pattern specific.
- For single-phase flow, an increase in oil velocity results in harder deposits, but with a lower deposit thickness.
- For stratified flow, a soft deposit, similar to that in single-phase laminar flow, is observed, but only at the bottom of the pipe.
- For stratified wavy flow, a soft deposit, similar to that in single-phase laminar flow is observed only at the bottom of the pipe, with a harder and thicker deposit along the edge of the wave boundary, *i.e.*, gas-liquid interface.
- The deposit in annular flow is uniform across the pipe circumference and very hard, especially at low oil superficial velocity.
- Intermittent flow results in a hard deposit with hardness increasing from top to bottom of the pipe. High gas superficial velocity intermittent flow results in harder deposits, but with a lower deposit thickness.
- A transition from stratified to annular flow yields a wax deposit thickness of the same order of magnitude, but there is a significant increase in its hardness.
- A transition from stratified to intermittent flow results in a lower deposit thickness but yields a deposit that is significantly harder.
- A transition from intermittent to annular flow results in a thicker deposit but without a significant change in the deposit hardness.

Vertical flow:

- Wax deposition appeared to be flow pattern specific.
- For single-phase flow, an increase in oil velocity results in harder deposits, but with a lower deposit thickness. The nature and the extent of wax deposit thickness in vertical flow are similar to horizontal flow.
- The deposit in annular flow is uniform across the pipe circumference and very hard for low oil superficial velocity. For high oil superficial velocity, the deposit is not as hard and not as thick.
- Intermittent flow results in a medium hard to a hard deposit with uniform hardness around the pipe circumference. An increase in velocities results in harder deposits, but yields a deposit thickness of the same order of magnitude.
- A transition from intermittent to annular flow yields a wax deposit thickness of the same order of magnitude and without a significant change in the deposit hardness.
- High oil superficial velocity or high mixture superficial velocity bubbly flow results in a hard deposit.

- At low oil superficial velocity, a transition from bubbly flow at high oil superficial velocity to intermittent flow results in a thicker deposit and a significant decrease in hardness.

- At high oil superficial velocity, a transition from bubbly flow to intermittent flow yields a wax deposit thickness of the same order of magnitude, but without a change in the deposit hardness.

In general, an increase in mixture velocity results in harder deposits, but with a lower deposit thickness. The wax buildup trend at low mixture velocities is similar to that observed in laminar single-phase flow tests. The wax buildup trend at high mixture velocities is similar to that observed in turbulent single-phase flow tests. A higher shear stress gives lower oil concentration in the wax deposit. Oil concentration in the wax deposit was found to vary between 40% and 80%, depending on the nature of the deposit. A lower oil concentration gives a harder deposit and a higher oil concentration yields a softer deposit. Wax deposit thermal conductivity was found to vary between 1.0 to 2.0 times oil conductivity. Higher oil concentration in the wax deposit gives a lower deposit thermal conductivity.

Flow pattern influences wax deposition in two-phase flow more at low oil superficial velocity than at high oil superficial velocity. The extent of wax deposition in high oil superficial velocity two-phase flow tests is comparable to that in a single-phase flow test of the same oil velocity. However, the extent of wax deposition in low oil superficial velocity two-phase flow tests is not comparable to that in a single-phase oil flow test of the same oil velocity.

The slow acquisition rate of the existing data acquisition system prohibits acquisition of the fast response times at high oil and gas flow rates required for a detailed flow pattern verification study. The failure to verify flow patterns for some flow pattern verification tests could also be attributed to the fact that the tests were conducted at a higher system pressure. Many of the flow pattern prediction methods were established at low system pressure.

Comparisons of the calculated two-phase convective film heat transfer coefficients and the experimental data from a heat transfer study were quite scattered. The reasons for the inconsistency may be partially due to uncertainties in experimental measurements and interpretation methods, and/or insufficient temperature difference to resolve two-phase flow heat transfer.

Modeling

The presented semi-empirical wax deposition kinetic model predicted wax thickness with an acceptable accuracy, especially at high oil flow rates. The model incorporated deposition rate reduction due to shear stripping and rate enhancement due to entrapment of oil and other mechanisms not accounted for by the classical Fick's mass diffusion theory. The incorporation was made through the use of dimensionless variables formulated for different flow patterns, and empirical constants derived from the wax deposition data. The higher or the lower predicted values of trapped oil concentration and the higher or the lower predicted values of the radial temperature gradient caused inaccuracies in some predictions in two-phase flow tests. Prediction inaccuracies in several intermittent flow tests were caused by not incorporating important hydrodynamic parameters such as slug length and slug frequency and slug impact forces in the kinetic model. The kinetic model, although semi-empirical, provides an insight for future model development.

Section 14
References

Agarwal, K.W., Khan, H.U., Surianarayanan, M., Joshi, G.C.: "Wax Deposition of Bombay High Crude Oil under Flowing Conditions," Fuel, 69 No. 6, pp. 794-796 (June 1990).

Ansari, A. M., Sylvester, N. D., Sarica, C., Shoham, O. and Brill, J.P.: "A Comprehensive Mechanistic Model for Upward Two-Phase Flow in Wellbores," SPE J. Production and Facilities, 143-152 (May 1994).

Apte[(a)], M.: "Investigation of Paraffin Deposition in Multiphase Flow," MS Thesis, The University of Tulsa, Tulsa, Oklahoma (1999).

Apte[(b)], M.S., Matzain A., Delle Case, E., Volk, M., Creek, J.L. and Brill, J.P.: "Investigation of Multiphase Flow Paraffin Deposition," paper presented at BHRG Multiphase Technology Conference, Cannes, France, (June 1999).

Barnea, D., Yacoub, N.: "Heat Transfer in Vertical Upwards Gas-Liquid Slug Flow," Intl. J. of Heat & Mass Transfer, Vol. 26, No. 9, pp. 1365 (1983).

Bern, P. A., Withers, V. R. and Cairns, R. J. R.: "Wax Deposition in Crude Oil Pipelines," EUR 206, 1980 European Offshore Petroleum Conference and Exhibition, London, England, (October 21-24).

Bird, R.B., Stewart, W.E., and Lightfoot, E.N.: "Transport Phenomena", John Wiley and Sons, pp. 636-648 (1960).

Brill, J.P. and Beggs, HD.: "Two-Phase Flow in Pipes," The University of Tulsa, 6th. Ed., (January 1988).

Brill, J.P. and Mukerjee, H: "Multiphase Flow in Wells," SPE Monograph, (1999).

Brown[(a)], T. B., Niesen, V. G. and Erickson, D. D.: "Measurement and Prediction of the Kinetics of Paraffin Deposition," paper SPE 26548 presented at the 68th SPE Annual Technical Conference and Exhibition, Houston, TX, (October 3-6 1993).

Brown, T.S., Niesen, V.G., and Erickson, D.D.: "The Effects of Light Ends and High Pressure on Paraffin Formation," SPE 28505 presented at the 69th ATCE SPE, New Orleans, LA, (September 25-28, 1994).

Brown, T.S., and Niesen, V.G.: "A Thermodynamic Model for Predicting the Vapor/Liquid/Solid Equilibria of Hydrocarbon Systems," The University of Tulsa Paraffin Deposition Prediction in Multiphase Flowlines and Wellbores Joint Industry Project, (1997).

Brown[(b)], T. S., Niesen, V. G. and Erickson, D. D.: "Thermodynamic Measurement and Prediction of Paraffin Precipitation in Crude Oil," SPE 26604 presented at SPE 68th Annual Technical Conference and Exhibition, Houston, TX (3-6 October 1993).

Bunz, A.P., Dohrn, R., Prausnitz, J.M.: "Three-Phase Flash Calculations for Multicomponent Systsms," Computers Chem. Eng., Vol. 15, No. 1, pp. 47-51 (1991).

Burger, E. D., Perkins, T. K. and Striegler, J. H.: "Studies of Wax Deposition in the Trans- Alaska Pipeline," J. of Petroleum Technology, 1075-1086 (June 1981).

Chen, X. T., Butler, T., Volk, M. and Brill, J. P.: "Techniques for Measuring Wax Thickness During Single and Multiphase Flow," SPE 38773, SPE Annual Technical Conference and Exhibition, San Antonio, Texas, Oct. 5-8, 1997.

Chilton, T.H. and Colburn, A.P., Ind & Eng. Chem., 26, 1183 (1934).

Chung, T.-H, Sarathi, P., Jones, R.: "Modeling of Asphaltene and Wax Precipitation," NIPER-498, Bartlesville, OK (January, 1991).

Coleman, H. W. and Steele, G. W.: "Experimentation Uncertainty Analysis for Engineers," John Wiley & Sons, 1989.

Creek, J. L. and Hobson, G. G., "ADEX 2 Wax Deposition Study, ANOA Pipeline Evaluation," Chevron petroleum Company internal report TM96000354, CPTC, La Habra, CA (May 1996).

Creek, J. L.: "Analyzing Why, How, and Under What Conditions Waxes, Hydrates, and Asphaltenes Will Form," presented at IIR Conference in Aberdeen (17 June, 1998).

Creek, J.L., Matzain A., Apte, M.S., Brill, J.P., Volk, M., Delle Case, E. and Lund, H.: "Mechanisms for Wax Deposition" paper presented at AIChE, National Spring Meeting, Houston, TX (March 1999)

Creek, J., Volk, M. and Marathon Oil Company: "Fluid Characterization and Property Evaluation – Final Report" (1999).

Cussler, E. L.: "*Diffusion Mass Transfer in Fluid Systems*", Cambridge University Press, (1987).

Davis, E.J., Cheremisinoff, N.P, and Sambasivan, G.: "Heat and Momentum Transfer Analogies for Two-Phase Transfer Stratified and Annular Flows," Proceedings of the Two-Phase Flow and Heat Transfer Symposium, Fort Lauderdale, pp. 577-608 (1976).

Davis, E.J., Hung, S.C., and Arciero, S.: "An Analogy for Heat Transfer with Wavy/Stratified Gas-Liquid Flow," AICHE Journal, 21(5), pp. 872-878 (1975).

Dawson, S.: "Simulation of Wax Deposition Case Study," paper presented at the 1995 IBC Advances in Multiphase Operation and Offshore Conference, London, England, (November 29-30, 1995).

Eaton, P. E. and Weeter, G. Y.: "Paraffin Deposition in Flow Lines", Paper No. 76-CSME/CSCH-22 presented at the 16th National Heat Transfer Conference, St. Louis, MO (August 1976).

Erickson, D. D., Niesen, V. G. and Brown, T. S.: "Measurement and Prediction of the Kinetics of Paraffin Deposition", SPE 26548 presented at SPE 68th Annual Technical Conference and Exhibition, Houston, TX (October 1993).

Forsdyke, I: Internal Report: British Petroleum (1995).

Fredenslund, A., Hansen, J.H., Pederson, K.S., and Ronningsen, H.P.: "A Thermodynamic Model for Predicting Wax Formation in Crude Oil," AIChE J., Vol 34, pp 1937-1942 (1988).

Fried, L.: "Pressure Drop and Heat Transfer for Two-Phase, Two-Component Flow," Chemical Engineering Progress Symp. Series, 50, pp. 47-51 (1954).

Hamouda, A. A. and Davidsen, S.: “An approach for Simulation of Paraffin Deposition in Pipelines as a function of Flow Characteristics with a reference to Teeside Oil Pipeline”, SPE 28966 presented at the SPE International Symposium on Oilfield Chemistry, San Antonio, TX (February 1995).

Hayduk, W. and Minhas, B. S.: “Correlations for Prediction of Molecular Diffusivities in Liquids”, *Can. J. Chem. Eng.* Volume 60, pp. 295-299 (April 1982).

Henson, R. D., T. J. Tangen and Horne, P. T.: “Evaluation of Paraffin-Treating Programs for Rod-Pumped Oil Wells,” SPE 27669 presented at the SPE Permian Basin Oil and Gas Recovery Conference, Midland, TX (16-18 March 1994).

Hestroni[(a)], G., Hu, B.G., Yi, J.H., Mosyak, A., Yarin, L.P., and Ziskin, G.: "Heat Transfer in Intermittent Air-Water Flows - Part 1 - Horizontal Tube," Intl. J. of Multiphase Flow, Vol. 24, No. 2 pp. 165-188 (1998).

Hestroni[(b)], G., Hu, B.G., Yi, J.H., Mosyak, A., Yarin, L.P., and Ziskin, G.: "Heat Transfer in Intermittent Air-Water Flows - Part 2 - Upward Inclined Tube," Intl. J. of Multiphase Flow, Vol. 24, No. 2 pp. 189-212 (1998).

Hsu, J.J., Santamaria, M.M., and Brubaker, J.P.: “Wax Deposition of Waxy Live Crudes under Turbulent Flow Conditions,” SPE 28480 presented at SPE 69th Annual Technical Conference and Exhibition, New Orleans, LA, (25-28 September 1994).

Hsu[(a)], J.J., and Brubaker, J.P.: “Wax Deposition Scale-Up Modeling For Waxy Production Lines,” OTC 7788 presented at 27th Annual Offshore Technology Conference, Houston, TX, (1-4 May 1995).

Hsu[(b)], J.J.C. and Brubaker, J.P.: “Wax Deposition Measurement and Scale-UP Modeling for Waxy Live Crudes under Turbulent Flow Conditions,” paper SPE 29976 presented at the 1995 SPE International Meeting on Petroleum Engineering, Beijing, China, (November 14-17 1995).

Hsu, J.C., Elphingstone, G.M. and Greenhill, K.L.: “Modeling of Multiphase Wax Deposition”, J. Energy Resources Technology- Transactions of ASME, 121 (2) 81-85 (June 1999).

Hughmark, G.A.: "Heat Transfer in Horizontal Annular Gas-Liquid Flow," Chemical Eng. Progress Symp. Series, 57, Vol. 61, pp. 176-178 (1963).

Jessen, F.W. and Howell, J.N.: “Effect of Flow Rate on Paraffin Accumulation in Plastic, Steel, and Coated Pipe,” Petroleum Transactions, AIME, pp. 80-84 (1958).

Jorda, R. M.: “Paraffin Deposition and Prevention in Oil Wells,” J. of Petroleum Technology, 1605-1612 (December 1966).

Kaminsky, R.D.: “Estimation of Two-Phase Flow Heat Transfer in Pipes,” paper presented at ASME ETCE, Houston, TX, (February 1999).

Kaya, A.S.: “Comprehensive Mechanistic Modeling of Two-Phase Flow in Deviated Wells,” MS Thesis, The University of Tulsa, Tulsa, OK, (1998).

Kim, D., Ghajar, A.J., Dougherty, R.L.: "A Heat Transfer Correlation for Turbulent Gas-Liquid Two-Phase Flow of Several Fluid Combinations and Different Flow Patterns in Vertical Pipes," paper presented at the 33rd ASME Natl. Heat Transfer Conference, Albuquerque, NM, (August 15-17, 1999).

Kim, C.P., Vimalchand, P., Donohue, M.D., and Sandler, S.I.: "Local Composition Model for Chainlike Molecules: A New Simplified Version of the Perturbed Hard Chain Theory," AIChE J., Vol. 32, 10, pp. 1726-1734 (1986).

Kim, D, Sofyan, Y., Ghajar, A.J. and Dougherty, R.L.: "An Evaluation of Several Heat Transfer Correlations for Two-Phase Flow With Different Flow Patterns In Vertical and Horizontal Tubes," Proc. National Heat Transfer Conference, Baltimore, MD (August 1997).

Knot, R.F., Anderson, R.N., Acrivos, A. and Petersen, E.E.: "An Experimental Study of Heat Transfer to Nitrogen-Oil Mixtures," Ind. & Eng. Chem. Vol.51 No.11, pp.1369-1372 (1959).

Kudirka, A.A., Grosh, R.J. and Mcfadden, P.W.: "Heat Transfer in Two-Phase Flow of Gas-Liquid Mixtures," Ind. & Eng. Chem. Fund. , Vol. 4, No. 3, pp. 339-344 (1965).

Lund, H. J.: "Investigation of Paraffin Deposition during Single-Phase Liquid Flow in Pipelines," Master Thesis, The University of Tulsa, 1998.

Marshall, G. R.: "Cleaning of the Valhall Offshore Oil Pipeline," Paper presented at the 20th OTC in Houston, TX, 517-525 (May 1988) cited in Brown *et al.* (1993).

Matlach, W. J. and Newberry, M. E.: "Paraffin Deposition and Rheological Evaluation of High Wax Content Altamont Crude Oils," SPE 11851 presented at Rocky Mountain Regional Meeting, Salt Lake City, Utah (23-25 May 1983).

Matzain A., Apte, M.S., Brill, J.P., Volk, M., Delle Case, E., Creek, J.L. and Wilson, J.W.: "Design and Operation of a high-pressure Paraffin Deposition Multiphase Flow Loop", BHRG Multiphase Tech. Conf., Banff, Alberta, Canada (June 1998).

Matzain, A.: "Single-Phase Liquid Paraffin Deposition Modeling," MS Thesis, University of Tulsa, OK (1996).

Matzain, A.: "Multiphase Flow Paraffin Deposition Modeling" Ph.D. Dissertation, The University of Tulsa, Tulsa, Oklahoma (1999).

Mendes, P. R. and Braga, S. L.: "Obstruction of Pipelines During Flow of Waxy Crude Oils," J. of Fluids Engineering Vol. 118, 722-728 (December 1996).

Michelsen[(a)], M.L.: "The Isothermal Flash Problem. Part 1. Stability," Fluid Phase Equilibria, Vol. 9, pp. 1-19 (1982).

Michelsen[(b)], M.L.: "The Isothermal Flash Problem. Part 2. Phase-Split Calculation," Fluid Phase Equilibria, Vol. 9, pp. 21-40 (1982).

MSI/Conoco PARAFFIN Prediction Program, available from MSI for WAX JIP member companies (1998).

Narayanan, L., Leontaritis, K.J., and Darby, R.: “Model for Predicting Wax Deposition from Crude Oils,” paper 55a presented at the 1993 AIChE Spring National Convention, (March 28-April, 1993).

Niesen, V. G. Brown, T. S. and Erickson, D. D.: “Thermodynamic Measurement and Prediction of Paraffin Precipitation in Crude Oil”, SPE 26604 presented at SPE 68th Annual Technical Conference and Exhibition, Houston, TX (October 1993).

Nyvlt, J., Vaclavu, V., Collect. Czechosl. Chem. Commun., 37, 3664 (1972) cited in the book of "The Kinetics of Industrial Crystallization" by Nyvlt, J., Sohnel, O., Matuchova, M., Broul, M., Elsevier Publication, pp. 176-181 (1985).

Oliver, D.R., and Wright, S.J.: " Pressure Drop and Heat Transfer in Gas-Liquid Slug Flow in Horizontal Tubes," British Chemical Engineering, Vol. 9(9), pp. 590-596.

Pate, C. B.: “MMS/Deepstar Workshop on Produced Fluids”, Offshore Technology Conference, Houston, TX (May 1995).

Peng, D.Y., Robinson, D.B.: “A New Constant Equation of States,” Ind. Eng. Chem. Fundam., Vol. 15, pp. 59-64 (1976).

Pletcher, R.H., and McManus, H.N.: "A Theory for Heat Transfer to Annular, Two-Component Flow," Intl. J. of Heat and Mass Transfer, 15, pp. 2091-2096 (1972).

Reid, R. C., *et al.*: “The Properties of Gases and Liquids,” 4th Edition, McGraw-Hill (1986).

Rezkallah, K.S. and Sims, G.E.: “An Examination of Correlations of Mean Heat Transfer Coefficients in Two-Phase and Two-Component Flow in Vertical Tubes”, *AIChE Symp. Series*, Vol.83, pp.109-114 (1987).

Rygg, O. B. *et al.*: “Wax Deposition in Offshore Pipeline Systems,” presented at 1st North American Conference, In all situations from Land-Based to Deep Water, MULTIPHASE TECHNOLOGY, Technology from the Arctic to the Tropics, Banff, Canada (9-11 June 1998).

Shah, M.M: “Generalized Prediction of Heat Transfer During Two Component Gas-Liquid Flow in Tubes and Other Channel,” AIChE Symp. Series, Vol. 77, No. 208, pp. 140-151 (1981).

Shoham, O., Dukler, A.E., and Taitel, Y.: "Heat Transfer during Intermittent/Slug Flow in Horizontal Tubes," Ind. Eng. Chem. Fundam., 21, pp. 312-319 (1982).

Soave, G., “Equilibrium Constants from a Modified Redlich-Kwong Equation of State,” Chem. Eng. Sci., Vol. 27, pp.1197-1203 (1972).

Svendsen, J. A.: “Mathematical Modeling of Wax Deposition in Oil Pipeline Systems”, *AIChE J.*, Vol. 39, No. 8, 1377-1388 (1993).

Taitel, Y. and Dukler, A.E.: “A Model for Prediction Flow Regime Transition in Horizontal and Near Horizontal Gas-Liquid Flow”, *AIChE J*., 22, 47–55 (1976).

Taitel, Y., Barnea, D. and Dukler, A.E.: “Modeling Flow Pattern Transitions for Steady State Upward Gas-Liquid Flow in Vertical Tubes”, *AICHE J*., 26, 345-354 (1980).

Weingarten, J. S. and Euchner, J. A.: "Methods for Predicting Wax Precipitation and Deposition," SPE J. Production Engineering, 121-126 (February 1988).

Wilke, C.R. and Chang, P.: "Correlation of Diffusion Coefficient in Dilute Solutions," AIChE J., Vol 1(2), pp. 264-270 (1955).

Won, K.W.: "Thermodynamics for Solid Solution-Liquid-Vapor Equilibria: Wax Formation from Heavy Hydrocarbon Mixture," Fluid Phase Equilibria, Vol. 30, pp. 265 (1986).

Xiao, J.J., Shoham. O., and Brill, JP.: "A comprehensive Mechanistic Model for Two-Phase Flow in Pipelines," SPE 20631 presented at the SPE Annual Technical Conference and Exhibition, New Orleans, LA, (September 1990).

Section 15
Nomenclature

A_i	=	inner surface area of pipe wall, (m^2)
A_1	=	wax buildup curve fitting parameter, (mm^2/s)
A_2	=	wax buildup curve fitting parameter, (1/s)
b	=	exponent for super-saturation
B	=	Blasius friction factor constant
C	=	diffusion constant, (cp-m^2/s)
C_1	=	empirical constant
C_2	=	empirical constant
C_3	=	empirical constant
Cp_g	=	specific heat capacity of gas, (J/kg-°C)
Cp_o	=	specific heat capacity of oil, (J/kg-°C)
C_{oil}	=	percentage of oil trapped in wax deposit, (%)
D	=	absorption constant
d_h	=	hydraulic diameter of outer jacket pipe, (m)
d_i	=	inside pipe diameter, (m)
D_{ow}	=	molecular diffusion coefficient for oil in wax, (m^2/s)
d_o	=	outside pipe diameter, (m)
d_{oc}	=	outer jacket pipe diameter, (m)
d_w	=	inside pipe diameter as a result of wax buildup, (m)
e	=	exponent for super-saturation
E	=	liquid holdup
f	=	Fanning friction factor
F_i	=	recorded parameter at time i
F_{i+1}	=	recorded parameter at time i + 1
H_D	=	oil level in drum, (m)
H_P	=	oil level in pipe, (m)
i	=	material i
I_b	=	natural background count rate
I_g	=	gas count rate
I_m	=	multiphase mixture count rate
K	=	mass absorption factor
k_{gl}	=	thermal conductivity of water-glycol, (W/m°C)
k_l	=	thermal conductivity of liquid, (W/m°C)
k_o	=	thermal conductivity of oil, (W/m°C)
k_p	=	thermal conductivity of pipe, (W/m°C)
k_w	=	thermal conductivity of wax, (W/m°C)
l_i	=	path length of material i, (m)
L	=	axial length, (m)
$\dot{m}_g$	=	gas mass flow rate, (kg/s)
$\dot{m}_o$	=	oil mass flow rate, (kg/s)
m_w	=	total mass of wax, (kg)
MW	=	molecular weight
n	=	Blasius friction factor exponent
n_w	=	total moles of wax, (kg-mole)
N_{NU}	=	Nusselt number

N_{PE} = Peclet number
N_{PR} = Prandtl number
N_{RE} = Reynolds number
N_{SR} = dimensionless number
p = pressure, (kg/m-s^2)
Q = heat loss due to cooling of oil, (W)
q = heat flux, (W/m^2)
$\tilde{Q}_o$ = volumetric flow rate, m^3/s
r = radial distance, (m)
r_i = inside pipe radius, (m)
r_o = outside pipe radius, (m)
S_i = inside pipe wetted wall fraction
S_o = outside pipe wetted wall fraction
S_w = inside pipe wetted wall as a result of wax buildup
SF = data smoothing factor
T = time, (s)
T = temperature, (°C)
$\overline{T}_{gl}$ = average glycol temperature, (°C)
T_{gl} = bulk glycol temperature, (°C)
T_{LM} = log-mean temperature, (°C)
$\overline{T}_m$ = average mixture temperature, (°C)
T_m = bulk two-phase mixture temperature, (°C)
T_o = bulk oil temperature, (°C)
T_w = wall temperature, (°C)
$\overline{T}_w$ = average wall temperature, (°C)
u = mass absorption coefficient
U_i = overall heat transfer coefficient based on inside area (W/m^2 °C)
U_o = overall heat transfer coefficient based on outside area (W/m^2 °C)
v = velocity, (m/s)
V = molar volume, (cm^3/mol)
v_l = liquid velocity, (m/s)
v_o = oil velocity, (m/s)
v_{sg} = gas superficial velocity, (m/s)
v_{sl} = liquid superficial elocity, (m/s)
V_w = wax volume, (kg/m^3)
w_w = concentration of wax in solution, (weight %)
x = axial distance, (m)
x_l = liquid height or distance, (m)
x_w = mole fraction of wax, (kg-moles)

Greek letters

a_{gl} = outside convective heat transfer coefficient of glycol, (W/m^2 °C)
a_l = inside convective heat transfer coefficient of liquid, (W/m^2 °C)
a_m = inside convective heat transfer coefficient of two-phase mixture, (W/m^2 °C)

a_o	=	inside convective heat transfer coefficient of oil, (W/m^2 °C)
Δ	=	differential
d	=	wax thickness, (m)
e	=	absolute roughness, (m)
r_g	=	density of gas, (kg/m^3)
r_i	=	density of material i, (kg/m^3)
r_{ind}	=	density of a reference medium measured using Micro Motion meter, (kg/m^3)
r_l	=	density of liquid, (kg/m^3)
r_m	=	density of two-phase mixture, (kg/m^3)
r_o	=	density of oil, (kg/m^3)
r_{ref}	=	density of a reference medium measured using Gamma Densitometer, (kg/m^3)
r_w	=	density of solid wax, (kg/m^3)
m_b	=	bulk mixture viscosity, (kg/m-s or cp)
m_g	=	gas viscosity, (kg/m-s or cp)
m_{gl}	=	glycol-water mixture viscosity, (kg/m-s or cp)
m_l	=	liquid viscosity, (kg/m-s or cp)
m_o	=	oil viscosity, (kg/m-s or cp)
m_w	=	mixture viscosity at wall interface, (kg/m-s or cp)
h	=	viscosity ratio exponent
k_d	=	mass transfer coefficient for the rate of diffusion of species into crystal lattice, (kg/m^2-s)
k_g	=	mass transfer coefficient for the combined rate of incorporation and diffusion of species into crystal lattice, (kg/m^2-s)
k_i	=	mass transfer coefficient for the rate of incorporation of species into crystal lattice, (kg/m^2-s)
k_x	=	mass transfer coefficient, (kg-moles/m^2-s)
t_w	=	wall shear stress, (kg/m-s^2)
P_1	=	empirical relationship
P_2	=	empirical relationship
Y	=	association parameter

Additional Subscripts

b	=	at bulk location
f	=	at film or wall location
ff	=	friction only
g	=	gas phase
hyd	=	hydraulic
l	=	liquid phase
tp	=	two-phase
sl	=	superficial liquid

Section 16
Appendices

Appendix A Techniques of Wax Thickness Measurement Methods

Appendix B Error Analysis of Wax Thickness Measurement

Appendix C Literature Review

Appendix D GUI Inputs – Adjustment Parameters for the Wax Deposition Program

Distribution CD

1995 Reports

DOE 3rd Quarter Report – Advisory Board Meeting Brochure, October 26, 1995
DOE 4th Quarter Report – October – December 1995

1996 Reports

Software Vendor Proposal
Flow Loop and Deposition Studies Meeting Minutes
DOE 1st Quarter Report – Advisory Board Meeting Brochure, April 25, 1996
Thermodynamics and Fluid Characterization Literature Survey
DOE 2nd Quarter Report
Multiphase Heat Transfer in Flowlines and Wellbores Literature Survey – Part 1
DOE 3rd Quarter Report – Advisory Board Meeting Brochure, October 4, 1996
DOE 4th Quarter Report

1997 Reports

Multiphase Heat Transfer in Flowlines and Wellbores – Final Report – Phase I
Multiphase Heat Transfer in Flowlines and Wellbores – Literature Survey – Part II
Single-Phase Liquid Paraffin Deposition Modeling
DOE 1st Quarter Report – Advisory Board Meeting Brochure, April 24, 1997
DOE 2nd Quarter Report
A Thermodynamic Model for Predicting the Vapor/Liquid/Solid Equilibria of Hydrocarbon Systems – Multiphase Solutions, Inc.
DOE 3rd Quarter Report – Advisory Board Meeting Brochure, October 1, 1997
DOE 4th Quarter Report

1998 Report

DOE 1st Quarter Report – Advisory Board Meeting Brochure, April 22, 1998
DOE 2nd Quarter Report
DOE 3rd Quarter Report – Advisory Board Meeting Brochure, September 24, 1998
DOE 4th Quarter Report
Investigation of Paraffin Deposition During Single-Phase Liquid Flow in Pipelines

1999 Reports

Multiphase Heat Transfer in Flowlines and Wellbores Final Report – Interim Phase
Fluid Characterization and Property Evaluation – Final Report
DOE 1st Quarter Report – Advisory Board Meeting Brochure, April 29, 1999
DOE 2nd Quarter Report
DOE 3rd Quarter Report – Advisory Board Meeting Brochure, September 30, 1999
Investigation of Paraffin Deposition During Multiphase Flow in Pipelines and Wellbores – M.S. Thesis by Mandar S. Apte
Multiphase Flow Paraffin Deposition Modeling – Ph.D. Dissertation by Ahmadbazlee Matzain

2000 Report

Paraffin Deposition Prediction in Multiphase Flowlines and Wellbores – Final Report

Papers Presented

BHRG
ETCE
ISCOP 99
AIChE
8th International Conference
SPE

Models CD

Source Code
GUI User's Manual

Single-Phase Data CD

Gardenba
Kerozene
Readme
Southpel
Waterrou

Two-Phase Data CD

Test10Mapr5
Test11Mapr21
Test12Mmay03
Test12MRSJul12
Test13May10
Test13MRSJuly16
Test14Mmay12
Test14MRSJuly14
Test15Mmay19
Test16Mmay26
Test17Mjune8
Test18Mjune9
Test19Mjune14
Test1Moct14
Test20Mjune16
Test21Mjune21
Test22Mjune23
Test23Mjuly7
Test4Mfeb23
Test4MRSJune2
Test4MRS
Test5Mmar11
Test6Mmar18
Test7Mmar23
Test7MRSJul9
Test8Mmar25
Test9Mmar30
Test9MRSJul5

Appendix A
Techniques of Wax Thickness Measurement Methods

Figure 1 shows the test section with all relevant variables required to calculate wax deposit thickness.

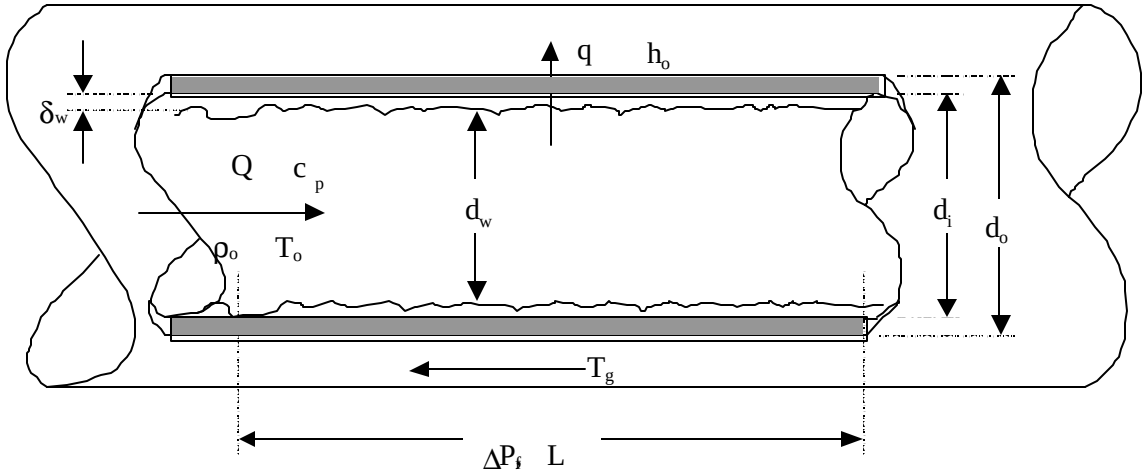

Figure 1 - Test Section with Relevant Variables for Wax Thickness Calculation

LD-LD Method

The test section in the multiphase process facility was equipped with LD-LD measurement setups for both the axial and circumferential distribution of wax. However, during this study it was found that the differential pressure transducers used in the circumferential wax deposition section were not sensitive enough to detect small changes in the liquid level. Hence, the circumferential LD-LD system was not used during this study.

The principle of this method is quite simple (Chen *et al.*, 1997). When the liquid in the test section is transferred to a drum (normally a pipe of same geometry), its volume can be measured from the level increase in the drum. Then, the wax thickness (assumed uniform) can be calculated from the liquid level decrease in the test section and the known liquid volume displaced from the test section. The equation for the calculation is

$$d_w(z) = 0.5 d_i (1 - \sqrt{DH_D / DH_P}). \qquad \text{(A.1)}$$

where d_i is the internal diameter of the test section. DH_D and DH_P are the liquid level increment in the drum and the liquid level decrement in the test section, if the working liquid (normally the liquid of the test) is transferred from the test section to the equivalent (in length and diameter) drum in a vertical position. z is the position along the test section. If the liquid density in the drum is the same as that in the test section, the ratio DH_D/DH_P can be replaced with the ratio of the differential pressures, DP_D/DP_P,

$$d_w(z) = 0.5 d_i (1 - \sqrt{DP_D / DP_P}). \quad \text{(A.2)}$$

Pressure Drop Method

This method is based on the concept that wax deposition in a pipe section reduces the hydraulic diameter of the flowing fluid inside the pipe, resulting in an increase in frictional pressure drop over the pipe section. The wax thickness on the inner pipe wall can be calculated with the equation,

$$(d_i - 2d_w)^{5-n} = \frac{2CrL}{DP_f}\left(\frac{m}{r}\right)^n \left(\frac{4Q}{p}\right)^{2-n} \quad \text{(A.3)}$$

In this equation, the friction factor at the pipe internal wall is applied, assuming the surface is smooth. The Reynolds number corresponding to the highest single-phase liquid velocity (6 ft/s) in our test is no more than 15000. The relative roughness of the stainless steel pipe is about 0.0009. From previous tests (single-phase oil), the roughness of the surface of the wax deposit was about 0.05 mm (Lund, 1999). If this value is applicable to the multiphase tests, the relative roughness of the surface of the deposit is 0.001. From the Fanning diagram shown in Fig. 2, clearly the assumption of a smooth pipe is valid for the Reynolds numbers considered.

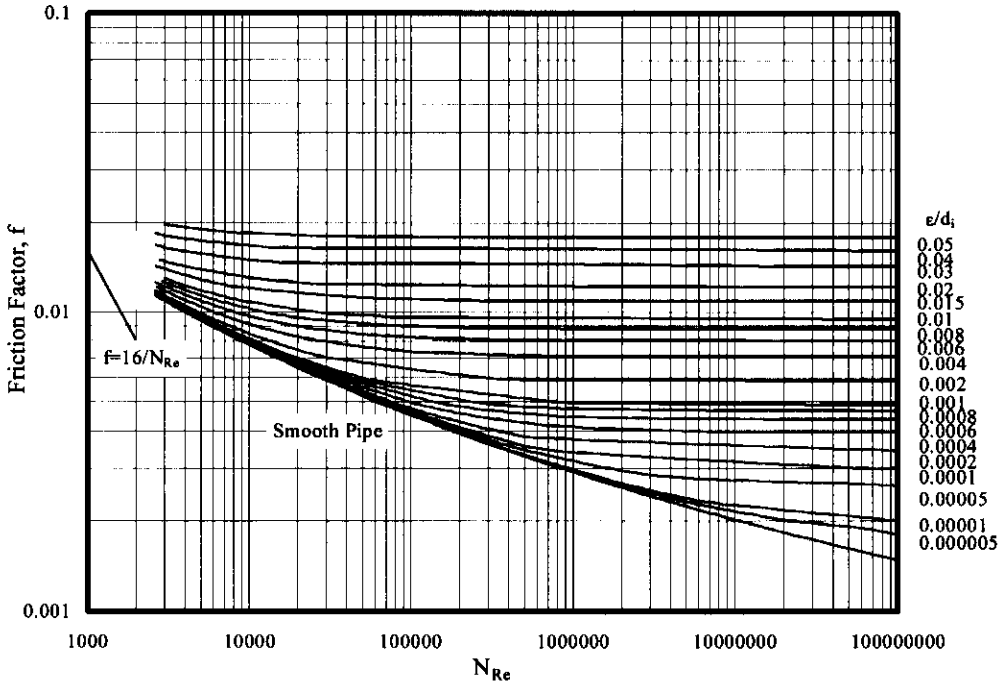

Figure 2 - Fanning Diagram

If there is no change during the experiment for the fluid properties, flow rate, flow state, and the surface roughness of the inside pipe wall, the wax thickness can be calculated with a simpler equation,

$$\delta_w = 0.5 d_i \left[1 - \left(\frac{\Delta P_{f0}}{\Delta P_f} \right)^{\frac{1}{5-n}} \right]. \qquad \text{(A.4)}$$

where DP_{f0} and DP_f are the initial pressure drop and the pressure drop during the experiment over the test section. The constant n is 1 for laminar flow and 0.2 for turbulent flow.

While using this technique, it is assumed that the wax deposit is evenly distributed inside the pipe, both in the radial and in the axial directions. It is assumed that the deposit is immobile, although deposits in laminar tests are very soft. The oil is assumed to behave as a Newtonian fluid. Although a radial temperature gradient exists, all physical properties, especially the fluid viscosity, are calculated at the bulk oil temperature. This would be reasonable for turbulent single-phase oil flow, but may not be valid for laminar flow conditions.

Heat Transfer Method

Before the occurrence of a wax layer on the pipe wall, the total resistance to heat transfer from the flowing fluid to the environment is comprised of the resistances due to convective heat transfer from the flowing fluid to the pipe wall, heat conduction through the pipe wall and any insulation or other coatings, and an appropriate heat transfer process to the environment (e.g. convective heat transfer if the pipe is exposed to water, air or other cooling fluid). After a layer of wax deposit is formed on the inside pipe wall, convective heat transfer with paraffin solidification will take place on the interface between the flowing fluid and the deposited wax layer. A thermal resistance term due to heat conduction through the wax layer is added to the total resistance to heat transfer from the flowing fluid to the environment. This added thermal resistance is approximately in direct proportion to the thickness of the wax layer on the pipe wall. Hence, the wax thickness can be determined from measurements of relevant thermal parameters by solving the heat transfer equation.

Heat transfer from the internal flowing fluid to the outside environment is described by

$$\frac{T_o - T_g}{q} = \frac{1}{h_w} \frac{r_o}{r_i - \delta_w} + \frac{r_o}{k_w} \ln \frac{r_i}{r_i - \delta_w} + \frac{r_o}{k_p} \ln \frac{r_o}{r_i} + \frac{1}{h_o}, \qquad \text{(A.5)}$$

where T_o is the bulk fluid (oil) temperature in the pipe, T_g is the environmental (glycol) temperature, q is the heat flux through the outside pipe wall, r_o and r_i are the outside and inside radii of the pipe, respectively, h_w and h_e are the film heat transfer coefficients from the flowing fluid to the wax layer and from the outside wall to the environment, respectively, k_p and k_w are the thermal conductivities of the pipe wall and the deposited wax, respectively, and d_w is the thickness of the wax layer. q can be obtained from a heat balance. The heat lost from the fluid over a certain length of pipe must equal the heat transfer to the surroundings. Thus,

$$q = \frac{C_p \rho_o Q \Delta T_o}{2\pi r_o L} \qquad \text{(A.6)}$$

where DT_o is the oil temperature drop over the test section, Q is the volume flow rate, ρ_o is the density and C_p is the specific heat of the waxy crude oil. DT_o is measured with two thermal couples at the inlet and the outlet of the test section,

$$\Delta T_o = T_{in} - T_{out} \tag{A.7}$$

At the beginning of the test, the wax thickness is zero. The heat transfer equation becomes

$$\frac{T_{o0} - T_{g0}}{q_0} = \frac{1}{h_w}\frac{r_o}{r_i} + \frac{r_o}{k_p} ln\frac{r_o}{r_i} + \frac{1}{h_o}. \tag{A.8}$$

Combining Eqs. (A.5), (A.6), (A.7) and (A.8), we obtain

$$\frac{2\pi r_o L}{C_p \rho Q}\left(\frac{T_o - T_g}{T_{in} - T_{out}} - \frac{T_{o0} - T_{g0}}{T_{in0} - T_{out0}}\right) = \frac{1}{h_w}\frac{r_o \delta_w}{r_i(r_i - \delta_w)} + \frac{r_o}{k_w} ln\frac{r_i}{r_i - \delta_w}. \tag{A.9}$$

The first term on the *RHS* of Eq. (A.9) is the change of the convective resistance inside the pipe due to a change of the surface area. The area change is very minimal if the wax thickness is minimal compared with the pipe diameter. Therefore, this term is negligible compared with the second term. Then, the wax thickness can be expressed explicitly as,

$$\delta_w = r_i\left(1 - exp\left[\frac{2\pi k_w L}{C_p \rho Q}\left(\frac{T_{o0} - T_{g0}}{T_{in0} - T_{out0}} - \frac{T_o - T_g}{T_{in} - T_{out}}\right)\right]\right). \tag{A.10}$$

Ultrasonic Method

Christian Michelsen Research (CMR), in collaboration with Norsk Hydro and Chevron Petroleum Technology Company, developed a prototype for an ultrasonic sensor to measure the thickness of a solid wax deposit under single-phase flow conditions. The probe is installed flush mounted with the inner pipe wall. The probe emits an ultrasonic pulse and then measures the time for the pulse to reflect from the opposing wall and return to the probe. Based on the speed of sound in the liquid in the pipe and the travel time, the deposit thickness on the wall opposite of the probe can be calculated. The speed of sound must be accurately known for the test fluid for this technique to be used. This sensor is still under development, and was used in the single-phase flow loop to test the sensor's capability.

Visual Observation and Manual Measurements

At the end of each test, the spool piece was depressurized and then removed. Careful observations of the wax deposit were made. Before depressurizing, gas was used to push the oil in the test section back to the separator. The softer deposits might be stripped off from the pipe wall during this process.

A vernier caliper or a depth gauge was then used to measure the thickness of the wax deposits. Samples of the wax deposit were then taken and sent to Chevron Petroleum Technology Company for High Temperature Gas Chromatography (HTGC) analysis.

For some tests the volume of water needed to fill the spool piece with wax was also measured. This was compared with the volume of water needed to fill the clean spool piece. The difference in the readings would give an estimate of the total volume of wax in the spool piece. Knowing the dimensions of the spool piece, an estimate of the average thickness of the wax deposit was made. Unlike other thickness measurements, this measurement was done after the test section was depressurized. The wax deposit may swell due to the expansion of the gas trapped in the deposit.

Appendix B
Error Analysis of Wax Thickness Measurement

Error Analysis for Single-Phase Test

In Lund's (1998) M.S. thesis, an error analysis was performed for the single-phase tests to determine how sensitive the different deposit thickness measurement methods are to errors in the data. Following are the descriptions and the results of the analysis.

LD-LD Method

The error associated with the height measurements in the LD-LD (Liquid Displacement-Level Detection) method was evaluated based on the equations used in the LD-LD method. An error of ±7.62 mm H_2O (±0.3 in.) in the pressure measurements to determine fluid height would give an error of ±0.1 mm (±0.0039 in.) in the deposit thickness for the spool piece studied. An error of ±7.62 mm H_2O (±0.3 in.) should be well within the precision and accuracy of our current measurement capabilities.

For laminar tests there is an additional question of how representative is the amount of wax being measured by the LD-LD method compared to what was actually in the spool piece during the test. It is believed that in some cases a significant portion of the laminar deposits were removed when the test fluid is transferred out of the test section. Therefore, all the LD-LD measurements made after laminar tests should give less deposit thickness than what was in the spool piece at the end of the test. This was not a problem in the turbulent tests, as they yielded a much firmer wax deposit.

Pressure Drop Method

The following error sensitivity analysis is based on a case with an oil inlet temperature of 40.6ºC (105°F). The inlet glycol temperature is 32.2ºC (90°F); ε is the error in pressure drop; ξ is the error in deposit thickness; δ is the deposit thickness for a given pressure drop ΔP.

As shown in Table 1, when the entire loop is used to measure pressure drop, we find no problem with the turbulent case. An error of ±254 mm H_2O (±10 in.) in pressure drop only produces a ±0.13 mm (±0.0051 in.) error (±6%) in the computed thickness. The laminar case is more serious. Here, an error of only ±5.08 mm H_2O (±0.2 in.) in pressure drop causes a 0.17 mm (0.0067 in.) error (±8%) in the deposit thickness calculated from the pressure drop data.

	DP	f(DP)	e	d	x
	mm H_2O (in. H_2O)	mm (in.)	mm H_2O (in. H_2O)	mm (in.)	mm (in.)
Laminar	146 (5.73)	2.00 (0.079)	5.08 (0.2)	2.17 (0.085)	0.17 (0.0067)
Turbulent	7620 (300)	1.93 (0.076)	254 (10.0)	2.06 (0.081)	0.13 (0.0051)

Table 1 - Effect of Pressure Drop Errors on Errors in Calculated Deposit Thickness - Length is 50 m (164 ft)

The problem in laminar cases is even more acute if the 5 m (16.4 ft) test sections are used to determine thickness, as shown in Table 2. Table 2 shows that an error of only ±0.508 mm H_2O (±0.02 in.) causes an error of ±0.17 mm (0.0067 in.) in the computed deposit thickness during a laminar test. Again, the turbulent case appears relatively accurate.

	DP	f(DP)	e	d	x
	mm H_2O (in. H_2O)	mm (in.)	mm H_2O (in. H_2O)	mm (in.)	mm (in.)
Laminar	14.5 (0.57)	1.97 (0.078)	0.508 (0.02)	2.14 (0.0843)	0.17 (0.0067)
Turbulent	774.7 (30.5)	2.00 (0.079)	25.4 (1.0)	2.13 (0.0838)	0.13 (0.0051)

Table 2 - Effect of Pressure Drop Errors on Errors in Calculated Deposition Thickness - Length is 5 m (16.4 ft)

In summary, the pressure drop must be measured to ±0.25 mm H_2O (±0.01 in.) to determine the deposit thickness to ±0.1 mm (0.004 in.) when the 5 m (16.4 ft) test sections are used in laminar flow. For turbulent or laminar flow when the entire loop is involved, suitable precision of ±0.1 mm (0.004 in.) may be obtained with pressure measurements to the nearest ±2.54 mm H_2O (±0.1 in.). The Rosemount differential pressure transducers were factory calibrated to ±9.7 mm H_2O (±0.38 in.) for the 50 m case, and ±0.97 mm H_2O (±0.038 in.) for the 5 m case. The turbulent cases can still present problems if the deposits are thin, as we encountered in the ΔT = 8.3ºC (15°F) test. Here, the deposit thickness was 0.2 mm (0.0079 in.), requiring a pressure drop measurement accuracy of ±2.54 mm H_2O (±0.1 in.) to obtain a maximum ±5% error in the calculated thickness.

Heat Transfer Method

The error analysis for the heat transfer method had to be performed in two stages. First, laminar flow was considered, then turbulent flow. The equations were solved iteratively for the deposit thickness, δ, by successive substitution of estimated thickness values. The temperature profile in the flow loop was simulated with the aid of D-WAX (1996) for the laminar and turbulent cases. This gave order of magnitude results for the temperatures of the fluids and the wall that are required for these calculations.

The laminar flow case is relatively insensitive to temperature measurement errors. An error of ± 0.1°C (0.18ºF) gave an error of about ±0.3 mm (±0.012 in.) in the deposit thickness. The required accuracy for ±0.1 mm (±0.0039 in.) in the deposit thickness should be on the order of ±0.056ºC (±0.1°F). The Rosemount temperature transducers were factory calibrated to ±0.27ºC (±0.48°F).

The turbulent case indicated that an error of ±0.01°C (±0.018ºF) gave an error in calculated deposit thickness of about ±0.1 mm (±0.0039 in.). This implies that our measurement accuracy would need to be on the order of ±0.011ºC (±0.02°F) to obtain the desired precision, a value not attainable with the instruments used.

Error Analysis for Multiphase Test

Error analyses were also conducted for the LD-LD method, pressure drop method and heat transfer method used to measure the thickness of the wax deposit in the multiphase flow tests. The results show that the LD-LD method can give the most reliable measurement. When the largest differential pressure (corresponding to full pipe liquid displacement) is used, the error in the wax thickness is only ±0.015 mm. The pressure drop method can give accurate measurement at high flow rate, but is not applicable for low flow rates. On the other hand, the heat transfer method is only applicable when the flow rate is low and the difference between the inlet and outlet oil temperatures is sufficiently large. The uncertainty of the thermal conductivity of the wax deposit may cause significant error when using the heat transfer method.

LD-LD Method

The internal diameter of the test section given by the manufacturer is 2.067 in. (52.50 mm), from which the precision limit is estimated as ±0.001 in. (0.025 mm). From the manufacturer's catalog, the precision limit (accuracy) of the differential pressure transducers for both DP_D and DP_P is ±0.19 in. H_2O (±0.075% of span, 250 in. H_2O). There are two contributions to the bias limit of the differential pressure transducer. One is the ambient temperature effect (per 50 ^{o}F), ±0.19 in. H_2O [±(0.0125%URL+0.0625%span), URL is up range limit]. The other is the static pressure effect, which includes the zero error and the span error. The zero error can be calibrated out at line pressure. The span error is ±0.25 in. H_2O [±(0.2% × reading/1000 psi × span)]. Therefore, the bias limit is ±0.31 in. H_2O by use of the root sum square (RSS) method.

If the wax thickness is assumed to be 1 mm, DP_D/DP_P is 0.925 from Eq. (B.2). Therefore, we may use the same nominal value for DP_D and DP_P when estimating the error of d_w.

The partial derivatives needed for the error analysis are:

$$\frac{\partial d_w}{\partial d_i} = 0.5\left(1-\sqrt{\Delta P_D / \Delta P_P}\right) \tag{B.1}$$

$$\frac{\partial d_w}{\partial \Delta P_P} = \frac{d_i}{4}\sqrt{\Delta P_D / \Delta P_P}\,\frac{1}{\Delta P_P} \tag{B.2}$$

$$\frac{\partial d_w}{\partial \Delta P_D} = -\frac{d_i}{4}\sqrt{\Delta P_D / \Delta P_P}\,\frac{1}{\Delta P_D} \tag{B.3}$$

Then, the bias limit and precision limit of d_w can be found from the following expressions (Coleman and Steele, 1989):

$$B_{d_w} = \left[\left(\frac{\partial d_w}{\partial d_i} B_{d_i} \right)^2 + \left(\frac{\partial d_w}{\partial \Delta P_D} B_{\Delta P_D} \right)^2 + \left(\frac{\partial d_w}{\partial \Delta P_P} B_{\Delta P_P} \right)^2 \right]^{1/2} \quad \text{(B.4)}$$

$$P_{d_w} = \left[\left(\frac{\partial d_w}{\partial d_i} P_{d_i} \right)^2 + \left(\frac{\partial d_w}{\partial \Delta P_D} P_{\Delta P_D} \right)^2 + \left(\frac{\partial d_w}{\partial \Delta P_P} P_{\Delta P_P} \right)^2 \right]^{1/2} \quad \text{(B.5)}$$

The bias limit and precision limit for every variable in Eq. (A.2) are listed in Table 3. Also, the nominal values for these variables should be given to estimate the error in d_w. Obviously, the contribution from the error in the pipe internal diameter is negligible, since P_{di} is very small and the ratio of DP_D to DP_P is very close to 1. The differential pressure is about 230 in. H_2O when the test section pipe or the equivalent drum is full of liquid in the vertical position. We may use it as the nominal value of DP_D and DP_P in the error analysis.

Variable	Bias limit (B)	Precision limit (P)	Nominal value
d_i	0	±0.025 mm	52.50 mm
DP_D	±0.31 in. H_2O	±0.19 in. H_2O	230.0 in. H_2O
DP_P	±0.31 in. H_2O	±0.19 in. H_2O	230.0 in. H_2O

Table 3 - Bias Limits, Precision Limits and Nominal Values of Variables in Wax Thickness Determination Using LD-LD Method

Then, the bias and precision limits of d_w can be obtained as $B_{d\,w}$ = ±0.025 mm and $P_{d\,w}$ = ±0.015 mm. By use of the RSS method, the error in d_w can be calculated from $E_{dw}=(B_{dw}^2+ P_{dw}^2)^{1/2}$=±0.029 mm with a confidence of 95%. If the value of d_w changes from 0.1 to 1 mm, its relative error changes from ±29% to ±2.9%.

On the other hand, the error in d_w depends on how large the values of DP_D and DP_P are taken during the measurement for calculation of d_w. Table 4 lists the errors in d_w when the differential pressures change from small to large.

DP (in. H_2O)	B_{dw} (±mm)	P_{dw} (±mm)	Error of d_w (±mm)
40	0.144	0.086	0.166
80	0.072	0.043	0.083
160	0.036	0.022	0.042
230	0.025	0.015	0.029

Table 4 - Dependence of d_w Error on Value of DP

In our tests, blank pipe readings were obtained almost every time for the test section and the equivalent drum. In other words, the differential pressure transducers were calibrated every time under the same conditions of the LD-LD measurement. Therefore, the bias errors caused by the ambient temperature effect and the static pressure effect could be calibrated out. Then, the errors in d_w are equal to the precision limits listed in the third column in Table 4 for different values of the differential pressure.

Also, the differential pressures corresponding to full pipe (about 230 in. H_2O) were obtained during every LD-LD measurement, and the wax thickness values calculated from these full pipe readings were used for analyses of wax deposition. Therefore, the error in the LD-LD measurement is about ±0.015 mm from the above analysis.

Pressure Drop Method

From the manufacturer's catalog, the precision limit (accuracy) of the differential pressure transducers for DP_{f0} (and DP_f) is ±0.11 in. H_2O (±0.075% of 150 in. H_2O span). The ambient temperature effect (per 50 ^oF) on the bias limit of the differential pressure transducer is ±0.24 in. H_2O [±(0.0125%URL+0.0625%span)]. The static pressure effect is ±0.15 in. H_2O [±(0.2% × reading/1000 psi × span)]. Therefore, the bias limit is ±0.28 in. H_2O by use of the RSS method.

If the wax thickness is assumed to be 1 mm, DP_{f0}/DP_f is 0.83 from Eq. (A.4) for turbulent flow. Therefore, the same nominal value for DP_{f0} and DP_f may be used when estimate the error in d_w.

The partial derivatives needed for the error analysis are:

$$\frac{\partial \delta_w}{\partial d_i} = 0.5\left[1-\left(\frac{\Delta P_{f0}}{\Delta P_f}\right)^{\frac{1}{5-n}}\right] \tag{B.6}$$

$$\frac{\partial \delta_w}{\partial \Delta P_{f0}} = -\frac{d_i}{2(5-n)}\left(\frac{\Delta P_{f0}}{\Delta P_f}\right)^{\frac{1}{5-n}}\frac{1}{\Delta P_{f0}} \tag{B.7}$$

$$\frac{\partial \delta_w}{\partial \Delta P_f} = \frac{d_i}{2(5-n)}\left(\frac{\Delta P_{f0}}{\Delta P_f}\right)^{\frac{1}{5-n}}\frac{1}{\Delta P_f} \tag{B.8}$$

Then, the bias limit and precision limit of d_w can be found from the following expressions:

$$B_{d_w} = \left[\left(\frac{\partial \delta_w}{\partial d_i}B_{d_i}\right)^2 + \left(\frac{\partial \delta_w}{\partial \Delta P_{f0}}B_{\Delta P_{f0}}\right)^2 + \left(\frac{\partial \delta_w}{\partial \Delta P_f}B_{\Delta P_f}\right)^2 + 2\frac{\partial \delta_w}{\partial \Delta P_{f0}}\frac{\partial \delta_w}{\partial \Delta P_f}B_{\Delta P_{f0}}B_{\Delta P_f}\right]^{1/2} \tag{B.9}$$

$$P_{d_w} = \left[\left(\frac{\partial \delta_w}{\partial d_i}P_{d_i}\right)^2 + \left(\frac{\partial \delta_w}{\partial \Delta P_{f0}}P_{\Delta P_{f0}}\right)^2 + \left(\frac{\partial \delta_w}{\partial \Delta P_f}P_{\Delta P_f}\right)^2\right]^{1/2} \tag{B.10}$$

Because DP_{f0} and DP_f were measured with the same differential pressure transducer, their bias limits were fully correlated. The bias limit and precision limit for every variable in Eq. (A.4) are listed in Table 5. Also, the nominal values for these variables should be given to estimate the error in d_w. The differential pressure in the test section was about 12 in. H_2O when single-phase oil flowed at 4 ft/s (turbulent state, n = 0.2). We may use it as the nominal value of DP_{f0} and DP_f in the error analysis.

Variable	Bias limit	Precision limit	Nominal value
d_i	0	±0.025 mm	52.50 mm
DP_{f0}	±0.28 in. H_2O	±0.11 in. H_2O	12.0 in. H_2O
DP_f	±0.28 in. H_2O	±0.11 in. H_2O	12.0 in. H_2O

Table 5 - Bias Limits, Precision Limits and Nominal Values of Variables in Wax Thickness Determination Using Pressure Drop Method

Then, the bias and precision limits of d_w can be obtained as B_{dw} = ±0 mm and P_{dw} = ±0.07 mm. The error in d_w is identical to the precision limit, E_{dw} = ±0.07 mm, with a confidence of 95%. If the value of d_w changes from 0.1 to 1 mm, its relative error changes from ±70% to ±7%.

Table 6 lists the errors in d_w for different values of the differential pressure, DP_{f0} (or DP_f). From Table 6 it is obvious that, at low flow rate (*e.g.* 2 ft/s corresponding to about 3 in. H_2O of differential pressure), measurement of the wax thickness may not be reliable. Therefore, the pressure drop method is not applicable at low flow rate situations, especially laminar flow.

DP (in. H_2O)	Error of d_w (±mm)
3	0.28
6	0.14
12	0.07
24	0.035
48	0.018
96	0.009

***Table 6 - Dependence of d_w Error on Value of* DP**

Heat Transfer Method

In Eq. (A.10) k_w, C_p and r can be assumed as constants. The errors in r_i, L and Q are negligible compared with the errors in temperature measurements. The oil temperatures, T_o, T_{in} and T_{out}, were measured with thermal couples (Rosemount NIST Type T). From the manufacturer's catalog, the precision limit (digital accuracy plus D/A accuracy) of the sensors is ±0.45 °F. The bias limit of the sensors (the ambient temperature effect on the digital and D/A accuracies per 36 °F) is ±0.19 °F. The environmental temperature (glycol temperature), T_g, was measured with an RTD (Rosemount Pt 100). Its precision limit is ±0.18 °F and its bias limit is ±0.08 °F.

The partial derivatives needed for the error analysis are:

$$\frac{\partial d_w}{\partial T_{o0}} = -\frac{2\pi r_i k_w L}{C_p \rho Q (T_{in0} - T_{out0})} \exp\left[\frac{2\pi k_w L}{C_p \rho Q}\left(\frac{T_{o0} - T_{g0}}{T_{in0} - T_{out0}} - \frac{T_o - T_g}{T_{in} - T_{out}}\right)\right] \tag{B.11}$$

$$\frac{\partial d_w}{\partial T_{g0}} = \frac{2\pi r_i k_w L}{C_p \rho Q (T_{in0} - T_{out0})} \exp\left[\frac{2\pi k_w L}{C_p \rho Q}\left(\frac{T_{o0} - T_{g0}}{T_{in0} - T_{out0}} - \frac{T_o - T_g}{T_{in} - T_{out}}\right)\right] \tag{B.12}$$

$$\frac{\partial \delta_w}{\partial T_o} = \frac{2\pi r_i k_w L}{C_p \rho Q (T_{in} - T_{out})} \exp\left[\frac{2\pi k_w L}{C_p \rho Q}\left(\frac{T_{o0} - T_{g0}}{T_{in0} - T_{out0}} - \frac{T_o - T_g}{T_{in} - T_{out}}\right)\right] \tag{B.13}$$

$$\frac{\partial \delta_w}{\partial T_g} = -\frac{2\pi r_i k_w L}{C_p \rho Q (T_{in} - T_{out})} \exp\left[\frac{2\pi k_w L}{C_p \rho Q}\left(\frac{T_{o0} - T_{g0}}{T_{in0} - T_{out0}} - \frac{T_o - T_g}{T_{in} - T_{out}}\right)\right] \tag{B.14}$$

$$\frac{\partial \delta_w}{\partial T_{in0}} = \frac{2\pi r_i k_w L (T_{o0} - T_{g0})}{C_p \rho Q (T_{in0} - T_{out0})^2} \exp\left[\frac{2\pi k_w L}{C_p \rho Q}\left(\frac{T_{o0} - T_{g0}}{T_{in0} - T_{out0}} - \frac{T_o - T_g}{T_{in} - T_{out}}\right)\right] \tag{B.15}$$

$$\frac{\partial \delta_w}{\partial T_{out0}} = -\frac{2\pi r_i k_w L (T_{o0} - T_{g0})}{C_p \rho Q (T_{in0} - T_{out0})^2} \exp\left[\frac{2\pi k_w L}{C_p \rho Q}\left(\frac{T_{o0} - T_{g0}}{T_{in0} - T_{out0}} - \frac{T_o - T_g}{T_{in} - T_{out}}\right)\right] \tag{B.16}$$

$$\frac{\partial \delta_w}{\partial T_{in}} = -\frac{2\pi r_i k_w L (T_o - T_g)}{C_p \rho Q (T_{in} - T_{out})^2} \exp\left[\frac{2\pi k_w L}{C_p \rho Q}\left(\frac{T_{o0} - T_{g0}}{T_{in0} - T_{out0}} - \frac{T_o - T_g}{T_{in} - T_{out}}\right)\right] \tag{B.17}$$

$$\frac{\partial \delta_w}{\partial T_{out}} = \frac{2\pi r_i k_w L (T_o - T_g)}{C_p \rho Q (T_{in} - T_{out})^2} \exp\left[\frac{2\pi k_w L}{C_p \rho Q}\left(\frac{T_{o0} - T_{g0}}{T_{in0} - T_{out0}} - \frac{T_o - T_g}{T_{in} - T_{out}}\right)\right] \tag{B.18}$$

The bias limits of the temperature sensors are much smaller than their precision limits. Therefore, we may only check the error caused by the precision limits:

$$P_{d_w} = \left[\begin{array}{l} \left(\frac{\partial \delta_w}{\partial T_{o0}} P_{T_{o0}}\right)^2 + \left(\frac{\partial \delta_w}{\partial T_{g0}} P_{T_{g0}}\right)^2 + \left(\frac{\partial \delta_w}{\partial T_o} P_{T_o}\right)^2 + \left(\frac{\partial \delta_w}{\partial T_g} P_{T_g}\right)^2 \\ + \left(\frac{\partial \delta_w}{\partial T_{in0}} P_{T_{in0}}\right)^2 + \left(\frac{\partial \delta_w}{\partial T_{out0}} P_{T_{out0}}\right)^2 + \left(\frac{\partial \delta_w}{\partial T_{in}} P_{T_{in}}\right)^2 + \left(\frac{\partial \delta_w}{\partial T_{out}} P_{T_{out}}\right)^2 \end{array}\right]^{1/2} \tag{B.19}$$

The parameters corresponding to a single-phase test with an oil flow rate of 4 ft/s are used for the error analysis. The precision limits and nominal values of the temperatures are listed in Table 7. Also, r_I = 26.25 mm, k_w = 0.21 W/m-K (1.5 times the oil conductivity), L = 6.096 m, C_p = 1894 J/s-m-K, Q = 0.00264 m^3/s, and ρ = 828.0 kg/m^3.

Variable	Precision limit (±°F)	Nominal value (°F)
T_{f0}	0.45	99.0
T_f	0.45	99.0
T_{e0}	0.18	60.0
T_e	0.18	60.0
T_{in0}	0.45	101.0
T_{out0}	0.45	97.0
T_{in}	0.45	101.0
T_{out}	0.45	97.0

Table 7 - Precision Limits and Nominal Values of Variables in Wax Thickness Determination Using Heat Transfer Method

Then, the error in d_w is calculated using Eq. (16) and E_{dw} = ±0.11 mm with a confidence of 95%. If the value in d_w changes from 0.1 to 1 mm, its relative error changes from ±110% to ±11%.

Table 8 lists the errors in d_w for different values of the temperature drop T_{in}-T_{out}. From Table 8 it is clear that, at high flow rate (*e.g.* 6 ft/s and above), the temperature drop may not be large enough to obtain accurate measurement of the wax thickness.

T_{in}-T_{out} (°F)	Error of d_w (±mm)
1	0.44
2	0.22
4	0.11
8	0.055

Table 8 - Dependence of $\mathbf{d_w}$ Error on Value of $\mathbf{\Delta T}$

The conductivity of the wax deposit may change significantly during a test or from one test to another due to the variation of the oil content trapped in the deposit. Previous experimental results showed that the conductivity could change from one to two times the oil conductivity. If we use 1.5 times the oil conductivity as the conductivity of the wax deposit and the uncertainty is ±0.5 times the oil conductivity, the resulted error range in the wax thickness will be from 0.71 mm to 1.44 mm from Eq. (A.10), based on the above experimental condition and assuming the wax thickness is 1 mm.

The above error analysis indicates that the heat transfer method may not be reliable to give an accurate measurement of the wax thickness because of the small difference between the inlet and outlet oil temperature, and the uncertainty of the thermal conductivity of the wax deposit.

Appendix C
Literature Review

Since its inception, the petroleum industry has been plagued by paraffin. Its long time nature as a nuisance, easily and inexpensively treated with chemicals and scrapers, has resulted in a lack of basic research regarding the actual deposition phenomena. However, paraffin deposition can be the determining factor for not producing deep-water fields, many of which are tied in to nearby platforms with sub-sea flowlines. It could lead to a potentially expensive, catastrophic event in the history of a project.

The cost of remediation due to pipeline blockage is proportionally greater as development depth increases (Pate (1995)). Many oil and gas related companies have conducted significant research on the phenomenon of paraffin deposition for several years, yet the physics of the actual deposition process remains poorly understood. The consensus of the petroleum industry is that, once a radial temperature gradient is established between the oil and pipe wall, and the oil temperature is below its WAT, deposition occurs (Creek *et al.* (1999)). The WAT is defined as the temperature at which paraffin particles first begin to precipitate from a hydrocarbon liquid solution, as indicated by the cloudiness of the liquid. Paraffin or wax could also form near the pipe wall even if the bulk oil is at a temperature above its WAT. Deposition will occur when the inner pipe wall surface temperature is below both the solution temperature and the solution WAT.

There are four possible mechanisms that have been identified for paraffin deposition: molecular diffusion, shear dispersion, Brownian diffusion, and gravity settling (Burger et al. (1981)). Burger et al. showed that gravity settling has no impact on paraffin deposition, and that Brownian diffusion can be ignored. Investigators (Brown et al. (1993)) consider molecular diffusion to be the dominant mechanism, although there is some discussion on the impact of shear dispersion (Burger et al.). Bern et al. (1980) stated that molecular diffusion transports paraffin in solution, while shear dispersion transports solid paraffin particles.

Paraffin deposition increases the frictional pressure drop in a pipe by reducing the effective diameter of the pipe, d_w. Some investigators report that the effective roughness also increases significantly due to paraffin deposition (Bern et al.). Any increase in roughness will result in an increase in the friction factor (under turbulent flow) , f, which will result in an increase in the pressure drop as shown in Eq. C.1, the Fanning equation for frictional pressure drop in pipes.

$$\frac{\Delta p}{\Delta L} = \frac{2 f \rho_o v_o^2}{d_w} \quad \text{..... (C.1)}$$

Paraffin deposition in multiphase flow is poorly understood. For single-phase flow of waxy crude oil, even though there has been a significant amount of work found in the literatures, the deposition mechanisms are still not well understood.

Paraffin Deposition in Single-Phase Flow Systems

Several authors have investigated the phenomenon of paraffin deposition in single-phase oil flow systems. Matzain (1996) and Lund (1998) reported thorough reviews of the existing literature on the theory of wax deposition during single-phase flow. Four mechanisms were identified as possible causes

for paraffin deposition: molecular diffusion, shear dispersion, Brownian diffusion, and gravity settling. It has been shown that gravity settling has no impact on paraffin deposition and that Brownian diffusion can be ignored (Burger *et al*. (1981), Bern *et al*. (1980)). Most investigators claim that molecular diffusion controls wax deposition and that shear dispersion is not a major contributor (Brown *et al*.[(d)] (1993), Bern *et al*. (1980)).

Hamouda and Davidsen (1995), and Eaton and Weeter (1976) have shown that the shear dispersion mechanism is not significant. Based on experimental observations, Creek *et al*. (1999) also acknowledge that shear dispersion, Brownian diffusion and gravity settling are not major contributors to the deposition phenomenon. .....

Molecular Diffusion

The difference in the temperature between the oil and the pipe wall produces a concentration gradient of the wax phase. This is due to the temperature dependency of solubility of paraffin species in oil. The concentration gradient leads to a mass transfer of dissolved wax molecules towards the pipe wall, and this mass flux is usually expressed in terms of Fick's law of mass flow. According to Cussler (1987), Fick's law states that the mass flux J_i of diffusing species in a given volume is proportional to the concentration gradient. The constant of proportionality is called the diffusion constant, D_i, and is a property of that system. Fick's Law is expressed as:

$$J = A\sum_{i=1}^{n}\left\{D_i\frac{\partial C_i}{\partial r}\right\} = A\frac{\partial T}{\partial r}\sum_{i=1}^{n}\left\{D_i\frac{\partial C_i}{\partial T}\right\} . \quad \text{..... (C.2)}$$

Usually, all higher carbon number components constituting the wax phase are lumped into one single, independent, constituent of the oil. The diffusion coefficient, $D_{ow,}$ is determined between this wax phase and the oil. The rate of transport of the dissolved wax phase can then be expressed as:

$$\frac{dm_w}{dt} = -\rho_o D_{ow} A_i \frac{dC_w}{dr} = -\rho_o D_{ow} A_i \frac{dC_w}{dT}\frac{dT}{dr} . \quad \text{..... (C.3)}$$

The molecular diffusion coefficient, D_{ow}, is often expressed either as an experimental constant divided by the viscosity or by empirical correlations developed for normal paraffins by Wilke and Chang (1955) or Hayduk and Minhas (1982). The Wilke-Chang (1955) correlation is given in Eq. C.4 for diffusion of solute A in solvent B.

$$D_{AB} = \frac{7.4x10^{-12}\left(\phi M_B\right)^{1/2}T}{m_B V_A^{0.6}} \approx \frac{C}{m_B} \quad \text{..... .(C.4)}$$

Rygg et al. (1998) used the correlation of Hayduk and Minhas (1982) developed for normal paraffin solutions and given in Eq. C.5.

$$D_{AB} = 13.3x10^{-12}\frac{T^{1.47}m_B^{10.2/V_A - 0.791}}{V_A^{0.71}} \approx \frac{C}{m_B} \quad \text{..... (C.5)}$$

where

$$C = 13.3x10^{-12}\ \frac{T^{1.47}\, m_B^{\left(\frac{10.2}{V_A}-0.791+1\right)}}{V_A^{0.71}} \quad \text{..... (C.6)}$$

In Eqs. C.4 and C.5, V is the molal volume, ϕ is the association factor, and M is the molecular weight. The viscosity is given in cp, and temperature is given in K. Equations C.4 and C.5 are both derived for binary mixtures at infinite dilution, but Reid et al. (1986) reported that D_{AB} is assumed to be representative even for concentrations of A in B up to 5%, but again for binary mixtures.

The available correlations for predicting diffusion coefficients are suited for binary mixtures only. Cussler (1987) describes the difficulty in predicting the diffusion coefficients for multicomponent mixtures.

Burger et al. reported that dT/dr in Eq. C.3 can be calculated in experiments based on the measured temperature decrease as shown in Eq. C.7.

$$\frac{dT}{dr} = \frac{Q\rho_o C_{po}\frac{dT}{dL}}{k_o \pi d_i} \quad \text{..... (C.7)}$$

Eaton and Weeter (1976) reported that deposition rate increases as the oil temperature decreases until maximum deposition rate is reached, after which the deposition rate decreases with decreasing oil temperature. They also reported that the deposition rate increased steadily with increasing dT/dr. Both observations agree with the molecular diffusion equation given in Eq. C.3.

Based on experimental observations, Creek *et al.* (1999) proposed that Fick's diffusion law could not solely and adequately describe the wax deposition phenomenon. The common approach for treating the summation in Eq. C.2 is to consider paraffin as one pseudo component as shown in Eq. C.3. Creek *et al.* (1999) pointed out that this is not appropriate, as wax was not a single compound but rather a combination of many hydrocarbon compounds with carbon chain lengths ranging from C_{15} up to C_{70+}.

Creek (1998) hypothesized that paraffin deposition is analogous to diffusion controlled crystallization. Among several pieces of information required for predicting paraffin deposition buildup rates, of special importance is the knowledge about the oil content of the wax deposit. Burger *et al.* (1981) determined that the trapped oil content ranged from 83% to 86%, while Rygg *et al.* (1998) used 60% for their gas-oil example with some success. Lund (1998) reported oil in wax concentration values of 90% for soft deposits and from 50% to 72 % for hard deposits.

Several researchers assumed the thermal conductivity of the wax deposit to be equal to the thermal conductivity of the oil (Mendes and Braga (1996), Svendsen (1993), Niesen *et al.* (1993)). This would be a reasonable approximation for soft deposits (~85 % oil). However, Lund (1998) reported much higher values of thermal conductivity for hard deposits (~50% oil). Among other phenomena, the aging of the deposit needs to be considered wherein the wax deposit characteristics change with time and result in significantly harder deposits. Such a behavior affects the physical properties of wax and wax deposition rates as experimentally reported by Lund (1998).

Shear Dispersion and Turbulent Effects

Burger et al. (1981) reported that lateral movement of small particles from areas of high velocity to areas of low velocity induced by shearing near the wall could cause paraffin deposition. This mechanism is referred to as shear dispersion, and it moves paraffin particles that have crystallized in the oil to the wall where they can deposit if the conditions are correct. Burger et al. expressed the rate of deposition due to shear dispersion as given in Eq. C.8.

$$\frac{dm_s}{dt} = A_i k^* C_w^* g \quad \text{..... (C.8)}$$

Although there is discussion of the magnitude of shear dispersion relative to molecular diffusion, there is a general agreement that shear rate has an effect on the paraffin deposition phenomenon. Brown et al.[(d)] (1993) reported that increasing the shear rate from 330 to 1330 s^{-1} decreased deposition rate by a factor of 2-6, and Bern et al. (1980) reported that depositional tendency decreases rapidly at low shear rates, and slowly at high shear rates. Jessen and Howell (1958) stated that the deposition rate reaches a maximum right before turbulent flow occurs.

Hsu et al. (1995) reported that even if shear dispersion does not contribute to deposition, shear rate can contribute to the deposition rate since many waxy crude oils are non-Newtonian and the effective viscosity is a function of the shear rate. Since the molecular diffusion coefficient can be expressed as a function of viscosity, it is also a function of the shear rate if the oil behaves as a non-Newtonian fluid.

Weingarten and Euchner (1988) observed sloughing at high shear rates in a 6.4-mm (0.25 in.) diameter flow loop. They also reported that the onset of sloughing was not related to the transition from laminar to turbulent flow. Creek and Hobson (1996) reported periodic sloughing in a 3.2-mm (0.13 in.) diameter flow loop.

Shear rate affects not only the deposition rate but also the nature of the paraffin deposits. Jessen and Howell reported that increasing the flow rate caused an increase in the hardness of the deposit. Matlach and Newberry (1983) reported that increasing the shear rate increases the hardness of the deposit as well as the median carbon number of the deposit. Brown et al.[(d)] (1993) reported that at high shear rates the deposits are hard and brittle, while at low shear rates the deposits are soft and pliable. Eaton and Weeter (1976) performed paraffin deposition tests using a rotating disk. They noted that the deposit changed significantly over a narrow range of rotational speeds. At 200 rpm they observed soft deposits, while at 300 rpm they found hard deposits. At 250 rpm they found an intermediate deposit.

Molecular Diffusion versus Shear Dispersion

It is necessary to know what mechanisms cause the deposition in order to predict paraffin deposition rates. Molecular diffusion and shear dispersion are the two mechanisms most often considered, but there are various opinions on the impact of the shear dispersion mechanism.

Mendes and Braga (1996) and Brown et al. used only molecular diffusion in their models; while Hamouda and Davidsen (1995) reported that other mechanisms should not be over looked, although molecular diffusion is the dominant mechanism. Weingarten and Euchner (1988) believe that shear dispersion deposition is important in low shear cases, although they did not observe any deposition without a wall colder than the oil. Burger et al. (1981) reported that molecular diffusion was dominant at high temperatures and high heat flow, but that shear dispersion was important at low temperatures and low heat flow. Hsu et al. (1995) stated that it is important to consider both shear effects and molecular

diffusion. Eaton and Weeter (1976) reported that on the basis of numerous experiments there is never deposition in the absence of a temperature gradient, even in the presence of an initial deposit which can act as a seed crystal.

Thermal Conductivity of Paraffin Deposits

Although a thermal conductivity value for the deposit is necessary for all the paraffin deposition models, values used by the models are rarely mentioned. Mendes and Braga (1996) assumed the thermal conductivity of the deposits to be the thermal conductivity of the oil. They also explained what would happen if the thermal conductivity of the deposit were less than that of the oil. Svendsen et al. (1993) assumed that the thermal conductivity of the deposit is equal to that of the oil, as the deposit is mainly oil. The MSI/Conoco paraffin deposition prediction program (1998) also uses the thermal conductivity of the oil for the deposit thermal conductivity.

Surface Roughness

Paraffin deposition may increase pressure drop by decreasing the effective diameter of the pipe, and by increasing the effective roughness of the pipe. There is some question about the roughness of deposits based on the existing literature. Bern et al. (1980) presented field data from a Forties sealine indicating that the roughness of the deposit equals the deposit thickness. Marshall (1988) presented field data from the Valhall pipeline indicating the deposit roughness is equal to, or greater than, the deposit thickness. On the other hand, Rygg et al. (1998) presented field data in which the deposit roughness in an oil and gas line only increased marginally, and the deposit roughness in an oil line (with 0.5% water) was approximately 15 percent of the deposit thickness.

Jorda (1966) studied the impact of pipe roughness on paraffin deposition. He found that increasing the roughness of a cold-finger increases the deposition rate as well as the nature of the deposit. Using a camera he was able to document that paraffin deposits first in the crevices of the steel surface of the cold-finger probe. Henson et al. (1994) also reported that paraffin sticks to rough surfaces more than to smooth surfaces. Brown et al.[(d)] (1993) observed tests where deposition was delayed several hours due to some effect at the tube surface. Svendsen (1993) reported that wall friction must be sufficiently large for wax crystals to stick to the wall.

Oil in Deposit Concentration

Paraffin deposits contain wax crystals and trapped oil. All known paraffin deposition models predict the rate of deposition of wax crystals, and then multiply by some factor to account for trapped oil. Knowledge of the oil in deposit concentration is thus a necessity to predict paraffin deposition accurately. Although some investigators have reported oil in deposit concentrations, or porosity, no attempts to correlate operating parameters to the porosity have been found in the literature.

Hsu et al. (1994 and 1995) reported that oil in deposit concentration could be as high as 80 %, while Weingarten and Euchner (1988) used 82 % oil concentration. Burger et al. (1981) reported oil in deposit concentrations ranging from 83 - 86 %. Rygg et al. (1998) assumed 85 % for an oil (with 0.5% water) based on the Burger et al. study, but assumed 60 % for an oil-gas turbulent field case. Rygg stated that the oil in deposit concentration is a potential tuning parameter. Hamouda and Davidsen (1995) reported 60 % at a deposition temperature of approximately 24°C (75°F), and 75 % at a deposition temperature of approximately 13.5°C (56°F). They reported a linear increase in the wax molecular weight with increasing deposit temperature. Hamouda and Davidsen also reported that shear rate has a

small effect on the oil in deposit concentration. Brown et al.[(d)] (1993), on the other hand, reported that the oil in deposit concentration, or porosity, decreases with increasing shear rate. Chung et al. (1991) reported that at lower temperatures the precipitated wax contains more low-molecular-weight paraffins. This is supported by Hamouda and Davidsen who found an increasing wax molecular weight with increasing temperature. Eaton and Weeter (1976) reported that at low velocities the deposit was initially soft, but that after 240 hours the deposit had become hard. They also reported that deposits formed at high velocities were hard even without aging.

Classical Mass Diffusion and Sloughing Mechanisms

The rate at which the volume of paraffin increases on the inner pipe circumferential area was obtained from Eq. C.9. Typically, the rate at which paraffin thickness increases on the inner pipe circumferential area is obtained by rearranging Eq. C.9 and substituting the volume expression that is a function paraffin thickness. The resulting expression is given by Eq. C.10.

$$\frac{dV_w}{dt} = \frac{1}{\rho_w}\left[\frac{dm_w}{dt}\right] \quad \text{(C.9)}$$

$$\frac{d\delta}{dt} = -\frac{\rho_o}{\rho_w} D_{ow}\left[\frac{dw_w}{dT}\frac{dT}{dr}\right] \quad \text{(C.10)}$$

In Eq. C.10, the change of dissolved paraffin concentration with respect to temperature and the temperature gradient in the radial direction were obtained at the inner pipe wall if no wax is present, or at the wax-crude oil interface if wax deposits are present. Wilke *et al.* (1955) and Hayduk *et al.* (1982) correlations are typically used to predict the diffusion coefficient. Many investigators however, have applied a fitting parameter to the diffusion coefficient parameter in order to fit the deposition model to the experimentally measured deposition rates data (see Brown[(a)] et al. (1993), Burger et al. (1981), Hsu[(a)] et al. (1994), Hsu[(b)] et al. (1995), Hsu[(c)] et al. (1995), and Weingarten and Eucner (1988)). Experience has shown that most available correlations for predicting diffusion coefficients do not appear to be accurate when the results of deposition simulators are compared with laboratory and field deposition rates. The resulting fitting parameter is expressed in terms of a constant, *C* as given by Eqs. C.3 or C.4.

Note that in Eq. C.10, the resulting paraffin thickness buildup rate is a function of the oil and paraffin densities, the diffusion coefficient; that is typically designated as a transport property of the dissolved paraffin in solution oil mixture, and the radial concentration gradient which is expressed in terms of a product of a temperature concentration gradient and a radial temperature gradient. Typically, one would assume that the density of paraffin equals the density of oil. The degree of uncertainty in the buildup rate when applying such assumption is not known but could possibly be very small.

One of the disadvantages when solely applying the classical Fick's mass diffusion theory in predicting paraffin buildup is that it does not incorporate the shear stripping or sloughing of paraffin from the pipe wall. Shear stripping of paraffin from the pipe wall was often seen by many investigators. Burger *et al.* (1981) concluded that the sloughing mechanism was a possible explanation for the reduction in deposition. Hsu *et al.*[(a)] (1994) revealed that flow turbulence or shear dispersion effects depress wax deposition significantly due to sloughing. Agarwal *et al.* (1990) deduced that turbulence is the main factor for the decrease in deposition with increasing flow rate, while diffusion is responsible for the increase in deposition with increasing flow rate in the laminar region. Matzain (1996) and Lund (1998) confirmed that paraffin thickness was greater in laminar flow than in turbulent flow, and decreased in Reynolds number in turbulent flow.

The sloughing effect generated under turbulent flow conditions has significant impact on paraffin deposition rate and can not be neglected in paraffin deposition modeling. Most developed prediction models do not include the sloughing effect, or if the sloughing effect is included, it is only based upon a fitting parameter that was obtained from sets of laboratory data. Most developed prediction models are either based only on a molecular diffusion theory, or are mainly semi-empiric in order to scale-up the wax deposition model and to include the net effects between positive wax deposition due to molecular diffusion and other mechanisms, and negative wax deposition due to sloughing by flow generated forces.

Interfacial Mass Transfer

One reason for the failure in describing the diffusion problem may be that the classical mass diffusion theory is an isothermal, quiescent process that may not directly apply for flowing non-isothermal systems. The deposition scenario is a non-isothermal flowing system and appears to be driven by the heat flux. The appropriate deposition flux coefficient relation may be a combination of mass and thermal diffusion. However, in many ways, the mechanism for the rate of transport of dissolved paraffin has been described as a transfer of mass due to a concentration difference. In many chemical engineering applications, the solutions of many mass transfer problems at low-mass transfer rates were obtained by analogy with corresponding problems in heat transfer. For slow mass transfer of dissolved species in a closed channel with known interfacial area, it is convenient to employ a local one-phase mass-transfer coefficient, k_x to obtain the rate of transport of dissolved species in a non-diffusing solution mixture (see Bird at al (1960). The interfacial mole flux varies with the difference in mole fractions.

$$\frac{dn_w}{dt} = \kappa_x A_i \left(x_{w,b} - x_{w,f} \right) \qquad \text{(C.11)}$$

The rate of transport of dissolved species, dn_w/dt given by Eq. C.11 has the units of moles per time. $x_{w,b}$ and $x_{w,f}$ are the mole fractions of dissolved species in the bulk fluid and in the wall film, respectively. For the simultaneous heat, mass, and momentum transfer problem, it is convenient to apply the close similarities among the transfers of heat, mass and momentum brought out by the Reynolds analogy (see Bird at al (1960). Chilton and Colburn (1934) later modified these similarities to include mass transfer resistance of the fluid near the solid or liquid boundary. Dawson (1995) applied the interfacial mass transfer theory to obtain the rate of transport of paraffin from the warm oil, where the paraffin is soluble, to the cooler pipe wall, where the paraffin crystallizes to form wax. The mass transfer coefficient was determined by making use of the Chilton and Colburn analogy.

Crystal Growth Theory-Diffusion Layer Model

Only recently has the kinetics of paraffin deposition in single-phase flow been associated with the theory of crystal growth. Although there is limited published work applying the theory of crystal growth to paraffin, there are a number of published reports available on the kinetics of crystal growth from non-organic supersaturated solutions. From the point of view of the kinetics of crystal growth based on the diffusion layer model, the dissolved substance in a supersaturated solution must initially be transported from the bulk solution to the crystal surface through the diffusion process, before it can be incorporated into the crystal lattice. This transport occurs through a stationary solution layer that is in dynamic equilibrium with the crystal surface and with the bulk phase of the supersaturated solution. The classical Fick's law generally describes the diffusion process. The rate of incorporation of particles into the crystal lattice is dependent on the difference in concentrations of species within the boundary layer and that in the saturated solution. Nyvlt *et al.*[(a)] (1985) and Nyvlt *et al.*[(b)] (1985) described these processes by a simple rate-determining process as given by Eq. C.12. The rate equation given by Eq. C.12, and the

subsequent rate equations that follow, are written in terms of paraffin or wax in order to represent paraffin or wax as the dissolved substance.

$$\frac{dm_w}{dt} = \left[\frac{}{k_i A_i} (w_{w,b} - w_{w,f}) - \frac{dm_w}{dt} \frac{}{k_d A_i} \right]^s \quad \text{.....(C.12)}$$

If $k_d > k_i$, then the rate-determining process is diffusion. If $k_i > k_d$, then the rate-determining process is the incorporation of species into the crystal lattice. The overall growth rate is determined by the slowest of these processes. The incorporation of species into the crystal lattice is also best described as an aging process. The parameter s is an exponent with a value dependent on the conditions, primarily on the super-saturation, within the limits of 1 to 2. For an s exponent equal to 1, it follows that,

$$\frac{dm_w}{dt} = \left(\frac{1}{k_d} + \frac{1}{k_i} \right)^{-1} A_i (w_{w,b} - w_{w,f}), \quad \text{.....(C.13)}$$

or more simply,

$$\frac{dm_w}{dt} = k_g A_i (w_{w,b} - w_{w,f}). \quad \text{.....(C.14)}$$

Note that Eq. C.14 is analogous to Eq. C.11, except that the rate of transport in Eq. C.14 has the units of mass per time. For an s exponent between 1 and 2, the rate equation becomes more complicated. However, the complicated functional dependence of the rate equation can be approximated by the relationship,

$$\frac{dm_w}{dt} = k_g A_i (w_{w,b} - w_{w,f})^b, \quad \text{.....(C.15)}$$

where exponent b assumes values between 1 and 2. Thus, the rate of crystal growth can generally be expressed by Eq. C.15 where proportionality constant k_g is dependent on the values of rate constants k_i and k_d. Measured kinetic data can be used to relate k_d and k_i by relating Eq. C.15 to Eq. C.12.

Paraffin Deposition in Multiphase Flow Systems

Paraffin deposition in multiphase flow is poorly understood. In this report, all references to multiphase flow are principally aimed at flows consisting of natural gas and crude oil. The effect of a water phase on paraffin deposition was not investigated. Paraffin deposition under multiphase flow conditions has not been systematically investigated and therefore remains poorly understood. In multiphase systems, the additional gas phase adds to the complexity of understanding the wax deposition phenomena.

There are limited published literature sources that specifically address the prediction of paraffin deposition in multiphase flowlines or wellbores. Furthermore, there are limited published experimental investigations that specifically address the nature of paraffin deposition in the multiphase flow conditions.

Rygg *et al.* (1998) and Dawson have presented models for multiphase paraffin deposition, but the proposed models contain several speculative assumptions that have never been verified with appropriate experimental data. Forsdyke (1995), Matzain et al. (1998) and Apte *et al.* (1999) provided a description of the possible effects of multiphase flow on paraffin deposition. They suggested that the principal effects of multiphase flow on wax deposition would be those of composition and flow patterns. Apte[(a)] (1999) conducted a preliminary investigation of wax deposition using a similar test facility as the present study and found that the wax deposition is flow pattern specific. A simulator that predicts wax deposition in the multiphase environments was developed and tested with the data collected.

Rygg *et al.* assumed that the radial temperature gradient in the two-phase flow mixtures makes dissolved wax diffuse from the bulk oil towards the wall. The diffusion process occurs in the laminar sub-layer region only. The volume rate of wax deposited by molecular diffusion is determined by summing up each individual paraffin component that is diffused due to concentration gradient in the laminar sub-layer region as a result of the radial temperature gradient. Rygg *et al.* assumes that the wetted inner surface perimeter depends on the local flow pattern and the liquid holdup. As a first approximation for annular, dispersed bubble and bubbly, and intermittent and churn flow patterns, the whole perimeter is assumed to be wetted. This approximation makes the paraffin buildup volume rate expression to become heavily dependent upon the concentration gradient, that is dependent upon the radial temperature gradient between the bulk two-phase flow mixtures and the pipe wall. Dawson presented the rate of paraffin deposition in the multiphase flow environment by applying a local mass transfer coefficient to describe the interfacial mass transfer of dissolved paraffin in a closed channel with known interfacial area as a result of a concentration difference. Interfacial mass transfer coefficients from the liquid to the wall are determined for each pipe segment depending on the local flowing conditions and fluid properties. By making use of the Chilton-Colburn analogy, which provides a relationship between mass and heat transfer, factors for heat transfer enhancement in multiphase flow are applied to mass transfer. The mass transfer coefficient calculated using this approach is modified to account for the effects of multiphase flow by replacing the true pipe diameter with a hydraulic diameter to account for the portion of the pipe that is occupied by the liquid.

Many investigators have proposed that the methods used for estimating paraffin deposition in single-phase flow be applied to multiphase flow conditions by including in the deposition mechanisms the effects of fluid compositions, flow pattern and the extent of liquid phase contact with the pipe wall (see Apte[(a)] (1999), Apte[(b)] et al. (1999), Dawson (1995), and Forsdyke (1995)). A modified pseudo-single-phase method can be used for all flow patterns, and the deposition rate can be modeled in a similar way to single-phase flow. In a single-phase liquid, molecular diffusion is generally considered to be the dominant mechanism, while shear dispersion effects are considered negligible. However, in multiphase flow, it is probable that a dominant factor governing paraffin build-up will be the forces stripping away the depositing paraffin. The nature of multiphase mixtures and fluid compositions may affect the paraffin solubility. In addition, the extent, duration and shear stress severity of the contact liquid at the pipe wall will depend on the flow pattern existing in the flowlines or wellbores.

Effect of Fluid Composition

The pressure and temperature along a multiphase flowline has been found to have a significant effect on the fluid compositions. The pressure along the flowline, even ignoring changes in elevation, will vary due to frictional losses. As the internal pressure drops along the line, the in-situ gas-oil ratio increases. Similarly, as the temperature drops along the line, the gas-oil ratio may increase or decrease, depending on the fluid composition. These changes in temperature and pressure may affect the fluid compositions and other liquid properties such as density, viscosity and thermal capacity. If these changes result in additional gas evolving from solution, the additional gas can increase the temperature and in situ

flow rates. The fact that a free gas phase under pressure is present means that the crude is more 'lively' and therefore a better solvent for paraffin. As a result, the paraffin solubility and the paraffin appearance temperature are affected and may vary along the line. A higher gas flow rate can also increase the wall shear stress, which may contribute to the increase in the stripping of deposits from the wall.

Effect of Flow Pattern

Flow patterns of multiphase flow mixtures in horizontal and near-horizontal flowlines are typically grouped into four categories: stratified (smooth and wavy), intermittent (slug and elongated bubble), annular, and dispersed bubble. Flow patterns of multiphase flow mixtures in a vertical pipe are also typically grouped into four categories: bubbly, dispersed bubble, intermittent (slug and churn) and annular. These flow patterns depend primarily on flow rates, pipe dimensions, and inclination angle. Brill *et al.*[(a)] (1988) and Brill *et al.*[(b)] (1999) give a comprehensive description of multiphase flow in wells and flowlines and the available methods for predicting multiphase flow parameters e.g. flow patterns, pressure gradients and liquid holdups. The mechanistic model by Xiao *et al.* (1990) is often used to predict flow patterns, pressure gradients and liquid holdups for pipe inclination angles from –15° to + 15°. The mechanistic models by Kaya (1998) and Ansari *et al.* (1989) are widely used to predict flow patterns, pressure gradients and liquid holdups for pipe inclination angles from +15° to +90° from horizontal.

Some investigators have proposed to address the nature of wax deposition in each individual flow pattern. The rate at which paraffin thickness increases on the inner pipe circumferential area in each individual flow pattern is determined by obtaining the rate at which the volume of paraffin deposition increases on the inner pipe circumferential area, and the extent of liquid phase in contact with the pipe wall.

Published literature sources that specifically address the prediction of paraffin deposition in multiphase flowlines or wellbores are indeed very limited. Paraffin deposition rate under multiphase flow conditions has been hypothesized in the past to be lower than that for single-phase flow for the following reasons:

- Greater wax solubility in live crude reduces the wax appearance temperature.
- Higher flow velocity due to presence of gas reduces the residence time and specific heat capacity, thus increasing the temperature profile.
- Higher flow rates increase the pipe wall shear stress.
- Presence of gas reduces the contact time of oil with the pipe wall.

The above hypotheses, however, have not been verified with experimental data. Clearly, there is a need for a more reliable predictive tool to estimate paraffin deposition in the multiphase flow environment.

Multiphase Heat Transfer

The wax deposition scenario has been described as a non-isothermal flowing system that appears to be driven by the heat flux. Consequently, the success in predicting wax deposition rates in single-phase and multiphase flow environment depends on how heat transfer characteristics are evaluated. They include the forced convective film heat transfer coefficient, bulk and wall temperatures and local heat flux across the pipe wall. Numerous heat transfer coefficient correlations and experimental data for forced

convective heat transfer during gas-liquid two-phase flow in vertical and horizontal pipes have been published over the past 40 years. These correlations were developed based on limited experimental data and are applicable to certain flow patterns. Kim *et al.*[a] (1999) proposed that a general and single heat transfer correlation could be applied to all turbulent gas-liquid two-phase flow in vertical pipes with different flow pattern. Approaches adopted by previous investigators fall in three categories; empirical - particularly for intermittent flow (see Kudirka et al. (1965), Rezkallah and Sims (1987), and Shah (1981)), modified single-phase flow methods - particularly for bubbly flow, dispersed bubble and intermittent flow (see Fried (1954), Knot et al. (1959), and Oliver and Wright (19xx)), and momentum transfer - heat transfer analogies - particularly for stratified and annular flow (see Davis[a] et al. (1976), Davis[b] et al. (1975), Hughmark (1963), and Pletcher and McManus (1972)). The local heat flux and temperatures are usually derived from a thermal balance.

In intermittent flow where spatial distribution of local holdup changes with time, heat transfer characteristics were mostly presented as time and space averaged over a slug unit. However, Shoham *et al.* (1982), Barnea[a] *et al.* (1983), Hestroni *et al.*[a] (1999) and Hestroni *et al.*[b] (1999) studied heat transfer characteristics for two-phase intermittent flow and reported that the time variation of temperature, heat transfer coefficients, and heat flux are very different in different zones of a slug unit. Substantial differences in heat transfer coefficient were found between the bottom and top of the slug. Recently, Kaminsky (1999) proposed a new heat transfer estimation method for non-boiling gas-liquid flow in pipes of high Prandtl number liquids, such as crude oil. The approach mathematically separates the heat transfer physics from the flow behavior. The method is in conjunction with existing prediction methods for two-phase flow pressure drop and liquid holdup, and is divided in two categories i.e. heat transfer in gas-liquid flow with turbulent liquid flow, and heat transfer in gas-liquid flow with laminar liquid flow. The method is valid for all flow patterns except annular-mist.

Vapor-Liquid-Solid Equilibrium Thermodynamics

The precipitation of paraffin or wax out of its liquid solution has been described in many literature sources to occur when the temperature of the pipe wall falls below the cloud point temperature of a hydrocarbon liquid (see Fredenslund et al. (1988), Erickson et al. (1993), and Narayanan et a. (1993)). The precipitation scenario appears to be dependent upon the amount of normal paraffins present in a hydrocarbon system. When vapor is present, rigorous treatments of the vapor-liquid-solid equilibrium state usually include the vapor phase. In that case a three-phase flash calculation must be performed. Four types of relations are required to described the three-phase flash; they are phase equilibrium of vapor-liquid and liquid-solid, component material balances, total material balance and stoichiometric. The multiphase flash problem usually can be solved by using either of two techniques i.e. Gibbs energy minimization and fugacity matching methods (see Bunz (1991)).

Vapor-liquid equilibria, usually called the equation of state, has been very well studied by many investigators e.g. Peng and Robinson (1975), and Soave (1972). Solid-liquid equilibria of a hydrocarbon system, however, has been studied by Won (1986), Erickson *et al.* (1993), Narayanan *et al.* (1993), and Fredenslund *et al.* (1988). Later, Brown *et al.*[b] (1994) utilized the model of Erickson *et al.* and included the effects of light ends, such as methane, ethane and propane and high pressures to describe the vapor-liquid-solid equilibria. Brown *et al.*[b] found that the simplified perturbed hard chain theory equation of state developed by Kim *et al.*[b] (1986) was better to represent the vapor-liquid equilibria of high-molecular-weight paraffins in light solvents.

A thermodynamic model for predicting vapor-liquid-solid equilibria of hydrocarbon systems developed by Brown *et al.*[c] (1997) was used in the present study. The model is essentially the same as described by Erickson *et al.* and Brown *et al.*[b]. The multiphase flash algorithms is based on the Gibbs

energy minimization methods as proposed by Michelsen [a] (1982) and Michelsen[b] (1982). The algorithms initially assume the system to be single-phase and the stability of this phase is evaluated with respect to vapor-liquid phase split. If the single-phase is unstable, a vapor-liquid flash is performed. The stability of the one or two-phase system is then evaluated with respect to formation of a solid paraffin phase. If the system is unstable, a two or three-phase flash is performed. For the stability analysis, the method of Michelsen[a,b] is used. Given an estimate of the composition of a new phase, the stability analysis converges on a composition for the new phase which, when split off in an infinitesimal amount, minimizes the Gibbs energy of the combined phases. If the Gibbs energy of the combined phases is less than that of the original system, the original system is unstable.

Simulation of Wax Deposition during Multiphase Flow

Although many oil companies that studied the problem of paraffin deposition have predictive capabilities for single-phase oil flow, these predictive capabilities may not be suitable for the multiphase flow conditions encountered in most flowlines. In the case of single-phase oil flow, molecular diffusion is generally considered to be the dominant mechanism, while shear dispersion effects are considered negligible. Fick's law as given by Eq. C.3 is then used to predict wax deposition buildup rates.

Rygg *et al.* (1998), Dawson (1995), Hsu *et al.* (1999) and Apte *et al.* (1999) have proposed models for predicting paraffin deposition during multiphase flow. These models contain several assumptions that have not been verified with appropriate experimental data.

Rygg *et al.* (1998) developed a computer program for the prediction of paraffin deposition that uses the Hayduk and Minhas (1982) correlation to calculate the molecular diffusion coefficient for each of the components. Dawson (1995) proposed the use of a mass transfer coefficient approach instead of molecular diffusion for predicting wax deposition rates. The mass transfer coefficient was modified using the Chilton and Colburn (1934) analogy. Hsu *et al.* (1999) modeled wax deposition phenomena in multiphase flow using semi-empirical measurements. The effects of diffusion and shear are incorporated in the model based on specific measurements obtained in a laboratory flow loop.

Forsdyke (1995) and Apte *et al.* (1999) suggested that the approach for estimating paraffin deposition in multiphase flow could be similar to that for single-phase flow. They described the possible effects of different flow patterns on wax deposition and speculated on the nature of the wax deposits that could occur during each flow pattern.

Appendix D
GUI Inputs – Adjustment Parameters for the Wax Deposition Program

The single-phase and multiphase test results show that the oil content in the deposits decreased during the turbulent tests. An appropriate estimation of the oil content in the deposits is essential for the prediction of the deposit thickness. At the same time, as the result of the oil content decrease, the thermal conductivity of the deposits increases. The change of thermal conductivity of the deposits will further influence the temperature gradient on the wall and the paraffin deposition rate.

The surface roughness in the pipe becomes different from that of the bare pipe due to the paraffin deposition. A single-phase turbulent test showed that the roughness is slightly higher than the pipe roughness after 24 hours. On the other hand, sloughing of the wax deposit was observed to occur during the turbulent tests.

The Wilke-Chang and Hayduk-Minhas correlations are the most frequently used correlations in predicting the molecular diffusion coefficient. From comparison with the test results, these correlations usually under predict wax deposition rate significantly.

The purpose of the adjustment parameter input options is to allow users to incorporate the effects of the oil content change, the thermal conductivity change, the wall roughness change, the shear striping and to have the options of using different diffusion coefficients based on their own experimental or field experiences.

The following recommended input ranges for the adjustment parameters are based on the single-phase and multiphase test results of the JIP, and the need for certain calculations.

1. Oil content in deposit

Input the oil fraction in the deposit (Coil: 0.2 ~ 0.9). The molecular diffusion coefficient will be magnified by a factor of 1.0/(1.0-Coil).

2. Thermal conductivity of deposit

Input a multiplier (Cwax: 1.0 ~ 3.0) for the oil thermal conductivity to simulate the thermal conductivity of the deposit (Kdep=Cwax*Koil). The thermal conductivity of the deposit is the same as that of oil if Cwax=1.0.

3. Pipe wall roughness

Input a parameter (Crou) to incorporate the contribution of the deposit to the roughness of the boundary surface of the flow

roughness=(ep+Crou*depthick)

roughness — absolute roughness of flow boundary surface

ep ——— absolute roughness of pipe inside wall without deposit

depthick ---- thickness of deposit on the pipe inside wall

Crou is between –ep/depthick and 1.0.

4. Shear stripping

Simulate the shear stripping by use of the shear dispersion formulation and a negative dispersion coefficient (-Cshr). The stripping rate should be smaller than 80% of the deposition rate of the molecular diffusion.

5. Multiplier for diffusion coefficient

Input a multiplier (Cdif: 0.0 ~ 10.0) for the Wilke & Chang correlation or Hayduk & Minhas correlation. There is no deposition if Cdif = 0.0.